Pleistocene Stratigraphy, Glacial Limits and Paleoenvironments of White River and Silver Creek, Southwest Yukon

by

Derek G. Turner

M.Sc., Simon Fraser University, 2008

Dissertation Submitted in Partial Fulfillment of the
Requirements for the Degree of
Doctor of Philosophy

in the
Department of Earth Sciences
Faculty of Science

SIMON FRASER UNIVERSITY

Fall 2014

Approval

Name:	**Derek Turner**
Degree:	**Doctor of Philosophy**
Title:	***Pleistocene stratigraphy, glacial limits and paleoenvironments of the White River and Silver Creek, southwest Yukon***
Examining Committee:	**Chair:** Dr. Dan Gibson Associate Professor, Simon Fraser University

Dr. Brent Ward
Senior Supervisor
Associate Professor
Simon Fraser University

Dr. Duane Froese
Senior Supervisor
Associate Professor
University of Alberta

Mr. Jeffrey Bond
Supervisor
Surficial Geologist
Yukon Geological Survey

Dr. Rolf Mathewes
Supervisor
Professor
Simon Fraser University

Dr. Olav Lian
Internal Examiner
Adjunct

Dr. Martin Roy
External Examiner
Professor
Universite du Quebec a Montreal

Date Defended/Approved: September 26, 2014

Partial Copyright Licence

Abstract

Quaternary glacial and non-glacial sediment exposed at White River and Silver Creek provide a record of environmental change in southwest Yukon for much of the late-Middle to Late Pleistocene. Eighteen sites at White River, located beyond the marine oxygen isotope stage (MIS) 2 glacial limit, contain thick accumulations of till, loess, peat, gravel and glaciolacustrine silt and clay, with tephras, paleosols, plant and insect macrofossils and large mammal fossils. Radiocarbon ages and eleven tephra beds constrain two tills to MIS 4 and 6. These tills correlate to the Gladstone and Reid glaciations and represent the penultimate and maximum all-time limits of the St. Elias lobe of the northern Cordilleran Ice Sheet. Two peat beds located between these tills indicate that interglacial conditions existed in the area during MIS 5e and 5a. Pond sediment deposited during mid-MIS 5 suggests that the sites were covered by an open birch tundra at this time. The MIS 3/2 transition was marked by a treeless, dry steppe-tundra populated by mammoth, horse and bison.

The eleven Silver Creek sites, located ~200 km up-ice, contain a similar record of glacial and non-glacial sediment. Infrared-stimulated luminescence (IRSL) and radiocarbon dating constrain the glacial deposits at these sites to MIS 2, 4, either MIS 7 or 6, and to two Early to Middle Pleistocene, Pre-Reid glaciations. Tilting of glaciolacustrine beds of up to 1.9 mm/yr may be from uplift along the Denali fault since MIS 7. Pollen and macrofossils analyses from overlying MIS 3-aged sediment suggest that the environment was dominated by herbs and forbs, with few shrubs and almost no tree pollen at this time. Combined, the White River and Silver Creek sites contain a record of glacial and non-glacial conditions in southwest Yukon since the Middle Pleistocene.

The glacial limits in southwest Yukon are markedly different from those in central Yukon. In southwest Yukon, the glacial limits are closely-spaced and were more extensive in the Middle to Late Pleistocene than in the Late Pliocene and Early Pleistocene. In central Yukon, glacial limits are separated by up to 300 km and were most extensive in the latest Pliocene and Early Pleistocene. This suggests that different forcing mechanisms controlled the extents of the St. Elias and Selwyn lobes during successive glaciations. Boundary conditions such as varying substrates, topography, moisture pathways and atmospheric circulation likely had a greater affect than tectonics and sea level on these glacial limits throughout the Plio-Pleistocene.

Keywords: Quaternary stratigraphy; Pleistocene; tephrochronology; paleoenvironments; glacial limits; dating

Dedication

This dissertation is dedicated to my grandfather, Dr. Donald E. W. Wormell, who inspired me at the earliest age to view the world with curiosity and wonder.

Acknowledgements

There were a great number of people who contributed in many ways to this dissertation. First, thank you to my supervisors. In particular, Dr. Brent Ward for being an excellent teacher, mentor and friend. Also, Dr. Duane Froese for encouraging me to expand my intellectual horizons and for putting up with me in his lab. Thank you to Mr. Jeffrey Bond for his ongoing optimism and support, both through our many discussions about the Quaternary geology of Yukon and with many aspects of the fieldwork.

One of the greatest things about working in such an inter-disciplinary field is the many exceptional scientists and people one regularly works with. Dr. Britta Jensen is greatly appreciated for teaching me the finer points of tephrochronology and for fixing my many mistakes. Drs. Michel Lamothe, Paul Sanborn, Alice Telka, Nancy Bigelow, Grant Zazula and Rolf Mathewes also all took the time to have long discussions about various aspects of the project. Drs. Olav Lian and Martin Roy were external reviewers whose input greatly improved the final product.

Thank you to the National Science and Engineering Research Council and the Northern Scientific Training Program for funding the field work. A special thanks to the Yukon Geological Survey, who go above and beyond to support student research in Yukon. I was especially grateful to receive the Bradshaw Scholarship, in honour of my friend Geoff Bradshaw, who is deeply missed. Without the YGS, I might still be stuck on the banks of the White River, both academically and literally. Thanks also to Melissa Dinsdale and Riley Gibson who provided excellent field assistance throughout the project.

Finally, thanks to Jillian Evers, Brennen Cross and Julia Turner for their patience, love and support while I pursued my Quaternological interests. Simply, without them this dissertation would not have been possible.

Table of Contents

List of Tables

List of Figures

Photo: Melissa Dinsdale

Chapter 1. Introduction

1.1. Background

The northern Cordilleran Ice Sheet repeatedly covered Yukon Territory throughout the latest Pliocene and Pleistocene. This ice sheet comprised multiple ice lobes that responded semi-independently to climatic forcing mechanisms (Fig. 1.1). The Selwyn lobe, sourced in the Selwyn Mountains to the east, covered central Yukon. The St. Elias and Eastern Coast Mountain lobes advanced across southwestern Yukon from the St. Elias and Coast Mountains, merging with the Cassiar lobe in southern Yukon. The Liard lobe flowed southeast from an ice divide that spanned the Cassiar, Pelly and Selwyn Mountains (Jackson et al., 1991).

The timing of the advances of these lobes is enigmatic, partly because of the lack of stratigraphy from within the glacial limits. The global marine oxygen isotope record (Martinson et al., 1987; Lisiecki and Raymo, 2005) suggests that extensive glaciations occurred in the Northern Hemisphere during even-numbered marine oxygen isotope stages (MIS) in the Middle to Late Pleistocene (e.g. MIS 2, 4, 6, 8, etc.), with the largest occurring during MIS 16, 12, 10, 6 and 2. However, the glacial records in Yukon and Alaska do not follow the major trends seen in these records. In central Yukon, the Selwyn lobe and ice from the Ogilvie Mountains was most extensive in the latest Pliocene and Early Pleistocene (Froese et al., 2000; Jackson et al., 2012; Hidy et al., 2013). The next most extensive glaciation was in MIS 6 (Ward et al., 2008), followed by MIS 2 (Hughes et al., 1969). Conversely, no pre-MIS 6 glacial limits are preserved in southern Alaska (Briner and Kaufman, 2008) and southwest Yukon (Bond et al., 2008; Turner et al., 2013) and the penultimate limit was mostly developed during MIS 4, not MIS 6 (Briner et al., 2005; Ward et al., 2007). Understanding the timing and extent of these ice lobes allows us to evaluate their regional response to various glacial forcing

mechanisms. This is significant for long-term models of climate change in Yukon and Alaska.

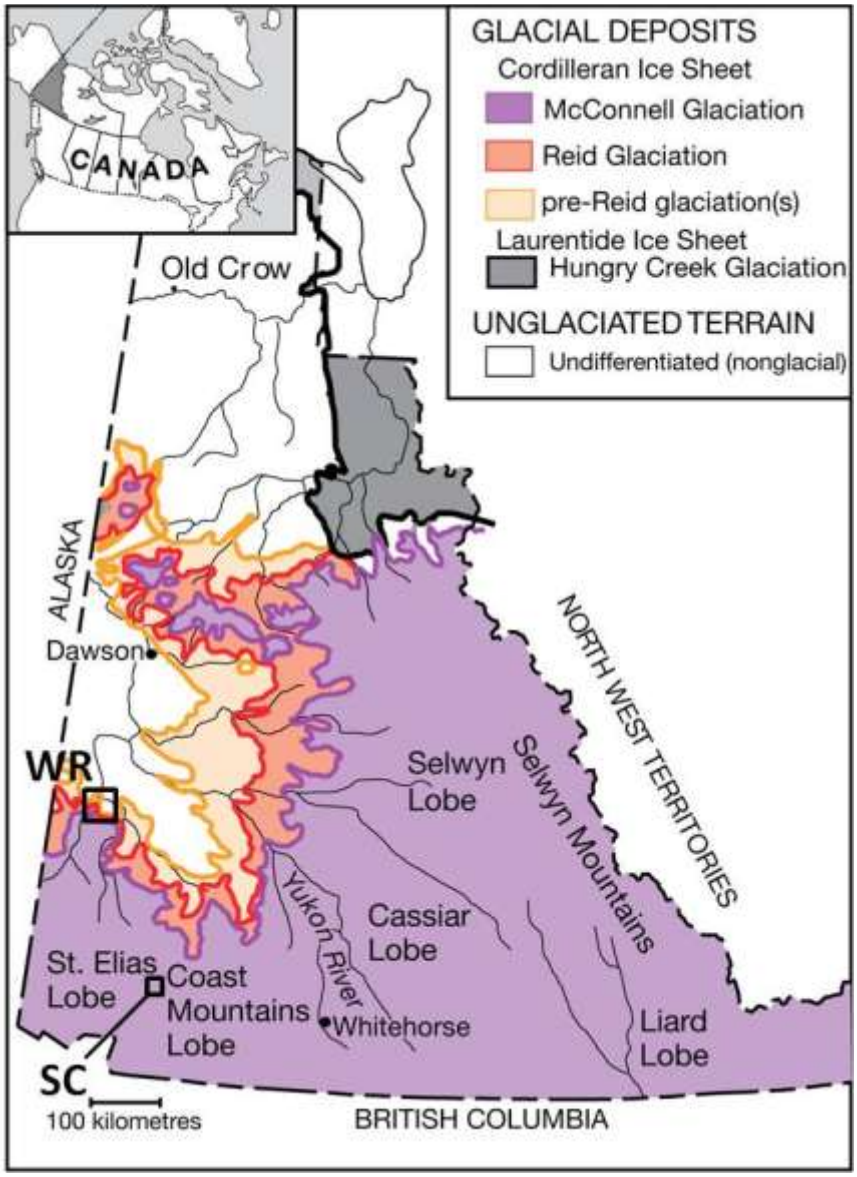

Figure 1.1. Location of the White River (WR) and Silver Creek (SC) study areas in relation to the glacial limits in Yukon and the ice lobes of the northern Cordilleran Ice Sheet (modified from Ward et al., 2007, with limits from Duk-Rodkin, 1999).

Detailed chronologies for glacial sediment are needed to resolve the differences in glacial extents of these ice lobes. This is particularly difficult for glaciations older than the maximum limit of radiocarbon dating (currently ~50 ^{14}C ka BP). Tephrochronology,

infrared stimulated luminescence (IRSL) and terrestrial cosmogenic nuclide dating offer potential alternatives to date older glacial deposits. Tephrochronology is a particularly useful tool as tephras are instantaneous marker horizons that can be correlated to other sites across Yukon and Alaska based on their unique glass morphology, major and minor element geochemistry, Fe-Ti oxides and stratigraphic and paleoenvironmental contexts. This dissertation uses tephrochronology, IRSL dating and accelerated mass spectrometry (AMS) ^{14}C dating to constrain the glacial and non-glacial stratigraphy at White River and Silver Creek and provide ages for the Pleistocene advances of the St. Elias lobe.

These two study areas were selected based on their locations relative to the glacial limits and their potential to contain datable, Middle to Late Pleistocene sediment. The White River sites were only recently exposed. The exceptional preservation of the stratigraphy at these sites and their proximity to the maximum extent of the St. Elias lobe made them ideal for detailed stratigraphic and paleoecological investigation. The Silver Creek site has been examined in the past (Denton and Stuiver, 1967; Schweger and Janssens, 1980) and is known to contain a record of numerous Pleistocene advances of the St. Elias lobe. This site was selected because of the presence of tephras and the potential to apply IRSL and modern AMS radiocarbon techniques to date the older glacial sediment and validate Denton and Stuiver's (1967) stratigraphy. These two complimentary areas, separated by ~200 km, provide an opportunity to increase our understanding of the timing of Pleistocene advances of the St. Elias lobe.

The resulting chronology also provides a framework to investigate the paleoecology of the non-glacial intervals between glaciations. Few paleoecological studies have focused on pre-MIS 2 deposits within the glacial limits of Yukon. Well-preserved pollen, plant and insect macrofossils and mammal fossils at White River offer a rich record for reconstructing paleoenvironments during MIS 5 and the transition from late MIS 3 to early MIS 2. Relatively poorly-preserved records at Silver Creek give insight into the environment during MIS 7 and MIS 3. Correlating these results to other well-constrained records across unglaciated Yukon and Alaska, such as those in the Klondike and those at Fairbanks, contributes to our understanding of regional ecosystem variations during previous non-glacial intervals.

1.2. Methodology

Similar methodologies were used to study the White River and Silver Creek sites. Methods for describing the sedimentology and stratigraphy and for analyzing the major element geochemistry analysis of tephras are described in detail, as these were the principle component of the research. The methodologies for paleoenvironmental analysis are summarized below and in Chapters 2 and 3. Laboratory analysis of the IRSL samples was performed in the Laboratoire de Luminescence Lux at the Université du Québec à Montréal, under the supervision of Dr. Michel Lamothe. These methods are described in Chapter 3.

1.2.1. Stratigraphy

The stratigraphy of the White River and Silver Creek sites was examined during field seasons in 2008, 2009 and 2010. The White River sites were discovered during reconnaissance field work by J. Bond and B. Ward in 2007. Recent forest fires in the area in 2003 and 2004 caused accelerated permafrost degradation and gullying, revealing fresh exposures (Fig. 1.2). The Silver Creek sites were initially described by G. Denton in the mid-1960s and the exposures have not changed substantially since then. Location coordinates, heights and distances were measured at both field areas using a Garmin 60CSX GPS unit and a TruPulse 200 laser rangefinder. Tephra, macrofossil and pollen samples were collected using cleaned instruments to avoid contamination and placed in Whirl-Pak sample bags for transportation. IRSL samples were collected using 4” diameter, opaque plastic tubes, with multiple samples taken at each location.

Figure 1.2. Example of the White River exposures in gully sidewalls. Erosion of these gullies accelerated following forest fires in 2003 and 2004. Sites WR99 and WR98 are on the left and right sidewalls of the gully, respectively.

1.2.2. Tephrochronology

Eighty tephra samples were collected in the White River study area. Of these, fifty-one were analyzed for their major element geochemistry. Eleven different tephras were identified (Appendix B). These tephras were mostly derived from either the Aleutian-Arc Peninsula (Type I) or the Wrangell Volcanic fields (Type II), following the classification scheme of Preece et al. (1999). Thirty-five tephras were sampled at Silver Creek. Although fourteen of these were analyzed and classified as Type II tephras, the glass was too heavily weathered to determine the major element geochemistry of the shards.

Most of the major element geochemistry analysis of the White River samples was completed at the University of Alberta in the fall, 2009 and spring, 2012, under the supervision of Dr. Duane Froese. Remaining samples were analyzed by Dr. Britta

Jensen. The samples were sieved into 250, 149, 74, 44 and <44 μm grain sizes and dried. Glass shards were separated from the heavy mineral fraction using tetrabromoethane (Fig. 1.3). They were then mounted into acrylic disks and coated with carbon to prevent a buildup of electrostatic charge from incident electrons (Fig. 1.4). The samples were analyzed using a JEOL electron microprobe (Fig. 1.5) with rhyolitic obsidian (IP 3506) and Old Crow tephra standards (c.f. Kuehn et al., 2011). The microprobe was operated with a defocused, 10 μm beam diameter at 6 ηA. The results were compared to the University of Alberta database. Potential correlations with high similarity coefficients (c.f. Hunt and Hill, 1993) were plotted on bivariate plots and re-analyzed together under the same microprobe conditions (c.f. Westgate et al., 2008). Correlations were further supported by comparing the stratigraphy, paleoenvironmental interpretations and glass morphology of the tephras.

Figure 1.3. **Separating the glass shards from the mineral content using tetrabromoethane. The glass has a lower density than the heavy mineral content. Darker samples typically have more organic material.**

Figure 1.4. **Acrylic disks with tephra samples for electron microprobe analysis. These disks have been coated in carbon.**

Figure 1.5. Electron backscatter images of glass shards using the JEOL electron microprobe at the University of Alberta.

1.2.3. Paleoecology

Paleoenvironmental analysis was based on plant and insect macrofossils and pollen to examine both the local and regional perspectives. The same samples were used for both pollen and macrofossil analysis whenever possible. Pollen analysis was completed by Dr. Nancy Bigelow at the Alaska Quaternary Center at the University of Alaska, Fairbanks. Volumetric pollen samples were sieved and exposed to acid and base washes to remove coarse organics and carbonates. The samples were separated using sodium polytungstate to concentrate the organic content. After centrifuging at 2000 rpm for five minutes, the suspended pollen was decanted onto a fibreglass filter. This paper was dissolved in hydrofluoric acid. After the remaining pollen underwent standard acetolysis, the samples were dehydrated with tert-Butyl alcohol and mounted in silicon oil. Samples were counted until 300 grains were encountered.

Plant and insect macrofossils collected at White River and Silver Creek were analyzed by Alice Telka of Paleotec Services. These samples were soaked in warm water and sieved into 0.15, 0.250, 0.425, 0.85 and 4.0 mm mesh sizes prior to identification using a binocular microscope. Details and references for the macrofossil

identification methodology are described in Chapters 2 and 3 and in Appendix C. Organic samples for AMS radiocarbon dating were submitted to either Beta Analytic in Florida or the Keck Carbon Cycle AMS Facility at the University of California, Irvine. Fragile macrofossils were preferentially selected for dating to limit the potential of reworking (c.f. Kennedy et al., 2010). Radiocarbon ages were calibrated using Oxcal v. 4.1 using the IntCal09 calibration curve (Reimer et al., 2009).

1.2.4. Dissertation objectives

The primary motivation of this dissertation is to use the glacial and non-glacial stratigraphies of the White River and Silver Creek sites to compare the glacial limits and paleoenvironments of southwest Yukon to other records in Yukon and eastern Alaska. To achieve this, the following objectives were established:

1) Interpret the stratigraphy of the White River sites and use tephrochronology and radiocarbon dating to determine the timing of the glacial limits at the maximum extent of the St. Elias lobe in southwest Yukon;
2) Determine the chronology of the glacial stratigraphy at Silver Creek and compare it to the White River glacial record;
3) Correlate the Pleistocene glacial limits of the St. Elias lobe in southwest Yukon to other records in Yukon and Alaska and to the global MIS record;
4) Use pollen and plant and insect macrofossils to interpret what environments existed in southwest Yukon during late-Middle to Late Pleistocene non-glacial periods, specifically MIS 7, 5 and 3.
5) Investigate what forcing mechanisms had the greatest influence on the different ice lobes of the northern Cordilleran Ice Sheet in Yukon throughout the Late Pliocene and Pleistocene.

1.2.5. Dissertation outline

This dissertation is based on three chapters, written in a journal-style, manuscript format. Each of these chapters presents a separate contribution, but may have repeated information, especially in methodologies and summaries of previous work. Because these chapters have been published or will be submitted for publication, they are presented here in their entirety.

Chapter 2 contains a description and interpretation of the stratigraphy along the White River. This site is beyond the MIS 2 glacial limit, but within the boundary of two closely-spaced glacial limits mapped by Bond et al. (2008). These two limits are represented in the stratigraphy by two tills separated by peat beds, loess and fluvial, glaciofluvial and glaciolacustrine sediment. Tephras and radiocarbon dates constrain the glacial limits to MIS 6 and 4 and the intervening non-glacial sediments to various sub-stages of MIS 5. The transition from MIS 3 to MIS 2 is also represented. The paleoecology of these well-preserved, non-glacial intervals is examined and correlated to other sites in Yukon.

Chapter 3 describes the stratigraphy and chronology of the exposures at Silver Creek. These sites contain five tills separated by thick accumulations of loess and fluvial, glaciofluvial and glaciolacustrine sediment. IRSL and radiocarbon ages suggest that these tills were deposited in either MIS 7 or 6, MIS 4, MIS 2 and two earlier Pre-Reid glaciations. Measurements of tilted, Middle Pleistocene glaciolacustrine beds allow an estimate of the amount of uplift along the Denali Fault in the Shakwak Trench. Pollen and macrofossils data from MIS 7- and 3-aged sediment provide a record of paleoenvironmental conditions in southwest Yukon during these non-glacial periods.

Chapter 4 summarizes the current understanding of the chronology of glacial limits in Yukon. The glacial limit records in central Yukon, the Southern Ogilvie Mountains and south and southwest Yukon are discussed, including the White River and Silver Creek sites. The record in southwest Yukon is then compared to a similar glacial limits record in the Delta River area in eastern Alaska using the potential correlation of the Sheep Creek – Canyon Creek tephra to one of the tephras at White River. Lastly, potential forcing mechanisms controlling the extent of successive glaciations in different parts of Yukon are described and evaluated based on these glacial limit records. This chapter summarizes the Yukon glacial limits literature in one source, something that was previously unavailable.

Chapter 5 summarizes the results of the dissertation and suggests possible future work on the glacial stratigraphy of southwest Yukon. Detailed site descriptions,

tephra data, macrofossil reports, pollen data, soil thin sections and an index of mammal fossils are included as appendices.

Chapter 2. Middle to Late Pleistocene ice extents, tephrochronology and paleoenvironments of the White River area, southwest Yukon

Derek G. Turner[1], Brent C. Ward[1], Jeffrey D. Bond[2], Britta J.L. Jensen[3], Duane G. Froese[3], Alice M. Telka[4], Grant D. Zazula[5], Nancy H. Bigelow[6]

[1]Derek G. Turner & Brent C. Ward, Department of Earth Sciences, Simon Fraser University, 8888 University Drive, Burnaby, B.C., V5A 1S6. Ph. 1-778-782-4564; Fax: 1-778-782-4198, dgturner@sfu.ca.

[2]Jeffrey D. Bond, Yukon Geological Survey, Yukon Government, P.O. Box 2703, Whitehorse, Yukon, Canada, Y1A 2C6.

[3]Britta J.L. Jensen & Duane G. Froese, Department of Earth and Atmospheric Sciences, University of Alberta, 1-26 Earth Sciences Building, Edmonton, Alberta, Canada, T6G 2E3.

[4]Alice M. Telka, PALEOTEC Services, 1-574 Somerset Street W., Ottawa, Ontario, Canada, K1R 2K2.

[5]Grant D. Zazula, Yukon Palaeontology Program, Department of Tourism & Culture, Yukon Government, P.O. Box 2703, Whitehorse, Canada, Y1A 2C6.

[6]Nancy H. Bigelow, Alaska Quaternary Center, PO Box 755940, University of Alaska, Fairbanks, Fairbanks, Alaska, USA

A modified version of this chapter was published in *Quaternary Science Reviews*, 75, 59-77, June 28, 2013

2.1. Abstract

Sedimentary deposits from two Middle to Late Pleistocene glaciations and intervening non-glacial intervals exposed along the White River in southwest Yukon, Canada, provide a record of environmental change for much of the past 200 000 years. The study sites are beyond Marine Isotope stage (MIS) 2 glacial limit, near the maximum

regional extent of Pleistocene glaciation. Non-glacial deposits include up to 25 m of loess, peat and gravel with paleosols, pollen, plant and insect macrofossils, large mammal fossils and tephra beds. Finite and non-finite radiocarbon ages, and eleven different tephra beds constrain the chronology of these deposits. Tills correlated to MIS 4 and 6 represent the penultimate and maximum Pleistocene glacial limits, respectively. The proximity of these glacial limits to each other, compared to limits in central Yukon, suggests precipitation conditions were more consistent in southwest Yukon than in central Yukon during the Pleistocene. Conditions in MIS 5e and 5a are recorded by two boreal forest beds, separated by a shrub birch tundra, that indicate environments as warm, or warmer than, present. A dry, treeless steppe-tundra, dominated by *Artemisia frigida*, upland grasses and forbs existed during the transition from late MIS 3 to early MIS 2. These glacial and non-glacial deposits constrain the glacial limits and paleoenvironments during the Middle to Late Pleistocene in southwest Yukon.

2.2. Introduction

Beringia, the mostly non-glaciated area of Yukon, Alaska and eastern Asia, was a large area created by periods of eustatically lowered sea levels during cold stages of the late Neogene (Hopkins, 1967, 1982; Fig. 2.1). The area was seemingly cold enough to support extensive glaciation, but the pronounced aridity resulted in much of this area remaining ice-free during the Pleistocene (Guthrie, 2001). This non-glaciated region provides an exceptional sedimentary record dating back through the late Cenozoic, much of it dateable beyond the limit of radiocarbon by the presence of widespread distal tephra beds (*e.g.* Westgate et al., 1990; Froese et al., 2009). Because of the excellent stratigraphic exposures and the potential for dating and correlating these tephra beds, much of the paleoenvironmental research has focused on the non-glaciated areas of Yukon and Alaska (e.g. Anderson and Lozhkin, 2001; Goetcheus and Birks, 2001; Froese, et al., 2009; Zazula et al., 2006a,b, 2007).

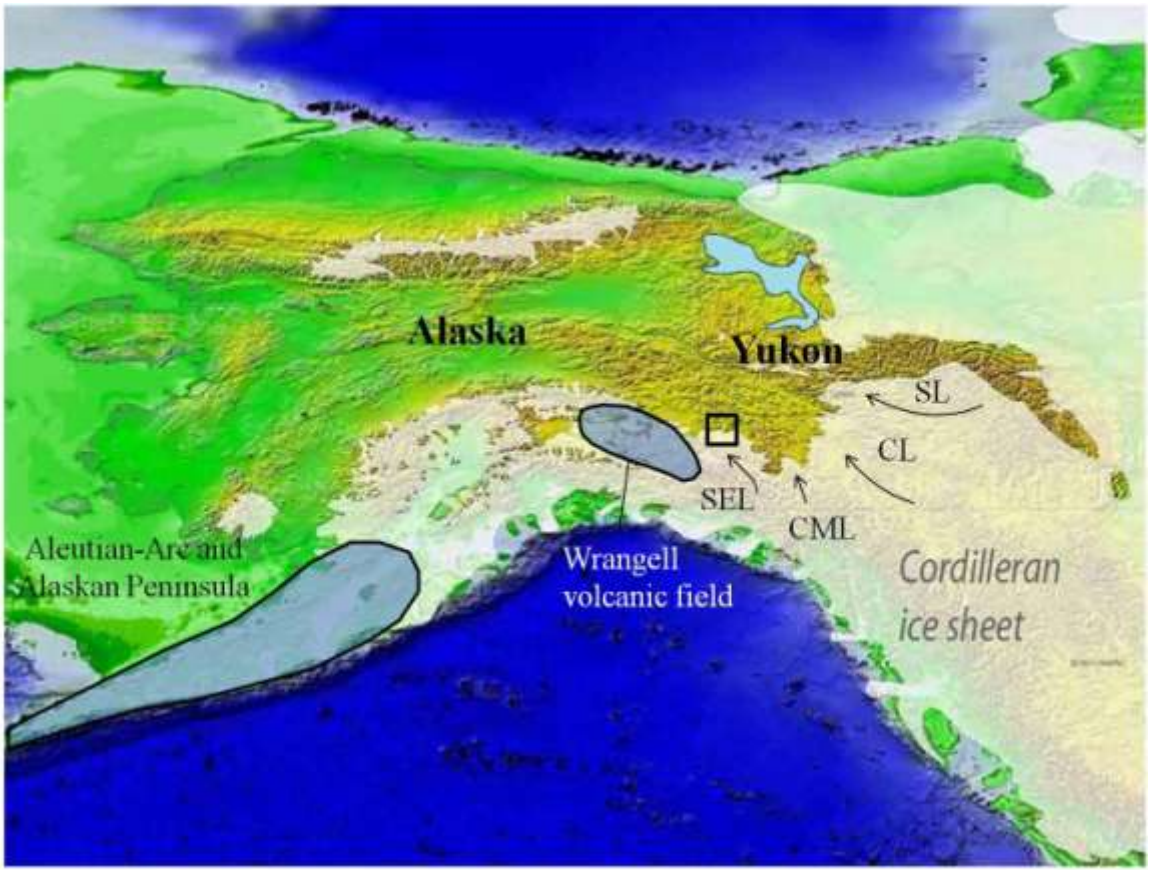

Figure 2.1. Eastern Beringia with sea level at 120 metres below sea level. MIS 2 ice extents are shown in white, including names of ice lobes of the northern Cordilleran Ice Sheet: St. Elias lobe (SEL), Coast Mountain lobe (CML), Cassiar lobe (CL) and Selwyn lobe (SL). Approximate locations of the sources for Type I (Aleutian-Arc and Alaskan Peninsula) and Type II (Wrangell volcanic field) tephras are outlined in blue. The study area is denoted by the black box. Glacial limits from Ehlers and Gibbard (2003).

The glaciated eastern fringe of Beringia, beyond the limit of the last Cordilleran Ice Sheet, preserves a record of earlier glaciations and includes rare, interbedded non-glacial deposits (Froese et al., 2000; Ward et al., 2008). These deposits, including distal tephra beds, can be used to unravel the complex, poorly understood chronologies of earlier glaciations in the Middle to Late Pleistocene (e.g. Westgate et al., 2001; Froese et al., 2003). In addition, the tephra beds offer the opportunity to link glacial extents and non-glacial intervals to longer and more continuous records from the non-glaciated regions of Beringia (e.g. Jensen et al., 2008).

In this paper, we present a record of glacial and non-glacial deposits at the maximum extent of the Cordilleran Ice Sheet in southwest Yukon. The purpose of this study is to date and compare the maximum and penultimate extents of the St. Elias lobe of the Cordilleran Ice Sheet to other areas in eastern Beringia, and to reconstruct a record of paleoenvironmental change during the Middle to Late Pleistocene.

2.3. Setting

The northern Cordilleran Ice Sheet was composed of multiple, quasi-independent ice lobes situated in the montane regions of northwest North America (Fig. 2.1; Jackson et al., 1991). The response of these localized, precipitation-limited lobes to climate change was complex and periodically out of phase with global ice volumes (Ward et al., 2007). This resulted in multiple glacial advances of differing age beyond the less extensive, MIS 2 (McConnell) glaciation. In central Yukon, the penultimate glacial limit deposited by the Selwyn lobe is MIS 6 in age (Ward et al., 2008; Demuro et al., 2012), and the most extensive limit is a composite of older, late Pliocene to Middle Pleistocene glaciations (Froese et al., 2000; Barendregt et al., 2010). No MIS 4 drift has been identified in central Yukon. In contrast, the penultimate limit at the maximum extent of the Coast Mountain lobe in southwest Yukon is MIS 4 in age (Ward et al., 2007). Understanding this difference requires higher resolution studies of glacial limits to understand how climate forcing mechanisms affected the timing and mode of local and regional glaciations through the Pleistocene (Ward et al., 2007, 2008).

This interdisciplinary study focuses on 18 gully-cut exposures in a ~60 m high terrace extending for 5 km along a north-south section of the White River in southwest Yukon, 100 km north of the eastern limit of the St. Elias Mountains (Fig. 2.2). It is less than 15 km north of the MIS 2 glacial limit, but within the limit of two, more extensive glaciations (Bond et al., 2008). These two, pre-MIS 2 glaciations were initially mapped as one limit by Rampton (1971), and correlated to either early Wisconsinan (MIS 4) or pre-Wisconsinan glaciations (Rampton, 1971; Denton, 1974). Although subsequent air photo mapping by Duk-Rodkin (1999) interpreted another, more extensive pre-Reid glacial limit, recent field work suggests that no such pre-Reid deposits are present (Bond et al., 2008).

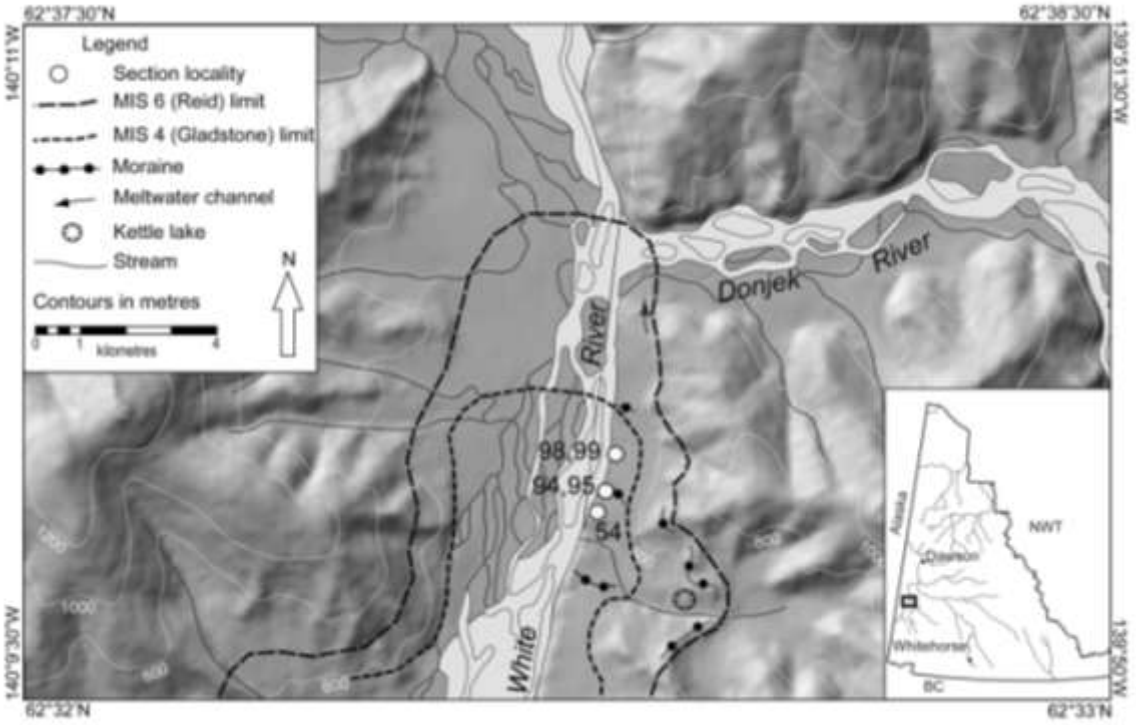

Figure 2.2. Study area along the White River, near the confluence with the Donjek River. Two glacial limits extend beyond the MIS 2 extent <15 km to the south.

2.4. Methods

Eighteen sites were examined along the White River. Of these sites, the five most significant are discussed in detail below (WR54, 94, 95, 98 and 99[1]). Sedimentological descriptions as well as macrofossil and pollen samples collected at each site were used to characterize the depositional environments and paleoecology of the organic units. Radiocarbon and tephra samples were collected for dating and correlating the deposits.

Eleven tephra beds were sampled at the study sites, deriving mostly from either the eastern Aleutian-Arc (Type I, following the classification of Preece et al., 1992, 1999) or the Wrangell Volcanic field and northern-most Alaska Peninsula volcanoes (Type II;

[1] The published manuscript used the following equivalent site names: site A = WR54; site B = WR94, site C = WR95; site D = WR98; site E = WR99.

Fig. 2.1). Beds that do not fit into this classification are listed as “other” following earlier studies (Preece et al., 1992, 1999; Westgate et al., 2008). Type I tephras are creamy or grey with bubble wall glass shards, <20% phenocrysts and have higher amounts of FeO and TiO_2 at a given SiO_2 weight percent (wt.%). Type II tephras have a more salt and pepper appearance, due to the greater abundance of phenocrysts, and contain higher amounts of Al_2O_3 and CaO at a given SiO_2 wt.%. Further correlation was supported by paleoenvironmental and stratigraphic data.

Tephra samples were sieved and glass from the 74 to 149 μm grain sizes was separated from the heavy mineral fraction using tetrabromoethane at a density of 2.4 g/mL. Major element geochemistry was determined on glass shards, analyzed by wavelength dispersive spectroscopy using a JEOL 8900 microprobe at the University of Alberta. The microprobe was operated with a defocused 10 μm beam at 15 keV accelerating voltage and 6 ηA beam current to minimize Na and K migration. Two samples of known composition, a rhyolitic obsidian (ID3506) and secondarily hydrated Old Crow tephra (Kuhn et al., 2011; Preece et al., 2011a), were analyzed with all tephra samples. The results were queried against the University of Alberta database using a similarity coefficient search (c.f. Hunt and Hill, 1993), and potential correlations were plotted on bivariate plots and re-analyzed together under the same microprobe conditions at the same time to confirm correlations (c.f. Jensen et al., 2008; Westgate et al., 2008).

Pollen and plant and insect macrofossil analyses were completed on splits from the same samples. Combining pollen, plant and insect macrofossil analyses provides a proxy for both regional and local environmental conditions. Pollen samples were prepared using standard techniques as well as separation with heavy liquids (s.g. 2.0; Faegri and Iversen, 1989). Wherever possible, samples were counted until 300 terrestrial tree, shrub, or herb grains were counted.

Plant and arthropod macrofossils were isolated from the sieved residue (0.425 mm mesh opening) in a manner similar to Birks (2001). Identification of vascular plant macrofossils and insect fossils are based primarily from comparison with modern reference specimens housed at the Geological Survey of Canada, Ottawa, and with

reference to illustrations, descriptions and checklists in several publications (e.g. Martin and Barkley, 1961; Bousquet, 1991; Danks and Downes, 1997; Cody, 2000). Only fragile, well preserved macrofossils were submitted to the Keck Carbon Cycle AMS Facility and Beta Analytic Inc. for Accelerator Mass Spectrometry (AMS) radiocarbon dating to limit the likelihood of reworking from older deposits (c.f. Kennedy et al., 2010).

2.5. Results

2.5.1. Stratigraphy

The stratigraphy of the examined sites along the White River are separated into 16 units and correlated between sites based on sedimentology, paleoenvironmental data and chronology (Figs. 2.3 and 2.4). Unit 1 is a consolidated, silty-sand diamict with ~25% striated, rounded-to-subangular clasts composed of a wide range of lithologies. This diamicton was exposed for 5 m in height, but likely extends at least 10 m lower, forming the basal unit at most of the sections studied. This unit is interpreted as a till, based on its extent, striated clasts, and clast fabric measurements that indicate ice flow to the north (Fig. 2.3b). Sporadic sand and gravel beds observed below Unit 1 suggest a fluvial environment preceded glaciation.

Above this till, Unit 2 is 1-2 m of moderate to well sorted, dominantly matrix-supported, cemented and oxidized pebble to cobble gravel with well rounded-to-subangular clasts. Its lower contact with Unit 1 is sharp. The gravel was observed at multiple exposures, but is significantly more weathered at WR99 than at the other sites. This weathering is gradational, decreasing in intensity downwards, with increased oxidation, disintegrated and frost shattered clasts, and ventifacts in the top metre. The presence of pedogenically precipitated, calcium carbonate rinds on the bottom of the clasts, some of which were rotated by cryoturbation, and silt and clay caps on some of the clasts, suggests that translocation occurred subsequent to deposition. There is also a small, 20 cm long intrusion of loess into the gravel that suggests an ice wedge pseudomorph. The degree of pedogenic development is similar to the Diversion Creek paleosol, a MIS 5-aged soil observed on MIS 6 glacial deposits in central Yukon (Smith et al., 1986; Tarnocai and Smith, 1989). Unit 2 is interpreted as outwash associated with

the retreat of ice that deposited the underlying till. The weathering gradient and the presence of ventifacts, calcium carbonate beards and fine-grained caps indicate that Unit 2 experienced a prolonged period of pedogenesis at WR99 prior to burial.

Unit 3 is composed of ~15 m of well sorted, bedded and laminated silt and sand with ripples. It has a sharp lower contact with Unit 2 at WR94 and 95. It contains concentrations of bivalves and gastropods, but few other organics. Pollen samples collected in this unit contained too few pollen grains for analysis. This unit is interbedded with multiple discontinuous, fining-up diamict beds and lenses, most with loaded lower contacts. Unit 3 is interpreted as glaciolacustrine sedimentation with frequent mass wasting events into the lake.

Unit 4 is 4 m thick, massive silt to fine-grained sand. Several <1 m thick diamict beds and lenses indicate that this unit was mixed with the surrounding materials. UA 1923, identified below as Old Crow tephra, is folded and faulted throughout the unit, suggesting rapid sedimentation, followed by intense deformation (Fig. 2.5e). Unit 4 is interpreted as loess that was deposited following drainage of the lake that deposited Unit 3. It is heavily cryoturbated and possibly deformed by the growth of ice wedges or potential loading from subsequent glaciation.

Unit 5 is a discontinuous, silty-sand diamict with 35-40% well rounded to angular clasts. It is consolidated and undulates by >2 m. Unit 5 is interpreted as colluvium deposited by gully fill processes similar to those that are currently active in the study area.

Unit 6 is composed of 2 m of bedded and laminated wood-rich peat exposed at WR54. It has an unconformable lower contact. On the west (downslope) side of WR54, Unit 6 is massive and includes a 50 cm diameter, beaver-chewed log. Adjacent to the log, the unit comprises bedded and laminated organic-rich silt and sand. Unit 6 pinches out to the west, towards the modern river, suggesting that it was deposited in an uneven, probably gullied, surface.

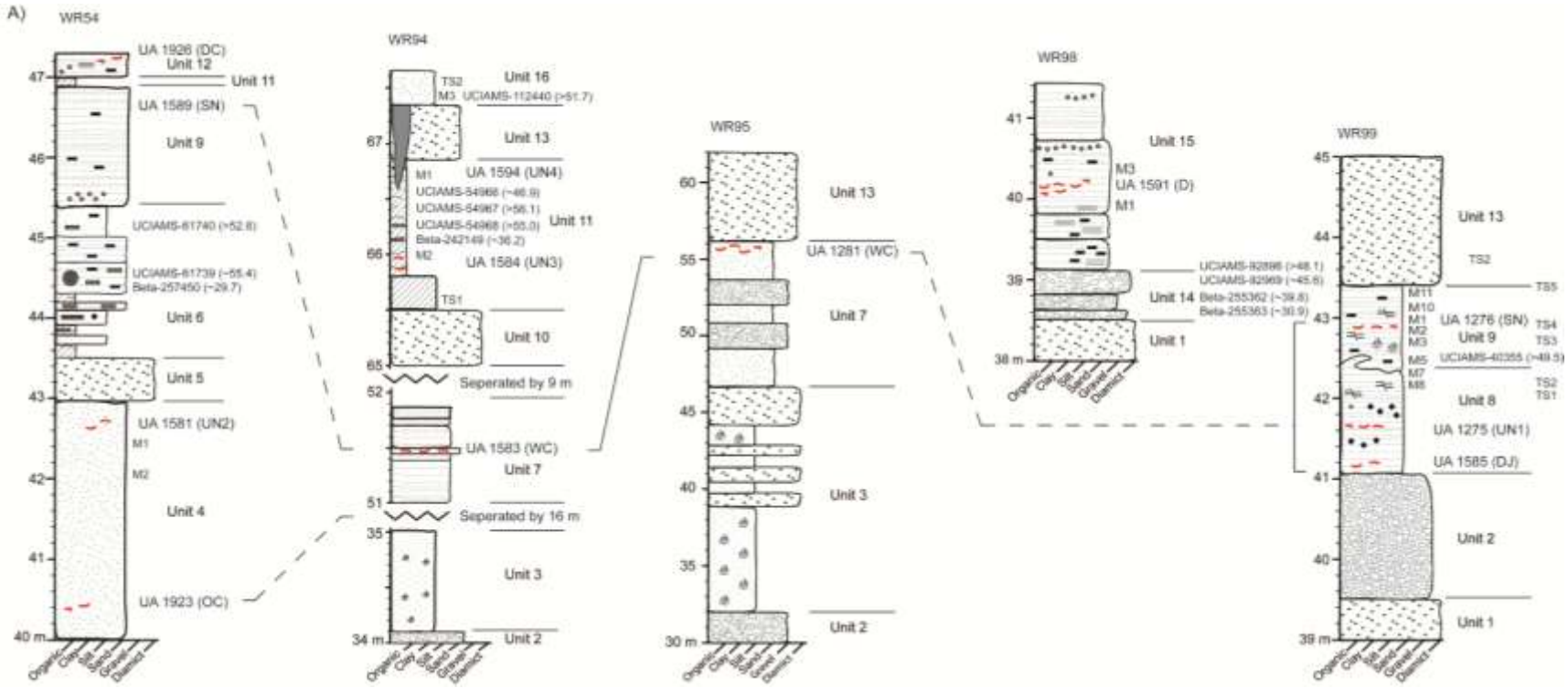
A)
WR54
UA 1926 (DC)
Unit 12
Unit 11
UA 1589 (SN)
Unit 9
UCIAMS-61740 (>52.8)
UCIAMS-61739 (~55.4)
Beta-257450 (~29.7)
Unit 6
Unit 5
UA 1581 (UN2)
M1
M2
Unit 4
UA 1923 (OC)
47
46
45
44
43
42
41
40 m
WR94
TS2
M3 UCIAMS-112440 (>51.7)
Unit 16
Unit 13
M1
UA 1594 (UN4)
UCIAMS-54966 (~46.9)
UCIAMS-54967 (>56.1)
UCIAMS-54968 (>55.0)
Unit 11
Beta-242149 (~36.2)
M2
UA 1584 (UN3)
TS1
Unit 10
Seperated by 9 m
UA 1583 (WC)
Unit 7
Seperated by 16 m
Unit 3
Unit 2
67
66
65
52
51
35
34 m
WR85
Unit 13
UA 1281 (WC)
Unit 7
Unit 3
Unit 2
60
55
50
45
40
35
30 m
WR98
Unit 15
M3
UA 1591 (D)
M1
UCIAMS-92896 (>48.1)
UCIAMS-92969 (~45.6)
Unit 14
Beta-255362 (~39.8)
Beta-255363 (~39.9)
Unit 1
41
40
39
38 m
WR99
Unit 13
TS2
TS5
M11
M10
M1
M2
M3
UA 1276 (SN)
TS4
Unit 9
TS3
M5
UCIAMS-40355 (>49.5)
M7
M8
TS2
TS1
Unit 8
UA 1275 (UN1)
UA 1585 (DJ)
Unit 2
Unit 1
45
44
43
42
41
40
39 m
Organic
Clay
Silt
Sand
Gravel
Diamict

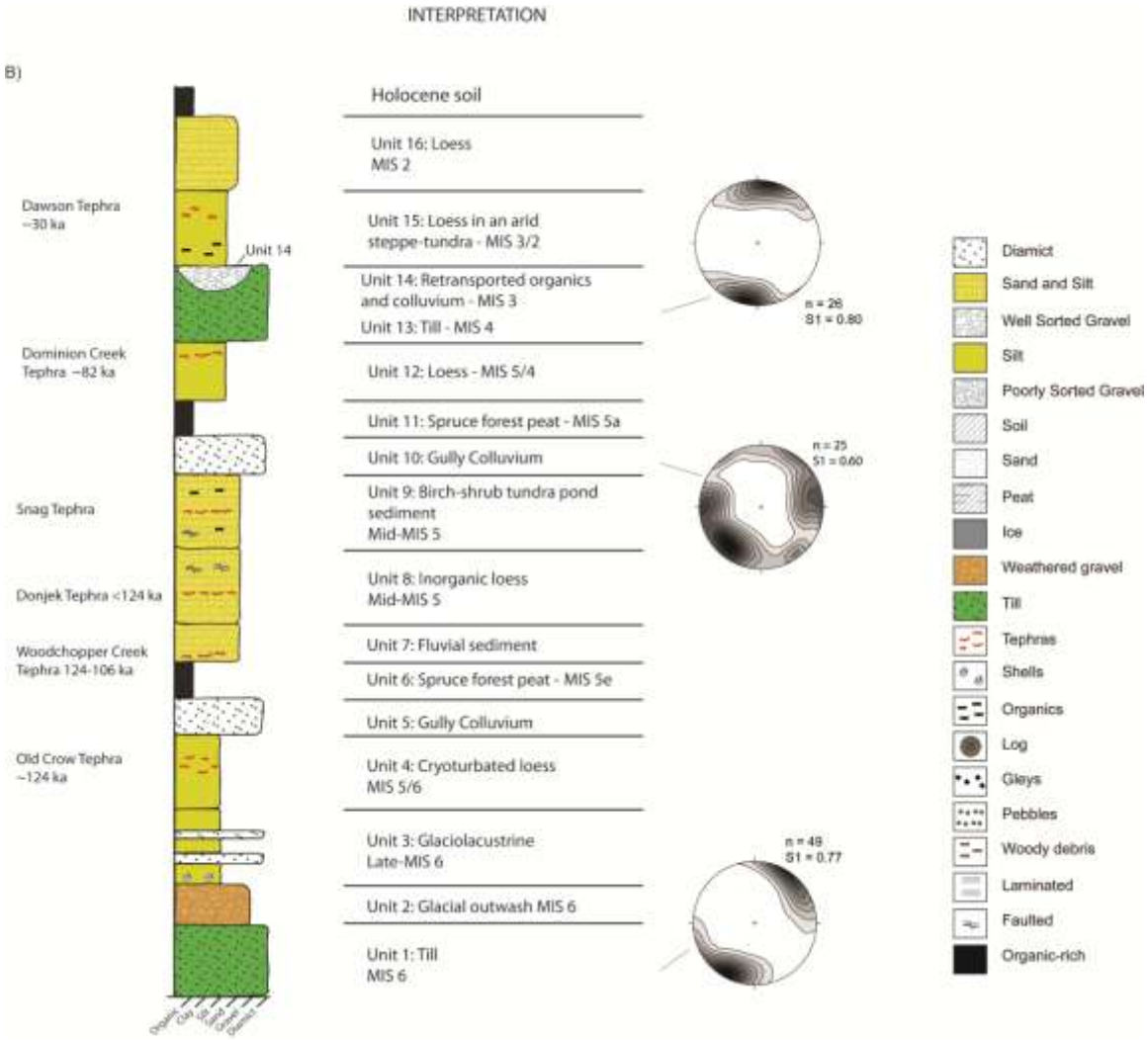

Figure 2.3. **A) Stratigraphy of White River sites discussed in detail. Heights are above river level. Scales vary between sites. Solid lines indicate the same tephra. Dashed lines indicate tephras of similar age. Ages for radiocarbon ages are in brackets (in ^{14}C ka BP). Tephra abbreviations are shown on Table 2.4; B) Compilation of the interpreted stratigraphy of all sites. Till and colluvium A-axis clast fabrics are equal area, lower hemisphere plots with contour intervals of 10. These plots include the number of clasts measured (n) and the calculated primary eigenvector (S1).**

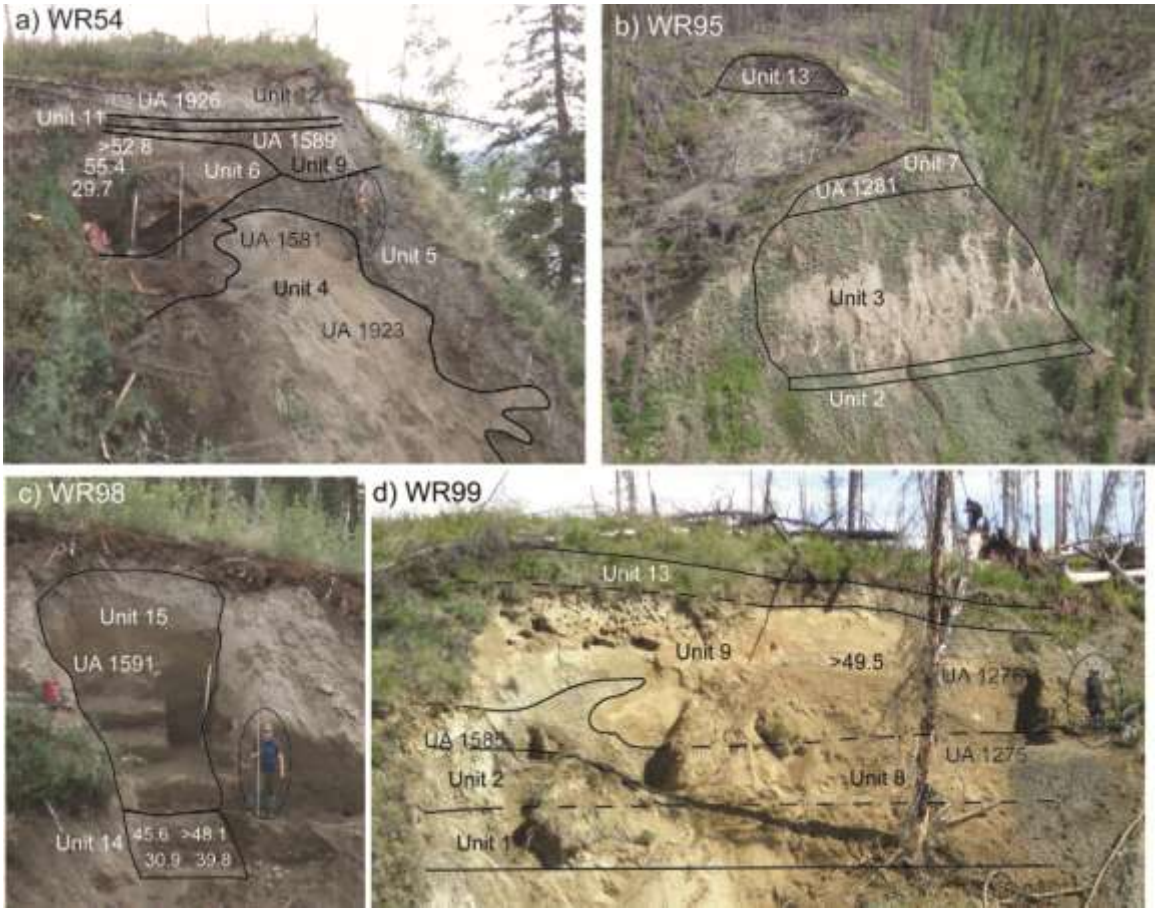

Figure 2.4. Site pictures with units and tephra sample locations for WR54, WR95, WR98 and WR99. Units are described in text and shown on figure 2.3. All radiocarbon ages are rounded to the nearest 100 years and are in ^{14}C ka BP. People are circled for scale, except in (b), where Unit 2 is 2 m thick.

Unit 7 consists of ~1 m of weakly-stratified, planar-bedded and laminated fine- to medium-grained sand, silt and clay. The sedimentology of this unit is enigmatic, but the sand beds contain burrows and other evidence of subaerial exposure at some sites. A coarse, laminated, pumiceous Type II tephra (UA 1281, 1583), identified below as Woodchopper Creek tephra, is exposed for 10-15 cm in a sandy bed near the top of this unit at WR94 and 95 (Fig. 2.5c), as well as in three other sites not discussed in detail. This tephra infills cracks and burrows and is composed of multiple fining up beds.

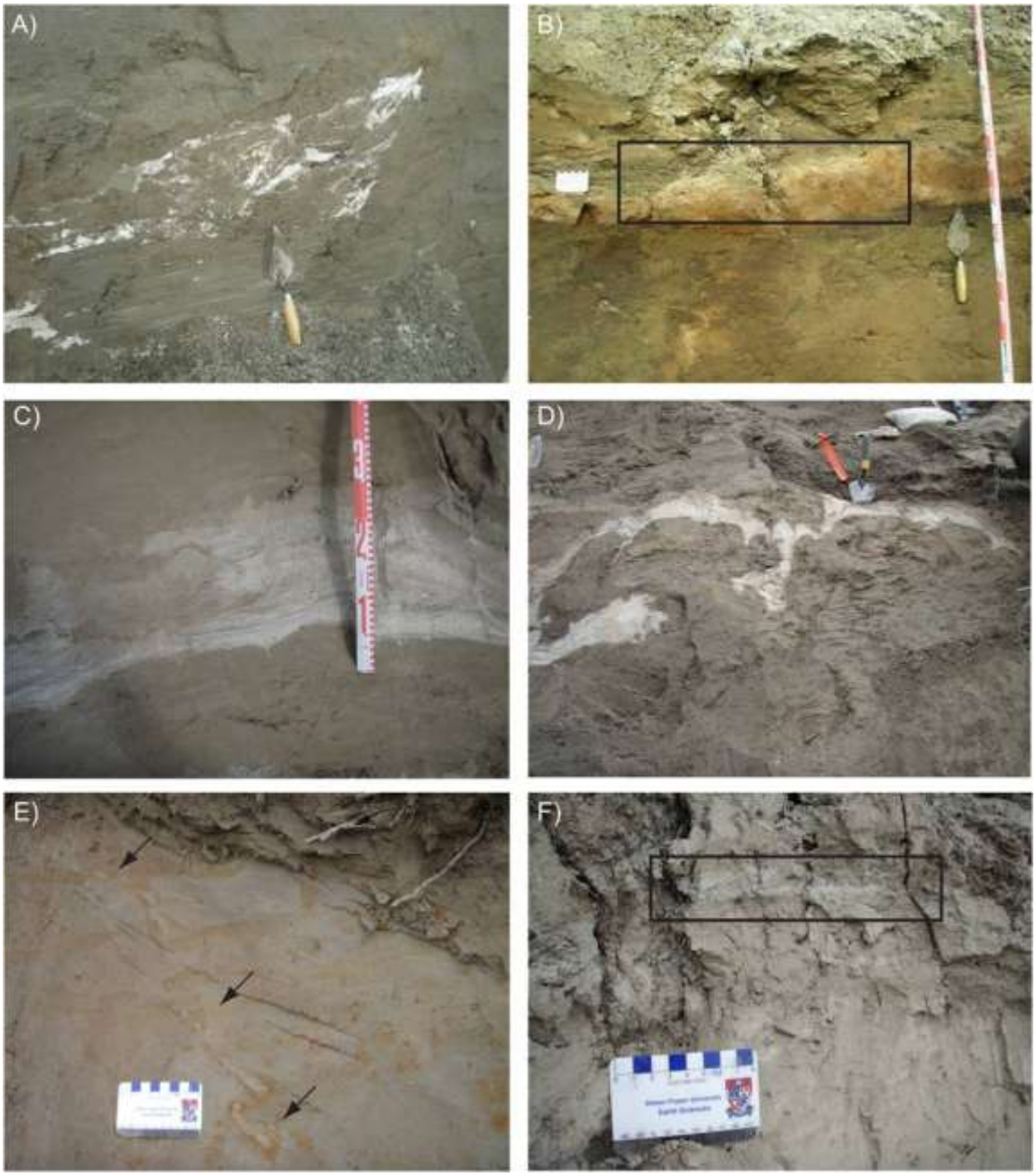

Figure 2.5. Tephras collected at White River. The tephras were exposed as both thin, discontinuous lenses indicative of reworking, and thick beds with primary sedimentary structures. A) Dawson tephra; B) Snag tephra; C) Woodchopper Creek tephra; D) Donjek tephra; E) Old Crow tephra (arrows), faulted to the right of the scale card and thins above and to the left; F) Dominion Creek tephra. Trowel is ~25 cm.

Both units 8 and 9 consist of silty fine sand. Unit 8 is 130 cm thick, weakly-stratified, light grey, has 5-10% granules and pebbles, and is unweathered, gleyed and

mostly inorganic. In contrast, Unit 9 is 1.5 to 4 m thick, bedded, laminated and contains dark brown to black organic beds, shells and iron-stained lenses of medium-grained sand. A tephra bed (UA 1585), named below as Donjek tephra, was observed in Unit 8 at WR99 and at other sites not discussed in detail (Fig. 2.5d). A Type I tephra (UA 1276, 1589), named below as Snag tephra, was sampled in Unit 9 at WR54 and WR99 (Fig. 2.5b). Unit 8 is interpreted as loess that was reworked by slope processes and cryoturbation. Unit 9 was deposited in an organic-rich pond environment. Both of these units are faulted. On the west side of WR99, 1.5 m of Unit 8 and the underlying Unit 2 is thrust one metre above Unit 9 (Fig. 2.4d). This faulting was probably caused by glaciotectonism.

Unit 10 is a silty diamict with 25-35% subrounded-to-angular clasts that is similar sedimentologically to Unit 5, and the diamict beds in Unit 3. Although it is >2 m thick and consolidated, it is not laterally extensive and has a weak clast fabric (Fig. 2.3b). It is therefore interpreted as colluvium.

Unit 11 is exposed at WR54 and WR94. At WR94 it is a 1.5 to 2 m thick, fibric-to-humic, wood-rich peat. It is well preserved at this location, with needles, cones, logs, seeds, moss, rodent fecal pellets and insect macrofossils. The top 20 cm of the peat is platy and hard with the plates oriented sub-vertically down-slope. At WR54, this upper platy peat is all that is exposed. The bottom of Unit 11 at WR94 comprises a 25 cm thick, very dark brown (7.5 YR 2.5/3) turbic cryosol.

Unit 12 is 50-80 cm of light to dark grey silt with rare pebbles and granules. It is weathered near its upper contact, with this weathering decreasing rapidly with depth. Approximately 20 cm above its lower contact at WR54 is a 2 cm thick, Type II tephra (UA 1926), identified below as Dominion Creek tephra (Fig. 2.5f). Unit 12 is interpreted as loess.

Unit 13 is a 1.5 m thick, continuous and consolidated sandy-silt diamict. It has well rounded-to-subangular clasts (25-45%) of various lithologies and a sharp lower contact. This unit is interpreted as a till based on its regional extent, the presence of keeled, striated and fractured clasts, and a strong clast fabric suggesting ice flow to the north (Fig. 2.3b).

Units 14 and 15 are only exposed at WR98. Unit 14 is composed of interbedded diamict, and matrix- and clast-supported gravel. Both gravel subunits contain a wide range in clast sizes, including boulders. Bones of steppe bison (*Bison c.f. priscus*), horse (*Equus* sp.), mammoth (*Mammuthus primigenius*), sheep (*c.f. Ovis dalli*) and meadow vole (*Microtus pennsylvanicus*) were recovered from the upper contact of this unit with Unit 15. Unit 15 comprises 2.5 m of bedded and laminated oxidized silty-sand with organics and woody debris. A single, 10-30 cm thick, reworked tephra bed (UA 1591) is present in this unit (Fig. 2.5a). It is identified below as Dawson tephra. Sample UA 1591 was cryoturbated and possibly reworked, but its thickness and infilling of burrows indicates that it is a primary tephra bed. The organic content in Unit 15 decreases upwards. Units 14 and 15 are interpreted as colluvium and loess infilling a gully, respectively. The bottom of Unit 15 at WR94 contains a 1.5 m wide ice wedge composed of vertically foliated ice that penetrated >2 m in Units 10, 11 and 13 below. Unit 16 is 50-100 cm of well-sorted, cryoturbated, massive sand with frost shattered pebbles, arctic ground squirrel (*Urocitellus parryii*) bones and fecal pellets.

2.5.2. Paleoecology

Six units were sampled for paleoenvironmental reconstruction: the loess in Unit 4, the peat beds in Units 6 and 11, the pond sediments in Unit 9, the colluvium in Unit 14 and the loess in Unit 15. Insect and plant macrofossils are listed in Tables 2.1 and 2.2, respectively. Pollen results are shown in Fig. 2.6 and mammal bones are reported in Table 2.3.

Pollen data from two samples in Unit 4 at WR54 are dominated by herbs and forbs, with few shrub and tree grains. This indicates that a cold, tundra environment existed between deglaciation and deposition of the organic-rich Unit 6 above.

Table 2.1. Insect and animal macrofossils. Sample locations shown on Figure 2.3a.

Site	99	99	99	99	99	99	99	94	94	98	98
Macrofossil sample	M8	M5	M3	M2	M1	M10	M11	M2	M1	M1	M3
PORIFERA											
Haplosclerina											
Spongillidae											
Spongilla type		26	375	500		>150*	50		5		
BRYOZOA											
Cristatella mucedo L.									7		
Plumatella sp.		7	46	60		14	12		>100*		
Fredericella sp.		2	1	50							
ARTHROPODA											
Insecta				1							3
Orthoptera											
Acrididae	11	1	1								
Hemiptera	2		1	1							
Corixidae		1		1	1						
Cicadellidae	4	1	1							2	33
Psyllidae									4		
Coleoptera	10			2	2					1	14
Carabidae	1		1	1	1					2	6
Dyschiriodes sp.				1	1						
Bembidion (*Eurytrachelus*) sp.	1										
Bembidion (Eurytrachelus) nitidum (Kirby)				1							
Bembidion (Peryphus) sp.											1

Site	99	99	99	99	99	99	99	94	94	98	98
Macrofossil sample	M8	M5	M3	M2	M1	M10	M11	M2	M1	M1	M3
Bembidion (Notaphus) sp.					2						
Bembidon sp.	4		1	1						1	1
Pterostichus sp.	1										
Amara littoralis Mannerheim											1
Amara sp.											1
Harpalus egregius Casey											1
Harpalus alaskensis Lth.											1
Harpalus sp.	2										5
Apristus sp.	2										
Syntomus americanus Dejean	1										
Cymindis unicolor Kby.											1
Cymindis sp.											1
Haliplidae			1		1						
Haliplus sp.		2									
Dytiscidae			1		1						
Hydroporus sp.					1				1		
Rhantus sp.					1						
Colymbetes sp.				1	1		1				
Graphoderus sp.		1					1				
Gyrinidae											
Gyrinus sp.					2						
Hydrophilidae					1				1		
Helophorus tuberculatus Gyll.									1		

Site	99	99	99	99	99	99	99	94	94	98	98
Macrofossil sample	M8	M5	M3	M2	M1	M10	M11	M2	M1	M1	M3
Helophorus sp.				1							
Hydrobius sp.					1						
Cymbiodyta sp.									1		
Cercyon sp.					6						
Hydraenidae											
Ochthebius sp.	1		1	1	1				2		
Staphylinidae	1				1						
Bledius sp.	5	1	3		1						
Omaliinae		1									
Olophrum consimile Gyll.									5		
Stenus sp.					1				1	1	
Lathrobium type	1								1		
Quedius sp.	2										
Tachinus sp.	1								1		
Tachyporous sp.	1			1							
Aleocharinae				1							
Gabrius brevipennis (Horn)				3							
Leiodidae											
Leiodes sp.	3										
Anisotoma sp.	3	1	1								
Catops sp.	2										2
Ptiliidae	2		1							1	

Site	99	99	99	99	99	99	99	94	94	98	98
Macrofossil sample	M8	M5	M3	M2	M1	M10	M11	M2	M1	M1	M3
Clambidae											
Calyptomerus sp.				1							
Histeridae											
Psiloscelis subopaca (LeConte)	1										
Scarabaeidae											
Aphodius corruptor W.J. Brown											2
Aphodius sp.	3			2	1	1				1	
Helodidae											
Cyphon sp.				1					11		
Byrrhidae											
Simplocaria sp.	1		2								1
Morychus sp.				1						1	3
Curimopsis sp.											2
Elateridae	2		1			1			1		
Denticollis varians (Germar)	1										
Anthicidae	2										
Coccinellidae											
Nephus sp.			1								
Lathridiidae											
Lathridium sp.									1		
Corticaria sp.									1		
Cerambicidae											
Acmaeops? sp.									1		

Site	99	99	99	99	99	99	99	94	94	98	98
Macrofossil sample	M8	M5	M3	M2	M1	M10	M11	M2	M1	M1	M3
Chrysomelidae			1	1							
Donacia sp.		1									
Calligrapha californica Linnel				1							
Chrysolina sp.											1
Ophraella sp.	1										
Phyllotreta zimmermanni (Crotch)	1										
Altica ambiens LeConte				1							
Altica sp.	1										
Chaetocnema protensa LeConte	1										
Curculionidae						1	1				
Connatichela artemisiae Anderson										4	105
Lepidophorus lineaticollis Kirby	16	1	9	5	7		1			29	208
Vitavitus thulius Kiss.										1	1
Stephanocleonus sp.											1
Hylobius pinicola (Couper)			1								
Scolytidae									1		
Scolytus piceae (Swaine)									1		
Phloeotribus? sp.									1		
Polygraphus sp.									1		
Pityophthorus spp.									1		
Trichoptera	1	3	10		10	1			1		
Ledpidoptera									3	3	1
Diptera	26		5	3	5		2	1	19	5	73

Site	99	99	99	99	99	99	99	94	94	98	98
Macrofossil sample	M8	M5	M3	M2	M1	M10	M11	M2	M1	M1	M3
Tipulidae											
Tipula sp.		1	2	1						2	
Chironomidae	1	133	34	78	211	19	9		>100*		
Bibionidae	1										
Hymenoptera	1	1									1
Ichneumonidae	3		3	2	3				3	20	48
Braconidae											
Cheloninae										1	3
Formicidae											
Camponotus sp.									1		
Formica sp.	3	1	2		2				2		
Myrmica sp.			1	3					4		
Crustacea											
Cladocera											
Daphnia & Simocephalus sp.		>275*	59	170	>414*	37	989		>100*	1	1
Ostracoda		>857*	100	>402*	>914*	>421*	433				
Arachnida											
Oribatei	16								>100*		
Hydrozetidae											
Hydrozetes type		2	25	17	6	>317*	4		15		
Araneae	2								4	1	
Erigonidae											
Erigone sp.									1	1	

Site	99	99	99	99	99	99	99	94	94	98	98
Macrofossil sample	M8	M5	M3	M2	M1	M10	M11	M2	M1	M1	M3
MOLLUSCA											
Gastropoda											
Horizontal (discoidal) type		357		95	276	1	15				
Vertical (conical) type	5	677		33	352		17			1	
Pelecypoda		7					3				

* discontinued enumeration due to abundance

Table 2.2. Plant macrofossils. Samples locations shown on Figure 2.3a.

Site	99	99	99	99	99	99	99	94	94	98	98
Macrofossil sample	M8	M5	M3	M2	M1	M10	M11	M2	M1	M1	M3
Fungal remains											
fungal sclerotia	244		183	15	2	2	94	>50*		469	43
Algal remains											
Characeae											
Chara sp. (oogonia)		>3059*	112	43	>103*	345	306				
Non-vascular plants											
Bryophytes	1%	2%	25%	50%	20%				30%		
Sphagnum sp.								10%	2%		
Vascular plants											
Equisetaceae											
Equisetum sp.									15		
Pinaceae											
Picea glauca (Moench) Voss									>1000*		
Picea sp.								5		4	
Potamogetonaceae											
Potamogeton spp.											
Potamogeton sp.		4	35	6	92						
Stuckenia pectinata (L.) Borner		5	3		6	17	6				
Ruppia cirrhosa (Petagna) Grande				2	1	17	13				

Site	99	99	99	99	99	99	99	94	94	98	98
Macrofossil sample	M8	M5	M3	M2	M1	M10	M11	M2	M1	M1	M3
Scheuchzeriaceae											
Triglochin sp.			5				1				
Poaceae	15	6	55			9	5			355	749
Poa type									4		
Cyperaceae										1	
Carex lenticular type		2	11	29	4	2	7			2	1
Carex trigonous type			3	5	15		3		2		
Carex aquatilis Wahlenb.									10		
Carex *canescens* L.									370		
Eriophorum sp.									1		
Schoenoplectus tabernaemontani (C.C. Gmel.) Palla		42	211	122	132		10				
Araceae											
Calla palustris L.									2		
Juncaceae											
Juncus sp.			29								
Salicaceae											
Salix sp.		4		2			1				
Betulaceae	4		2		10						
Alnus incana (L.) Moench											
Betula sp.											
Betula nana/glandulosa type	60		4	15	6		8				
Betula shrub/small tree type	6	1	4	3	4		2		84		
Betula arboreal type									1		
Polygonaceae											
Persicaria lapathifolia type							1				
Persicaria amphibia (L.) Delarbre		1									
Persicaria vivipara (L.) Ronse Decr.		1									
Polygonum sp.					2						
Rumex sp.											
Rumex maritimus L.					22	3					

Site	99	99	99	99	99	99	99	94	94	98	98
Macrofossil sample	M8	M5	M3	M2	M1	M10	M11	M2	M1	M1	M3
Chenopodiaceae											
Chenopodium spp.		4	4	114	>120*	7	3				
Caryophyllaceae											2
Cerastium sp.										8	3
Ranunculaceae											
Ranunculus sp. 1											
Ranunculus sp. 2											
Ranunculus sceleratus type		3	2	25	>142*	18	16				
Ranunculus sp.					5					3	
Ranunculus cymbalaria Pursh		2									
Papaveraceae											
Papaver sp.										1	6
Brassicaceae	135									136	75
Rosaceae											
Potentilla sp.										4	1
Potentilla smooth type	33	1	19	11	20	4				26	24
Comarum palustre L.									11		
Amelanchier alnifolia sanguinea type											21
Potentilla anserina L.	38	2	28	56	408		1				
Onagraceae											
Epilobium sp.									1		
Haloragaceae											
Myriophyllum sibiricum Kom.		2	1		3		3				
Plantaginaceae											
Hippuris vulgaris L.		4	2	1	10						
Ericaceae											
Arctostaphylos uva-ursi (L.) Spreng.			1		13		7				
Vaccinium sp.									2		
Genus 1											
Genus 2											

Site	99	99	99	99	99	99	99	94	94	98	98
Macrofossil sample	M8	M5	M3	M2	M1	M10	M11	M2	M1	M1	M3
Primulaceae											
Androsace septentrionalis L.	1	8	13	10	4	1	1			1	
Polemoniaceae											
Phlox hoodii Richardson										38	118
Boraginaceae											
Amsinckia menziesii (Lehm.) Nels. & Macbr.			4								
Lappula sp.										9	14
Asteraceae										48	
Artemisia frigida Willd.					1					373	1267
Artemisia sp.										13	
Taraxacum sp.										3	18
Genus ?	1	2	6						2		
Genus 1										33	22
Genus 2										15	1
Unknown plant macrofossil taxa			5		1				2	9	10

* discontinued enumeration due to abundance

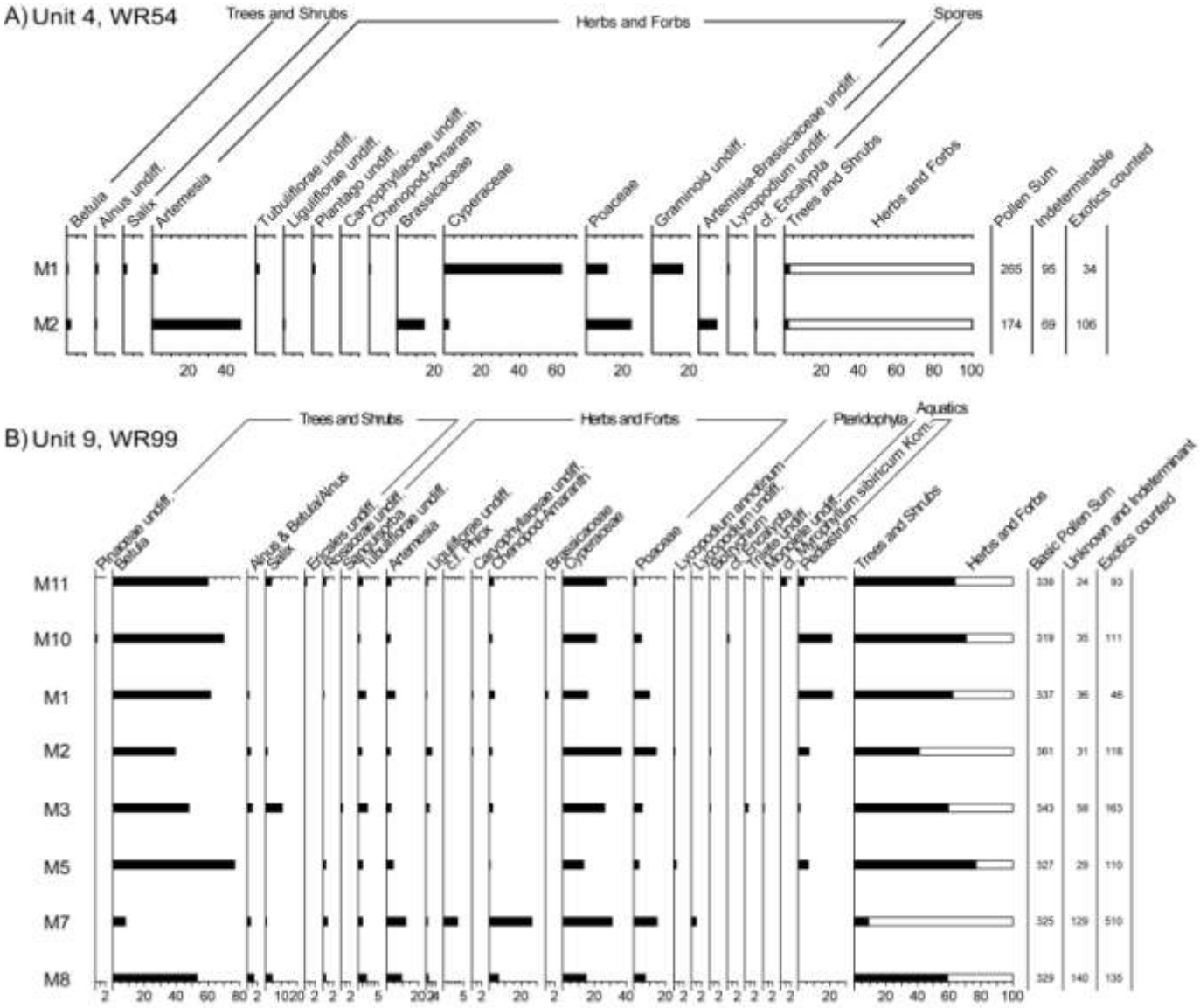
A) Unit 4, WR54
Trees and Shrubs
Herbs and Forbs
Spores
Betula
Alnus undiff.
Salix
Artemesia
Tubuliflorae undiff.
Liguliflorae undiff.
Plantago undiff.
Caryophyllaceae undiff.
Chenopod-Amaranth
Brassicaceae
Cyperaceae
Poaceae
Graminoid undiff.
Artemisia-Brassicaceae undiff.
Lycopodium undiff.
cf. Encalypta
Trees and Shrubs
Herbs and Forbs
Pollen Sum
Indeterminable
Exotics counted
M1
M2
265 95 34
174 69 106
20 40
20
20 20 40 60
20
20
20 40 60 80 100
B) Unit 9, WR99
Trees and Shrubs
Herbs and Forbs
Pteridophyta
Aquatics
Pinaceae undiff.
Betula
Alnus & Betula/Alnus
Salix
Ericales undiff.
Rosaceae undiff.
Salix/Myrica
Tubuliflorae undiff.
Artemesia
Liguliflorae undiff.
cf. Phlox
Caryophyllaceae undiff.
Chenopod-Amaranth
Brassicaceae
Cyperaceae
Poaceae
Lycopodium annotinum
Lycopodium undiff.
Bothrychium
cf. Encalypta
Triletes undiff.
Monolete undiff.
cf. Myriophyllum sibiricum Kom.
Podostemum
Trees and Shrubs
Herbs and Forbs
Basic Pollen Sum
Unknown and Indeterminant
Exotics counted
M11
M10
M1
M2
M3
M5
M7
M8
338 24 93
319 35 111
337 36 46
361 31 118
343 58 163
327 29 110
325 129 510
329 140 135
2 20 40 60 80
2 10 20
2 2 2 5 20
4 5
2 20
2 20 40
20
2 2 2 2 2 2 2
20
20 40 60 80 100

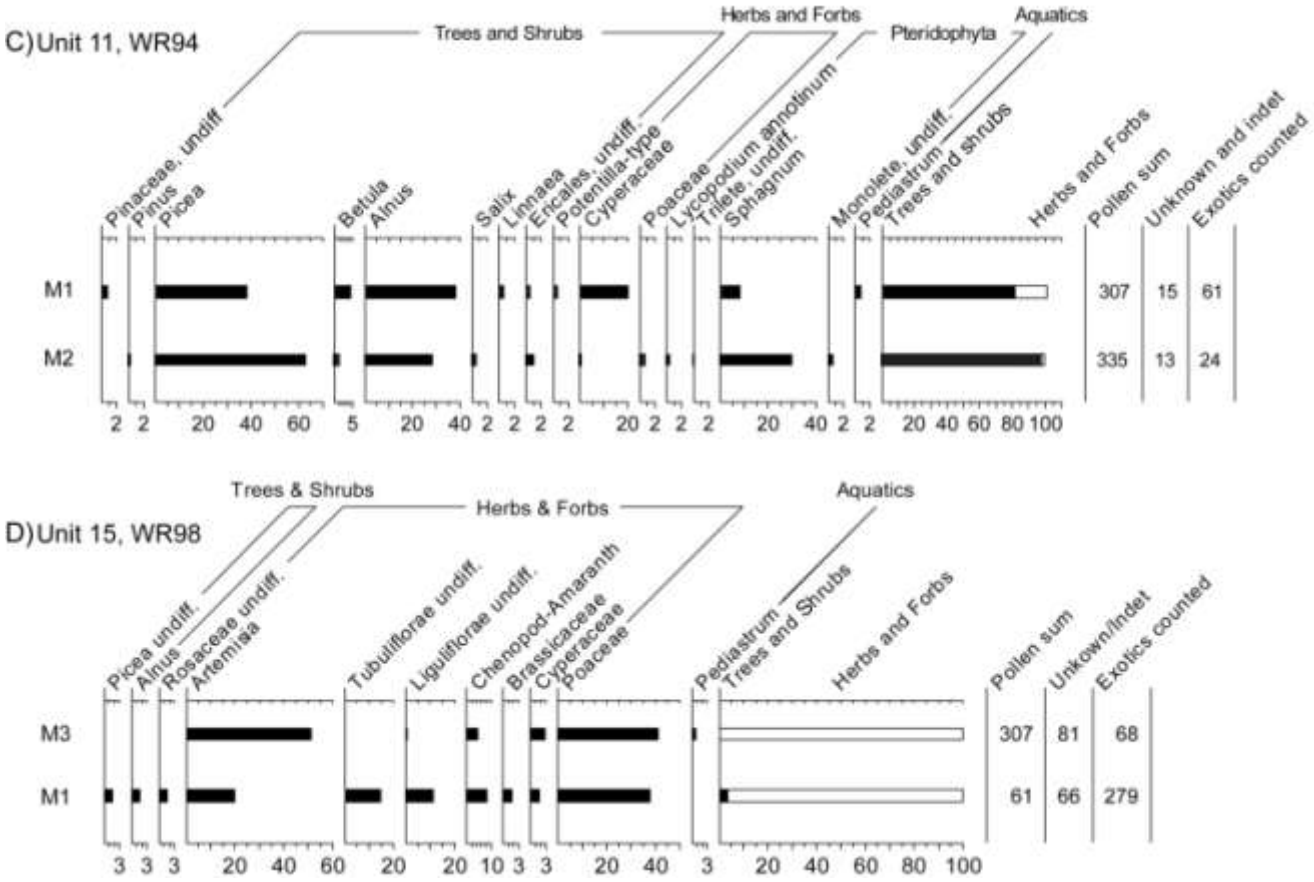

Figure 2.6. Pollen results from WR54, 99, 94 and 98. 6A) High amounts of sedges and grasses indicate a cold, tundra environment. 6B) The abundance of sedge and grass and the lack of conifer pollen suggest an aquatic setting in a birch-shrub tundra. M7 is more suggestive of a well-drained or disturbed environment. 6C) Abundant spruce and alder support a boreal forest setting. 6D) The abundance of *Artemisia* and other forbs, along with a near absence of tree and shrub pollen, indicates dry and cold conditions. Sample locations are shown in Figure 2.3a.

Table 2.3. Mammal fossils recovered from WR94, 98 and 99.

Taxon	Site	Unit	Common Name	Element	Yukon Government Species #
Urocitellus parryii	WR94	16	Arctic ground squirrel	Humerus	308.18
Microtus pennsylvanicus	WR98	14	Meadow vole	Mandibles and cranium	
Mammuthus primigenius	WR98	14	Mammoth	Tibia fragment	308.9
Mammuthus primigenius	WR98	14	Mammoth	Post-cranial	308.10
Equus sp.	WR98	14	Horse	Metatarsal	308.19
Equus sp.	WR98	14	Horse	Thoracic vertebra	354.12
Equus sp.	WR98	14	Horse	Thoracic vertebra	354.13
Bison c.f. *priscus*	WR98	14	Steppe bison	Cranium	400.1
Bison c.f. *priscus*	WR98	14	Steppe bison	Partial cranium	308.11
Bison c.f. *priscus*	WR98	14	Steppe bison	Mandibular molar	354.1
Rangifer tarandus	WR98	14	Caribou	Metatarsal fragment	354.7
c.f. Ovis dalli	WR98	14	Sheep	Naviculo-cuboid	354.15
Camelops hesternus	WR99	9	Western camel	Partial proximal phalanx	400.6

Nearly identical plant and insect macrofossil taxa were found in both Units 6 and 11. White spruce (*Picea glauca*) needles, twig terminals, cones and seed wings, bryophytes, bark beetles (*Polygraphus rufipennis* and *Pityophthorus* sp.), sedge (*Carex canescens* and *C. aquatilis*), and beaver-chewed wood collected from Unit 11 at WR94 suggest a wet environment with birch trees within a white spruce forest (Fig. 2.7). Abundant spruce was also found in the pollen samples, but there is no birch pollen. Although this may suggest birch was not regionally widespread, this may not be representative of the entire unit as only two pollen samples were analyzed. Despite the lack of pollen from obligate aquatic taxa, the abundance of *Sphagnum* spores does indicate hygric conditions. Similar macrofossils to those in Unit 11 were identified in Unit 6, including beaver-chewed wood, indicating a white spruce boreal forest was re-established before the subsequent glaciation represented by Unit 13. Spruce macrofossils were also recovered from the colluvium in Unit 14 in association with a

bison skull (Fig. 2.8a). These fossils indicate the presence of spruce, but not enough pollen or macrofossils were recovered to adequately characterize the environment.

Plant macrofossils, insect fossils and fossil pollen recovered from Unit 9 reveal a succession from a poorly-drained environment of wet tundra, to a pond filled with abundant aquatic plants. The plant cover at the base of Unit 9 (M8) is a mosaic of moist open meadow-grassland with dry areas. This mosaic supported herbs of Rosaceae, including cinquefoil (*Potentilla* sp.), common silverweed (*Potentilla anserina*), mustards (Brassicaceae) and grasses (Poaceae) with abundant dwarf birch shrubs (*Betula nana/glandulosa*). Phytophagous insects common to this environment include grasshoppers (Acrididae), leafhoppers (Cicadellidae) and members of leaf beetles (Chrysomelidae) of *Ophraella*, *Altica*, *Chaetocnema protensa* and *Phyllotreta zimmermanni*, the later being host-specific to Brassicaceae.

This poorly-drained environment changed into a calcareous pond (M5) filled with stoneworts (*Chara*) algae that are rapid colonizers of newly established water bodies (Wood and Imahori, 1965). Calciphile submergent plants (e.g. *Stuckenia pectinata*, sago pondweed and *Ruppia cirrhosa*, ditch grass) and other submergent aquatics eventually replaced the *Chara*-infilled pond. Shoreline plants included abundant bulrushes (*Schoenoplectus tabernaemontani*), celery-leaved buttercup (*Ranunculus sceleratus*) and common silverweed (*Potentilla anserina*). Fossil aquatic inhabitants were abundant in the pond, including aquatic beetles such as predaceous diving beetles (Dytiscidae), whirligig beetle (*Gyrinus* sp.), ostracodes and snails (Gastropoda). Overall, the absence of any conifer pollen and macrofossils typically found in MIS 5 interglacial boreal forest environmental reconstructions from Alaska/Yukon (e.g. Pewe et al., 1997; Muhs et al., 2001) indicates that this pond was in a shrub birch tundra ecosystem in a treeless environment, both regionally and locally during a cool interval in MIS 5. A partial proximal phalanx of a western camel (*Camelops hesternus*) bone was collected at the top of Unit 9, 50 cm below Unit 10 (Zazula et al., 2011).

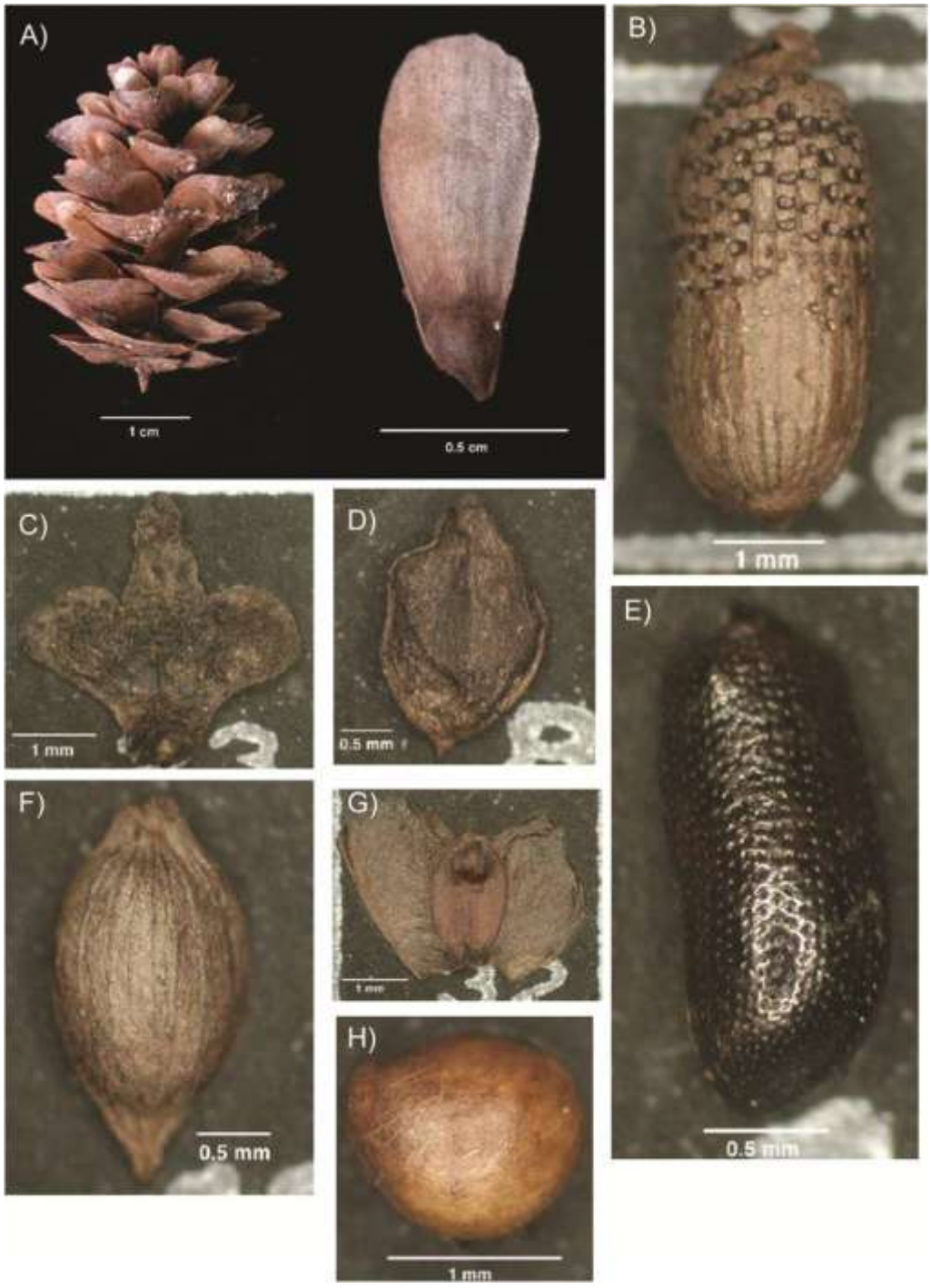

Figure 2.7. **Macrofossils collected from Unit 11 at WR94: A) White spruce (*Picea glauca*) cone and seed; B) Wild Calla (*Calla palustris*); C) Water birch (*Betula occidentalis*); D) Water sedge (*Carex aquatilis*); E) Bark beetle elytron (*Pityophthorus* sp.); F) Silvery sedge (*Carex canescens*); G) White birch (*Betula papyrifera*) nutlet; H) Marsh cinquefoil (*Potentilla palustris*). These macrofossils suggest a wet or boggy area in a boreal forest or marsh.**

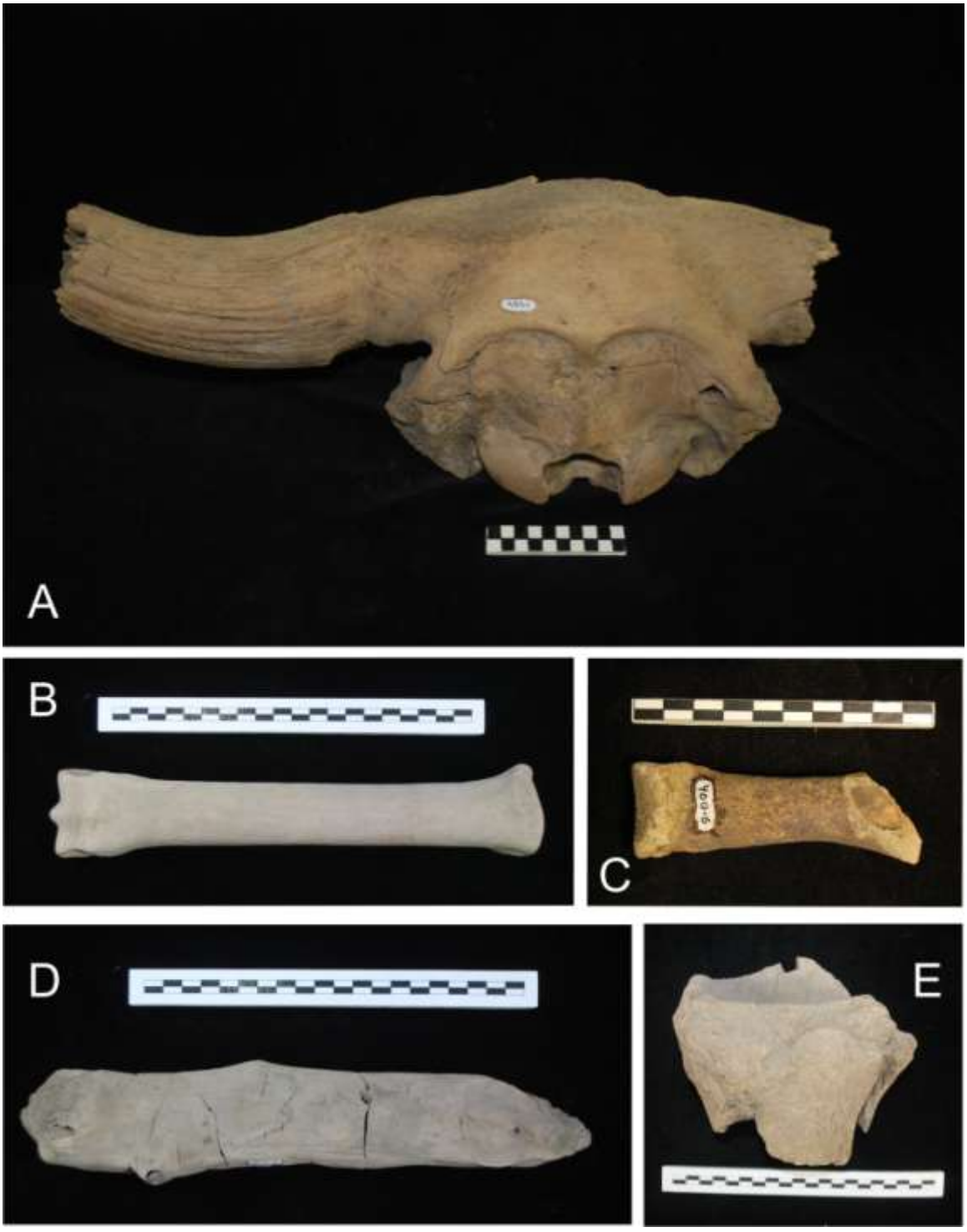

Figure 2.8. **Fossil remains from White River area: A) *Bison priscus*, partial cranium YG 400.1; B) *Equus* sp., metatarsal, YG 308.19; C) *Camelops hesternus*, partial proximal phalanx, YG 400.6; D) *Castor canadensis* chewed wood; YG 308.14; E) *Mammuthus primigenius*, tibia proximal end, YG 308.9.**

Plant and insect macrofossils sampled in Unit 15 are rich in upland grasses, xerophilous steppe forbes (e.g. *Phlox hoodii*), sage (*Artemisia frigida*), tundra beetles (*Vitavitus thulius*) and weevils (*Lepidophorus lineaticollis, Connatichela artemisiae*), indicating deposition in a dry and cold steppe-tundra environment rich in sage, upland grasses and forbs. This is supported by the pollen data that are dominated by *Artemisia*, Poaceae and other herbs. The bones found at the contact between Units 14 and 15 (Fig. 2.8) were identified as mammoth, bison, horse and sheep, corroborating an open, steppe-tundra ecosystem.

2.5.3. Tephrochronology

Fifty-one tephra samples were collected and analyzed from the White River sections, representing eleven different tephra beds. The tephras in this study are rhyolitic, with the exception of Snag tephra, which is a rhyodacite. The average major element geochemistries of these tephras are shown in Table 2.4 and graphically in figures 2.9 and 2.10.

Samples UA 1276, UA 1589, UA 1591 and UA 1923 are creamy, fine-grained, Type I tephras with well-preserved bubble wall glass shards and low phenocryst abundance. UA 1591 and 1923 have small SiO_2 wt% distributions, with relatively low Al_2O_3 and CaO wt%, and are clearly distinguished from one another by their average SiO_2, Na_2O and FeOt wt% values. Their glass major-element chemistry correlates well with the Dawson (UA 1591) and Old Crow (UA 1923) tephra beds (Fig. 2.10a, b). Old Crow tephra has been identified below last interglacial forest beds (MIS 5e) across Beringia (e.g. Westgate et al., 1985; Hamilton and Brigham-Grette, 1991; Muhs et al., 2001; Reyes et al., 2010a; Preece et al., 2011a), and is an informal marker bed for latest MIS 6 (c.f. Reyes et al., 2010a; Preece et al., 2011a). Its age has recently been refined to 124 ± 10 ka (Preece et al., 2011a). Dawson tephra is a well-constrained marker bed for the transition between MIS 3 and 2 (ca. 25 300 ^{14}C yr; 30 433 – 30 032 cal yr B.P.; Froese et al., 2006; Demuro et al., 2008; Brock et al., 2010). The major-element geochemistry of UA 1276 and 1589 have the highest SiO_2 wt% distribution of the tephra beds in this study (Fig. 2.10g, h). These two samples correlate and define a new tephra formally named here the Snag tephra, dating to an interval within MIS 5.

Samples UA 1281, UA 1583, UA 1585 and UA 1926 are coarse-grained, Type II tephras with frothy pumice and a salt and pepper appearance due to the abundance of phenocrysts. Both UA 1281 and 1583 have relatively high Al_2O_3 and CaO wt%, and their glass major-element chemistry correlates well with Woodchopper Creek tephra (Fig. 2.10 e, f). Woodchopper Creek tephra is constrained by Old Crow and VT (106 ± 10 ka; Jensen et al., 2011) tephra beds at Chester Bluff in east-central Alaska (Jensen et al., 2008, 2011), and is early to mid-MIS 5 in age. Samples UA 1585 and 1926 both are relatively high SiO_2 wt% tephra beds. UA 1585 has low Al_2O_3 and K_2O (Fig. 2.10 a, b) and is named here as Donjek tephra. Donjek tephra has been observed in close association with Woodchopper Creek and Snag tephra beds in the Klondike (Jensen, unpublished data), suggesting a similar age for these three tephras beds. UA 1926 has high K_2O and correlates to Dominion Creek tephra (Fig. 2.10 c, d). Dominion Creek tephra is commonly found above Sheep Creek-Klondike tephra in the Dawson area and has a fission track age of 82 ± 9 ka (Westgate et al., 2008).

2.5.4. Radiocarbon Chronology

Thirteen AMS radiocarbon ages from Units 6, 9, 11, 14 and 16 provide a mix of seven finite and six non-finite ages (Table 2.5). However, three of the finite ages are close to the effective limit of radiocarbon dating[1] and have large errors (UCIAMS-54966, -61739 and -92969). The other four finite ages (Beta-242149, -257450, -255362 and -255363) are considered minimum ages based on their proximity to non-finite samples or MIS 5-aged tephras. The sedimentology of the tephras indicates that they are primary beds are not reworked. These ages are likely not reliable and probably contain some younger carbon contamination.

[1] The stated conservative limit used by Beta Analytic is >43500.

Table 2.4. Average values and standard deviations (in brackets) of major glass chemistry of tephra samples, and reference samples ID3506 and Old Crow tephra. Tephra abbreviations: DC, Dominion Creek tephra; SN, Snag tephra; WC, Woodchopper Creek tephra; DJ, Donjek tephra; D, Dawson tephra; UN, Unnamed tephra.

Sample	UA 1589	UA 1276	UA 1583	UA 1281	UA 1585	UA 1591	UA 1923	UA 1926	UA 1275	UA 1581	UA 1584	UA 1594	UA 1594	ID3506	Old Crow
Site	WR54	WR99	WR94	WR95	WR99	WR98	WR54	WR54	WR99	WR54	WR94	WR94	WR94		
												Pop. 1	Pop. 2		
SiO_2	69.19	71.17	73.67	72.68	77.29	74.37	75.31	75.53	76.07	72.10	69.78	74.89	64.80	73.83	71.88
	(3.98)	(3.91)	(1.04)	(1.17)	(0.38)	(0.20)	(0.22)	(0.44)	(0.28)	(0.47)	(0.39)	(0.70)	(0.34)	(0.52)	(0.91)
TiO2	0.87	0.63	0.21	0.24	0.23	0.26	0.30	0.29	0.18	0.26	0.74	0.50	1.01	0.07	0.27
	(0.37)	(0.39)	(0.05)	(0.05)	(0.04)	(0.04)	(0.05)	(0.09)	(0.03)	(0.05)	(0.04)	(0.08)	(0.03)	(0.03)	(0.06)
Al_2O_3	14.44	14.14	15.29	15.64	12.84	13.50	12.97	13.23	13.73	15.92	14.97	12.86	16.05	13.10	12.34
	(0.84)	(0.86)	(0.42)	(0.49)	(0.15)	(0.12)	(0.12)	(0.22)	(0.22)	(0.20)	(0.14)	(0.28)	(0.22)	(0.13)	(0.22)
FeOt	3.97	3.09	1.41	1.56	1.45	2.08	1.76	1.45	1.07	1.81	3.38	1.99	5.12	1.58	1.63
	(1.52)	(1.37)	(0.20)	(0.21)	(0.08)	(0.06)	(0.06)	(0.24)	(0.09)	(0.13)	(0.21)	(0.19)	(0.16)	(0.06)	(0.11)
MnO	0.06	0.07	0.05	0.04	0.07	0.07	0.06	0.03	0.03	0.05	0.07	0.03	0.07	0.08	0.06
	(0.04)	(0.03)	(0.03)	(0.03)	(0.03)	(0.03)	(0.03)	(0.03)	(0.02)	(0.03)	(0.03)	(0.03)	(0.04)	(0.02)	(0.03)
MgO	0.96	0.71	0.47	0.55	0.30	0.23	0.29	0.20	0.34	0.62	0.75	0.27	1.66	0.05	0.26
	(0.58)	(0.60)	(0.08)	(0.10)	(0.03)	(0.03)	(0.03)	(0.05)	(0.09)	(0.07)	(0.076)	(0.05)	(0.09)	(0.02)	(0.04)
CaO	2.81	2.34	2.08	2.28	1.81	1.22	1.53	1.00	1.61	2.41	2.60	1.08	4.40	0.73	1.35
	(1.16)	(1.26)	(0.24)	(0.22)	(0.11)	(0.06)	(0.07)	(0.24)	(0.06)	(0.11)	(0.14)	(0.15)	(0.08)	(0.03)	(0.12)
Na_2O	4.30	4.12	4.09	4.21	4.04	4.44	3.73	3.73	3.88	4.40	4.14	3.67	4.26	4.00	3.61
	(0.23)	(0.27)	(0.29)	(0.53)	(0.18)	(0.12)	(0.14)	(0.30)	(0.13)	(0.20)	(0.15)	(0.17)	(0.08)	(0.13)	(0.16)
K2O	3.29	3.59	2.69	2.74	1.84	3.62	3.76	4.44	3.06	2.41	3.46	4.59	2.55	5.02	3.52
	(0.51)	(0.54)	(0.12)	(0.15)	(0.07)	(0.12)	(0.11)	(0.33)	(0.10)	(0.06)	(0.11)	(0.14)	(0.07)	(0.08)	(0.15)

Sample	UA 1589	UA 1276	UA 1583	UA 1281	UA 1585	UA 1591	UA 1923	UA 1926	UA 1275	UA 1581	UA 1584	UA 1594	UA 1594	ID3506	Old Crow
Site	WR54	WR99	WR94	WR95	WR99	WR98	WR54	WR54	WR99	WR54	WR94	WR94	WR94		
												Pop. 1	Pop. 2		
Cl	0.11	0.15	0.04	0.05	0.14	0.22	0.30	0.13	0.04	0.04	0.10	0.12	0.08	0.33	0.28
	(0.09)	(0.08)	(0.02)	(0.02)	(0.03)	(0.03)	(0.03)	(0.06)	(0.02)	(0.02)	(0.03)	(0.03)	(0.04)	(0.04)	(0.04)
H_2O	2.83	6.36	7.15	6.28	5.95	2.76	4.95	5.23	6.35	6.31	5.08	5.43	3.19	1.29	4.86
	(1.25)	(2.13)	(1.50)	(1.98)	(1.33)	(1.61)	(1.27)	(0.01)	(1.65)	(2.24)	(1.59)	(2.10)	(1.37)	(0.62)	(1.24)
n	23	38	14	14	39	25	23	17	24	16	14	38	7	30	28
Name	SN	SN	WC	WC	DJ	D	OC	DC	UN1	UN2	UN3	UN4	UN4	ID3506	Old Crow

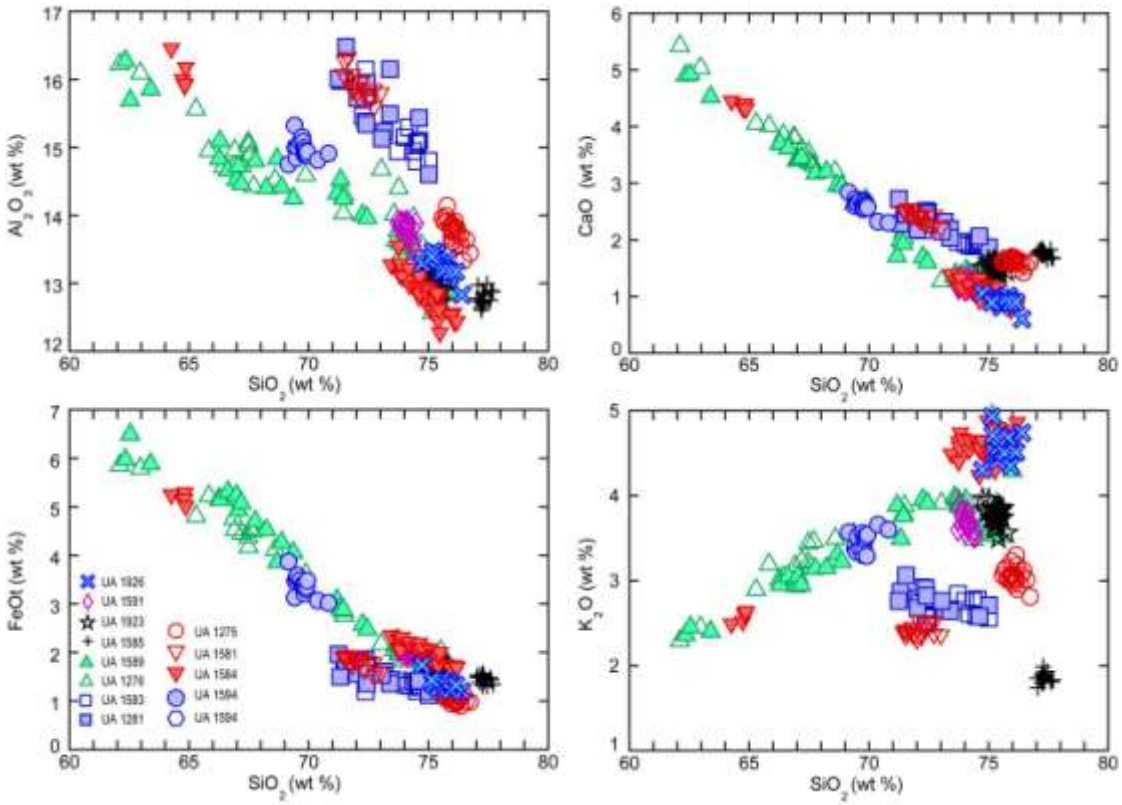

Figure 2.9. Major element glass chemistry plots of all tephra beds sampled at White River.

2.5.5. Pedological thin sections

Seven pedological samples were collected from the White River sites, two from WR94 and five from WR99. Thin sections from these samples were prepared by Dr. Paul Sanborn at the University of Northern British Columbia. Images of these thin sections in plain and cross-polarized light are shown in Appendix F.

Both thin sections 08DT94-TS1 and 08DT94-TS2 were sampled from turbic cryosols at WR94, the former at the bottom of Unit 11 and the latter in the modern soil. The mixing of organic and mineral material observed in these thin sections (e.g. 08DT94-TS2 in Appendix F) supports the field classification of turbic cryosols for these soil horizons. The thin section from sample 08DT94-TS1 has a banded fabric. Although structures similar to banded fabrics have also been observed in areas with only seasonal freeze and thaw cycles (Sanborn and Pawluk, 1989), it does indicate the presence of either seasonal or perennial ice lenses.

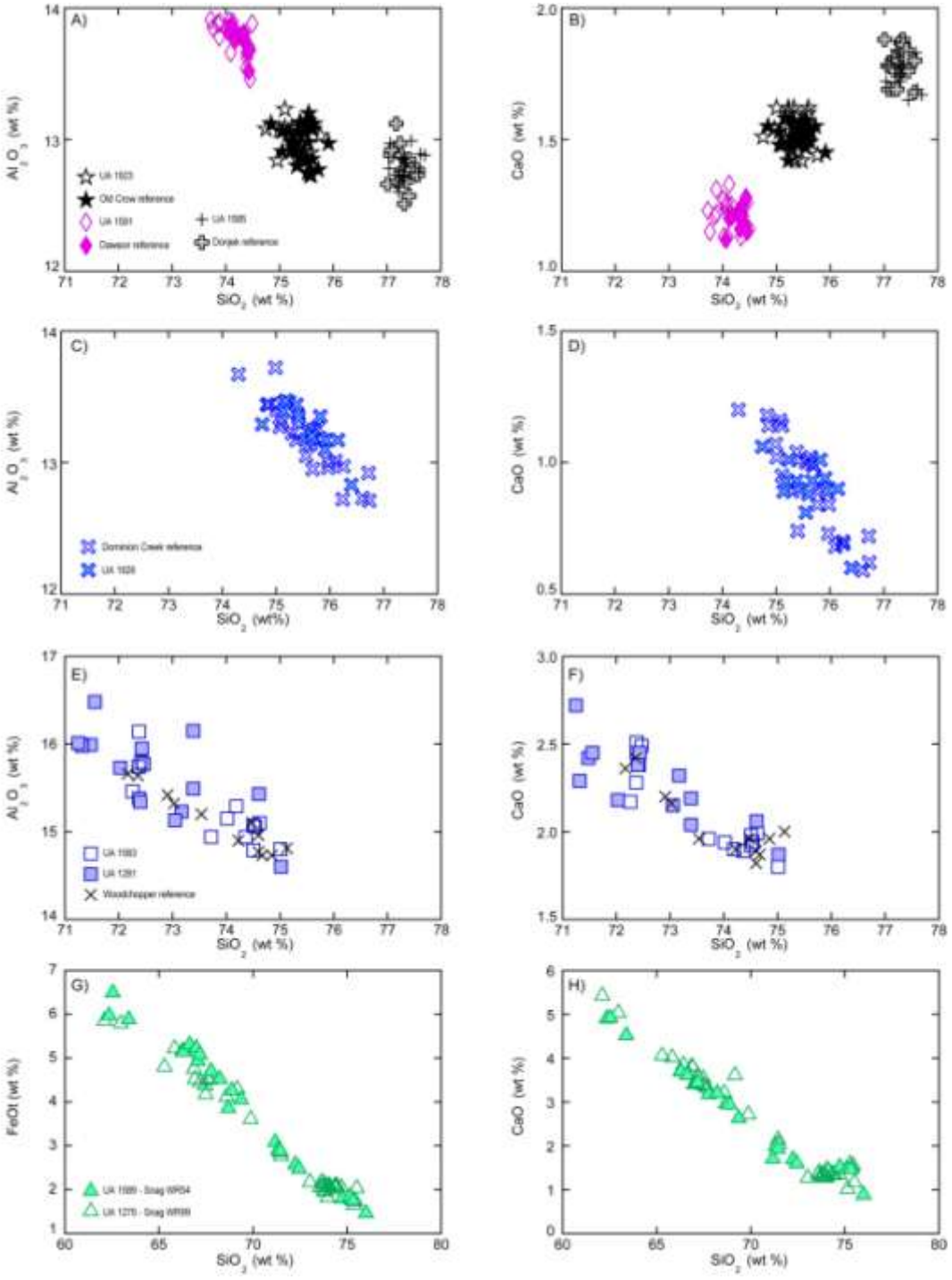

Figure 2.10. Comparison of the major element glass chemistry of tephra beds sampled at White River and reference samples: A) and B) UA 1585, 1591 and 1923 with Donjek, Old Crow and Dawson tephra reference samples; C) and D) UA 1926 with Dominion Creek tephra reference sample; E) and F) UA 1281 and 1583 with Woodchopper Creek tephra reference sample; G) and H) UA 1276 and 1589.

Table 2.5. Radiocarbon data from WR54, 94, 98 and 99.

Lab #	Site	Unit	Material / Taxon	Common Name	$d^{13}C$ (‰)	±	Fraction Modern	±	$D^{14}C$ (‰)	±	^{14}C age (BP)	±
UCIAMS-61739*	WR54	6	*Picea* twig terminal	Spruce	-25.5	0.1	0.0010	0.0004	-999.0	0.4	55400	3300
UCIAMS-61740	WR54	6	*Carex* achenes	Sedge	-27.0	0.1	0.0006	0.0004	-999.4	0.4	>52800	
Beta-257450*	WR54	6	*Picea* twig terminal	Spruce	-24.4						29680	190
UCIAMS-54966*	WR94	11	*Oxycoccus microcarpus* leaves	Small cranberry	-28.7	0.1	0.0029	0.0004	-997.1	0.4	46900	1200
UCIAMS-54967	WR94	11	Beaver-chewed wood		-26.3	0.1	0.0001	0.0004	-999.9	0.4	>56100	
UCIAMS-54968	WR94	11	*Picea* twig terminal	Spruce	-25.3	0.1	0.0002	0.0004	-999.8	0.4	>55000	
Beta-242149*	WR94	11	*Picea glauca* twig terminal with attached needles	White spruce	-24.9						36210	790
UCIAMS-112440	WR94	16	Charcoal		-25.1	0.1	-0.0002	-0.0008	-1000.2	-0.8	>51700	
Beta-255362*	WR98	14	*Mammuthus primigenius* tibia	Mammoth	-20.8						39750	630
Beta-255363*	WR98	14	*Bison* c.f. *priscus* cranium	Steppe bison	-20.0						30910	280
UCIAMS-92969*	WR98	14	*Picea* needles	Spruce	-27.2	0.1	0.0033	0.0005	-996.7	0.5	45600	1300
UCIAMS-92896	WR98	14	*Bison* c.f. *priscus* cranium	Steppe bison	-19.8	0.1	0.0013	0.0006	-998.7	0.6	>48100	
UCIAMS-40355	WR99	9	*Arctostaphylos uva-ursi* articulated nutlets	Bearberry	-26.6	0.1	0.0007	0.0007	-999.3	0.7	>49500	

* denotes ages interpreted to be erroneous or unreliable

Samples 08DT99-TS4 and 08DT99-TS5 were collected from units 9 and 13 at WR99. Sample 08DT99-TS4 contains abundant organic material (Appendix F). Sample 08DT99-TS5 was taken from the contact between Units 9 and 13. Thin sections from the silt and the overlying till contain roots. Some of these roots are birefringent under cross-polarized light, suggesting that they still contain cellulose. The sample was collected ~1.5 m below the surface, so this cellulose could either be modern or preserved in situ.

2.6. Discussion

2.6.1. Stratigraphy and chronology

Tephras and radiocarbon ages constrain the stratigraphy and chronology of the White River exposures (Fig. 2.3b). Old Crow tephra (124 ± 10 ka, Preece et al., 2011) was sampled between the till and the forest bed at WR54 and provides a minimum (and probable) MIS 6 age for the till in Unit 1. This also suggests that the glaciolacustrine deposits in Unit 3 and the tundra environment interpreted for Unit 4 were deposited during late MIS 6. This interpretation of the environment during deposition of Old Crow tephra is consistent with other sites across Eastern Beringia (Reyes et al., 2010a). The white spruce dominated boreal forest environment interpreted for Unit 6, overlying Old Crow tephra, likely represents MIS 5e.

This last interglacial forest bed is separated from a second boreal forest bed by units 7-9, containing Woodchopper Creek, Donjek and Snag tephras. At WR54, Snag tephra was observed between the two forest beds, indicating that the shrub tundra conditions interpreted for Unit 9 existed after MIS 5e, likely during another sub-stage of MIS 5[1]. The overlying forest bed (Unit 11) is constrained by Dominion Creek tephra above it to be >82 ± 9 ka (Westgate et al., 2008), and is likely MIS 5a in age. This is in agreement with other sites in central Yukon (Westgate et al., 2008; Schweger et al.,

[1] A subsequent IRSL date beside Donjek tephra returned a preliminary age of 88 ± 7 ka, supporting a mid-MIS 5 age for units 7-9.

2011). Non-finite radiocarbon ages from these units are consistent with a MIS 5 (*sensu lato*) age.

The till in Unit 13 is constrained to MIS 4 by the presence of Dominion Creek, Woodchopper Creek, Donjek and Snag tephras below it at WR54, 94, 95 and 99, and the location of the study area beyond the MIS 2 limit. The four radiocarbon ages recovered from a mammoth tibia, spruce needles and separate bison crania in Unit 14 (Beta-255362 and -255263, UCIAMS-92896 and -92969) range from ca. 30 to >48 ka ^{14}C BP, but are constrained by Dawson tephra to be either from MIS 5 or early MIS 3. If the ages are erroneous and this material is from MIS 5, it could have been reworked into gully sediment during MIS 3 or there could be an unconformity between Unit 14 and Dawson tephra in Unit 15.

The overlying steppe-tundra conditions associated with Unit 15 existed during the transition from MIS 3 to 2 associated with deposition of Dawson tephra. These environmental interpretations are consistent with other interpretations in eastern Beringia (e.g. Zazula et al., 2006b; Zazula et al., 2007) .The ice wedge at the bottom of Unit 16 is below a non-finite radiocarbon age (UCIAMS-112440) and likely formed in early MIS 3 or in MIS 4.

2.6.2. Glacial Limits

The chronology along the White River dates the penultimate glacial limit to MIS 4 and suggests the maximum Pleistocene glacial limit is MIS 6. The recognition of MIS 4 as the penultimate glaciation at the northern extent of the St. Elias lobe supports Ward et al.'s (2007) interpretation of diachronous penultimate limits in Yukon, and Rampton's (1971) original assignment of the pre-MIS 2 surface in the Snag-Klutlan area to the early Wisconsinan. It also indicates that the St. Elias and Coast Mountain lobes were coherent during MIS 4. This MIS 4 glaciation at White River correlates to Ward et al.'s (2007) Gladstone glaciation and likely Denton and Stuiver's (1967) Icefield glaciation in Yukon. In adjacent Alaska, Briner et al. (2005) and Matmon et al. (2010) present evidence for MIS 4-aged penultimate moraines in Alaska. The MIS 6 glaciation correlates to the Reid glaciation in central Yukon (Hughes et al., 1969; Ward et al., 2008;

Westgate et al., 2008; Demuro et al., 2012). A MIS 6 age for the maximum glacial advance of the St. Elias lobe supports interpretations of Hughes et al. (1969), Hughes (1990), Rampton (1971) and Bond et al. (2008) that no pre-Reid drift is present in this area.

Although the MIS 6 and 4 limits mark the most extensive Pleistocene glaciations in the area, the MIS 2, 4 and 6 limits are all within 15 km along the White River without any older, pre-Reid glacial deposits. This contrasts with the Selwyn lobe in central Yukon, where pre-Reid drift extends up to approximately 100 km past the MIS 6-aged Reid limit, but no MIS 4 deposits have been found at the surface (Duk-Rodkin, 1999; Bond and Lipovsky, 2010). Assuming precipitation was the principle variable controlling glaciation, this suggests that while moisture delivery varied during glacial intervals in the interior region of central Yukon, constraints on precipitation in southwest Yukon remained similar throughout the Pleistocene. Moisture delivery to eastern Beringia during Pleistocene glaciations was a complex combination of controls such as tectonics, increased continentality from eustatic sea level regression (Guthrie, 2001; Briner et al., 2005), changing extents of the Laurentide ice sheet (c.f. Barendregt and Irving, 1998) and variations in the jet stream precipitation delivery (c.f. Bromwich et al., 2004; see chapter 4).

2.6.3. Paleoenvironmental Record

The non-glacial sediments interbedded with the MIS 4 and 6-aged glacial sediments contain a detailed record of Late Pleistocene environmental change in southwest Yukon. Glaciolacustrine deposits above the MIS 6-aged till imply that a large, likely moraine-dammed glacial lake covered a portion of the study area following deglaciation. After this lake drained, rapid loess aggradation coincided with deposition of Old Crow tephra in a tundra environment. The presence of this tephra where the Alaska Highway crosses the White River (Rampton, 1969; Preece et al., 2011a) confirms that ice had retreated at least ~75 km when it was deposited.

The geomorphology during MIS 5e was likely similar to present day along the White River, with gullies forming and infilling with colluvium and material from the

surrounding landscape. Gully incision was probably accelerated by warming and shallow permafrost degradation, consistent with evidence for regional shallow permafrost degradation during MIS 5e (Reyes et al., 2010b). Macrofossil data from Unit 6 indicate that a white spruce boreal forest with beaver ponds existed during this time. Warm conditions with extra-limital species similar to this have been interpreted for MIS 5e across eastern Beringia (e.g. Matthews et al., 1990a; Hamilton and Brigham-Grette, 1991; Beget et al., 1991; Schweger and Matthews, 1991; Brigham-Grette and Hopkins, 1995; Pewe et al., 1997; Muhs et al., 2001). The degree of weathering in the gravel in Unit 2 at WR99 suggests a substantial period of time elapsed between deglaciation and deposition of Unit 8. This weathering probably occurred during MIS 5e and is similar to the weathering observed in the Diversion Creek paleosol (Smith et al., 1986; Tarnocai and Smith, 1989).

Subsequent cooling and loess aggradation coincided with deposition of Woodchopper Creek and Donjek tephras in Units 7 and 8. This cooling may have coincided with the development of an arctic ice sheet that extended into the Amundsen Gulf (Brigham-Grette and Hopkins, 1995), potentially limiting arctic moisture delivery to eastern Beringia. The chronology and paleoenvironment of Unit 9 indicate that this period of rapid loess deposition was followed by shrub birch tundra conditions and deposition of Snag tephra. This transition must have occurred during the sub-stages of mid-MIS 5.

The turbic cryosol and boreal forest peat bed in Unit 11 are stratigraphically above this tundra environment and formed in late MIS 5. This unit represents a return to a period as warm as, or warmer than, present. Although most MIS 5 forest beds are assumed to be from MIS 5e, Schweger (2003) described a boreal forest bed at Ash Bend in central Yukon that was later interpreted to be from MIS 5a (Westgate et al., 2008; Schweger et al., 2011). A MIS 5a age is therefore preferred for Unit 11. This highlights the need for caution when assigning a MIS 5e age for all *sensu lato* MIS 5 forest beds.

Following glaciation in MIS 4, a steppe-tundra environment existed in late MIS 3 and early MIS 2. The presence of spruce macrofossils in the unit below Dawson tephra

indicates that some spruce may have existed in early MIS 3, although a MIS 5-age is more likely for this material in Unit 14. The abundance of arid species and lack of spruce during deposition of Dawson tephra suggests that the White River area was more arid than the Klondike, ~150 km to the north, where some spruce remained (Zazula et al., 2006c). This highlights the regional differences in temperature and precipitation that existed across Beringia during the large Pleistocene climatic transitions (c.f. Elias, 2000; Guthrie, 2001; Goetcheus and Birk, 2001; Anderson and Lozhkin, 2001).

2.7. Conclusions

Sections along the White River provide a record of glacial limits and paleoenvironmental change during the Middle to Late Pleistocene in southwest Yukon. The exposures contain glacial and non-glacial deposits with multiple tephra beds that were used to extend the record beyond the limit of radiocarbon dating. Eleven different tephras were identified, including Old Crow, Woodchopper Creek, Donjek, Snag, Dominion Creek and Dawson tephras.

The response of the St. Elias lobe to Pleistocene climate changes was out of phase with both ice lobes in central Yukon and global ice volume. The St. Elias lobe was more extensive in MIS 4 and 6 than during any other time in the Plio-Pleistocene, unlike in central Yukon where ice reached its maximum limit before MIS 6 and was limited in MIS 4. Also, the limits in the White River area are within 15 km of each other, in contrast to central Yukon where they are separated by approximately 100 km. Climatic controls and other forcing mechanisms on glacial extent therefore varied more in central Yukon than in southwest Yukon during Pleistocene glaciations (refer to Chapter 4).

Macrofossil and pollen data in non-glacial sediments provide a paleoenvironmental record for multiple substages in MIS 5, and at the MIS 3/2 transition. During MIS 5e, conditions along the White River were as warm as, or warmer than, present, with a white spruce boreal forest ecosystem. In mid-MIS 5, a period of rapid loess deposition and development of a shrub birch tundra occurred. Conditions returned to a white spruce boreal forest again in late MIS 5, probably in MIS 5a. The transition

from MIS 3 to 2 is marked by the development of a steppe-tundra ecosystem that was likely more arid than in areas more distal to the ice sheet.

Chapter 3. Stratigraphy of Middle to Late Pleistocene glaciations in the St. Elias Mountains, southwest Yukon

Derek G. Turner[1], Brent C. Ward[1], Duane G. Froese[2], Michel Lamothe[3], Jeffrey D. Bond[4], Nancy H. Bigelow[5]

[1]Derek G. Turner & Brent C. Ward, Department of Earth Sciences, Simon Fraser University, 8888 University Drive, Burnaby, B.C., V5A 1S6. Ph. 1-778-782-4564; Fax: 1-778-782-4198, dgturner@sfu.ca.

[2]Duane G. Froese, Department of Earth and Atmospheric Sciences, University of Alberta, 1-26 Earth Sciences Building, Edmonton, Alberta, Canada, T6G 2E3.

[3]Michel Lamothe, Département des Sciences de la Terre et de l'Atmosphère, Université du Québec à Montréal, CP 8888, Succursale Centre-Ville, Montreal, QC, Canada, H3C 3P8.

[4]Jeffrey D. Bond, Yukon Geological Survey, Yukon Government, P.O. Box 2703, Whitehorse, Yukon, Canada, Y1A 2C6.

[5]Nancy H. Bigelow, Alaska Quaternary Center, PO Box 755940, University of Alaska, Fairbanks, Fairbanks, Alaska, USA

3.1. Abstract

A record of Middle to Late Pleistocene advances of the St. Elias lobe of the northern Cordilleran Ice Sheet in southwest Yukon is preserved at the Silver Creek site, on the northeastern edge of the St. Elias Mountains. Silver Creek is located 100 km up-ice of the marine oxygen isotope stage (MIS) 2 McConnell glacial limit. This site contains ~3 km of nearly continuous lateral exposure of glacial and non-glacial sediments, including multiple tills separated by thick gravel, loess and tectonically tilted lake beds. Infrared-stimulated luminescence (IRSL) and radiocarbon dating constrain the glacial deposits to MIS 2, 4, either MIS 6 or mid-MIS 7, and two Early to Middle Pleistocene advances.

This chronology and the tilt of the lake beds suggest possible Pleistocene uplift rates of up to 1.9 mm/yr along the Denali Fault since MIS 7. The non-glacial sediment consists of sand, gravel, loess and organic beds from MIS 7, MIS 3 and the early Holocene. IRSL and AMS radiocarbon dates constrain the MIS 3 deposits to between 30-36 ^{14}C ka BP. This is one of the few well-constrained MIS 3-aged sites in Yukon. Pollen and macrofossil analyses show that a meadow-tundra to steppe-tundra mosaic with abundant herbs and forbs and few shrubs or trees, dominated the environment at this time. The stratigraphy at Silver Creek provides a paleoclimatic record since at least MIS 8, including five Pleistocene glaciations, that comprise the oldest direct record of Pleistocene glaciation in southwest Yukon.

3.2. Introduction

An extensive record of Pleistocene climate change is preserved in the largely non-glaciated area spanning northwestern North America and northeastern Asia, collectively termed Beringia. Reconstructing the timing of repeated continental glaciations and intervening non-glacial intervals preserved in Beringia relies heavily on data from marine cores (Shackleton, 1987; Lisiecki and Raymo, 2005) and terrestrial sites in the non-glaciated region (e.g. Hamilton and Brigham-Grette, 1991; Muhs et al., 2001; Froese et al., 2009). Although rare, well-constrained terrestrial records within the glacial limit are useful for examining more detailed, direct records of glaciation and intervening non-glacial intervals. This study examines one such site at Silver Creek, located in the Shakwak Trench at the northeastern edge of the St. Elias Mountains in southwest Yukon (Fig. 3.1).

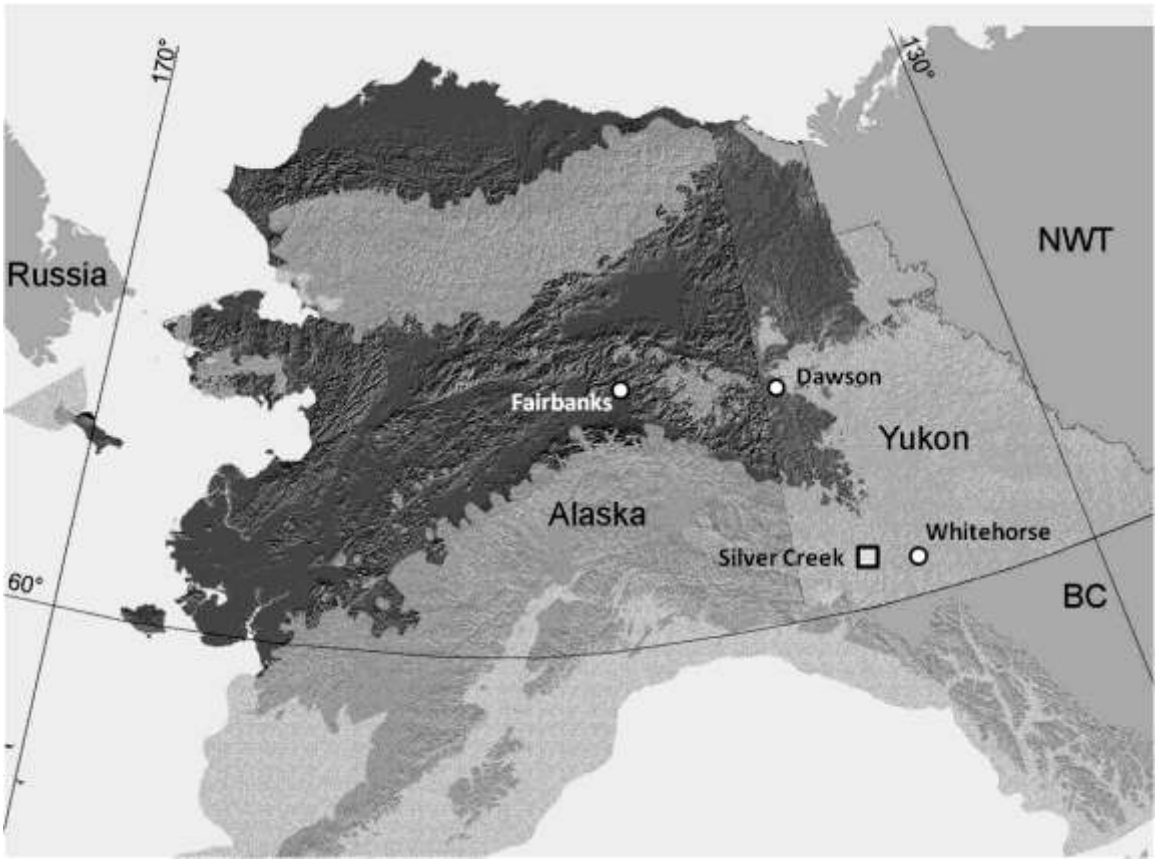

Figure 3.1. The Silver Creek study area in southwest Yukon. The shaded area shows the all-time maximum Pleistocene ice limits in Alaska and Yukon (Manley and Kaufman, 2002; Duk-Rodkin, 1999).

The Shakwak Trench was glaciated numerous times during the Pleistocene by the St. Elias lobe of the northern Cordilleran Ice Sheet (Denton, 1974). This ice sheet was composed of five distinct, topographically controlled lobes that acted semi-independently. The relative extents of these ice lobes varied during successive glaciations. The last glaciation in marine oxygen isotope stage (MIS) 2 was less extensive in central Yukon than the MIS 6 Reid glaciation and several Late Pliocene to Middle Pleistocene, Pre-Reid glaciations (Froese et al., 2000; Ward et al., 2008; Jackson et al., 2012). However, ice was most extensive in southern and southwest Yukon in MIS 6 and 4 (Ward et al., 2007; Turner et al., 2013). It is unknown if ice advanced out of the St. Elias Mountains during the Pre-Reid glaciations. This complex glacial record has raised questions about how regional climate controls affect glacial limits through the Pleistocene.

A significant problem in reconstructing Pleistocene environmental change is constraining the timing of events that occurred beyond the limit of radiocarbon dating. An alternative dating methods for older (ca. >50 1^4C ka BP) sediment is infrared stimulated luminescence (IRSL) dating. IRSL dating is increasingly being used to date pre-MIS 2 sediment in northern latitudes with promising results (e.g. Auclair et al., 2007; Demuro et al., 2008, 2012; Jensen et al., 2011). IRSL is especially useful for dating sediment in areas where other dating methods (e.g. tephrochronology, cosmogenic methods) are not readily applicable.

The objectives of this paper are to: 1) use radiocarbon and IRSL dating to constrain the age of the glacial stratigraphy at Silver Creek; 2) use pollen and plant and insect macrofossils to reconstruct environmental conditions in the intervening non-glacial periods; and 3) correlate these paleoenvironmental records to other records in Yukon.

3.3. Setting

Silver Creek is located on the northeastern side of a 30 km long massif of the Kluane Range, front ranges to the St. Elias Mountains to the southwest (Figs. 3.1, 3.2). The St. Elias Mountains are one of the highest mountain ranges in North America, with peaks above 5,000 masl. Silver Creek flows north from the Kluane Range into Kluane Lake in the Shakwak Trench, a deeply scoured, 10-15 km wide, northwest-southeast trending valley oriented parallel to the Denali Fault. This study focuses on approximately 3 km of near-continuous exposure in Silver Creek, south of the Alaska Highway.

During the last glaciation, ice flowed down Silver Creek from the Kluane Range and coalesced with the Kaskawulsh Glacier to the west and ice flowing northwest along the Shakwak Trench (Denton, 1974). This ice formed part of the St. Elias lobe of the northern CIS, which flowed along the trench for up to ~175 km before spreading out across the Wellesley Basin (Rampton, 1971; Duk-Rodkin, 1999). During glacial maximum, ice may have flowed across the trench and into the Ruby Range to the northeast (Duk-Rodkin, 1999). It is assumed that similar ice-flow configurations existed in earlier glaciations, but pre-MIS 2 ice flow directions are poorly preserved.

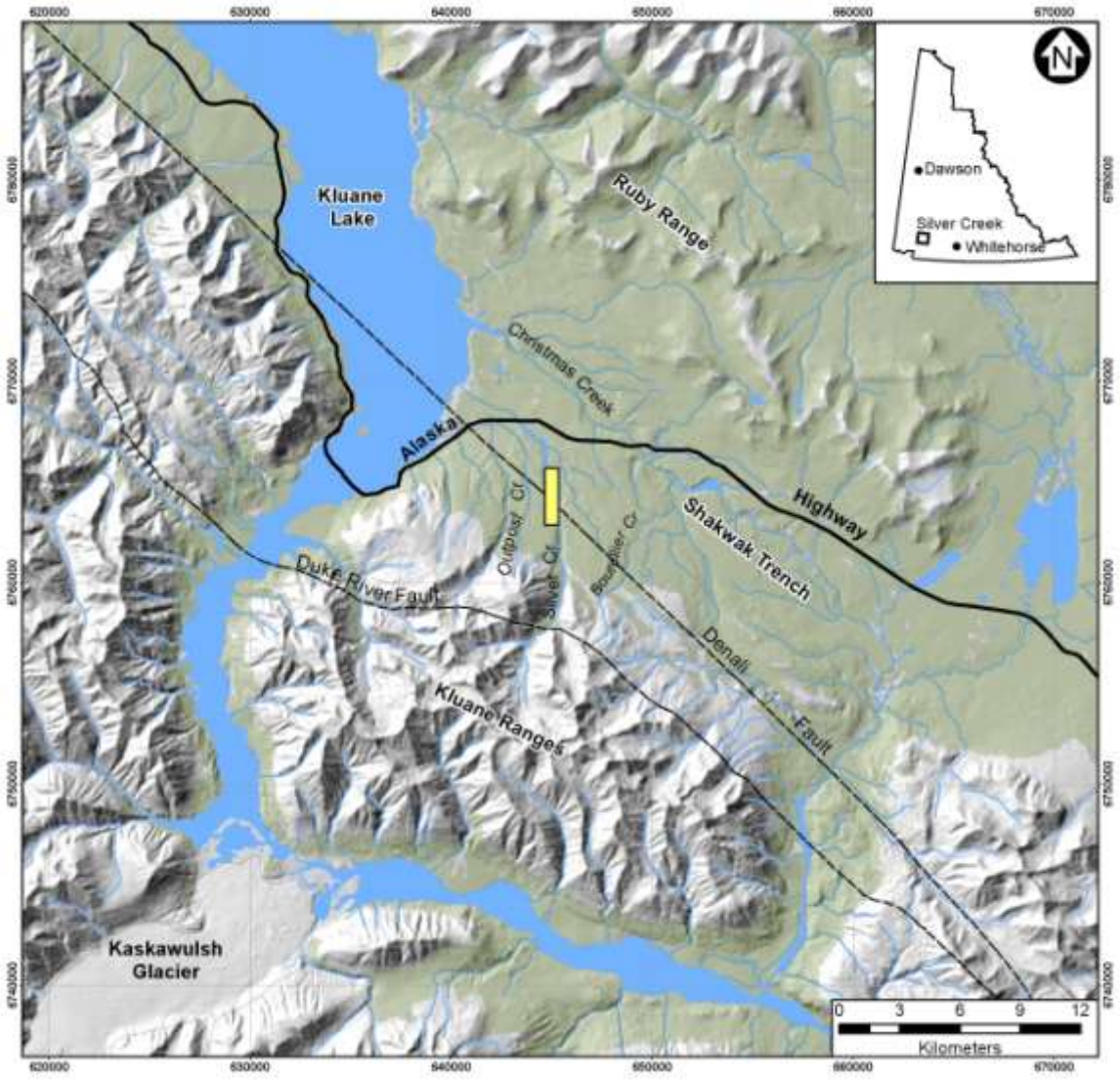

Figure 3.2. Location of Silver Creek study area (yellow box) and surrounding physiographic features mentioned in text. Dashed lines show the inferred location of the Denali and Duke River faults in the Shakwak Trench.

3.4. Previous Work

Denton and Stuiver (1967) identified three distinct drift units separated by three non-glacial intervals at Silver Creek, the Shakwak Trench and the neighbouring Outpost, Christmas and Boutellier creeks. They interpreted this stratigraphy as representing three glaciations, based on stratigraphy, sedimentology and bulk sediment radiocarbon

dates on organic-rich horizons. The glaciations were named, from oldest to youngest, the Shakwak, Icefield and Kluane glaciations and were represented by glaciolacustrine sediment, outwash, ice-contact stratified drift and thick tills with varying clast fabrics.

The three non-glacial intervals between the glacial deposits were termed the Silver, Boutellier and Slims (Denton and Stuiver, 1967). These interpretations relied on erosional surfaces, weathering zones that penetrate up to ~4.5 m into the till and, in the case of the Boutellier interval, interbedded sand, gravel and organic-rich silt beds.

Denton and Stuiver (1967) correlated these climatic events to existing continental records of the Cordilleran and Laurentide Ice Sheets and the intervening non-glacial episodes (Denton, 1974). Their bulk sediment radiocarbon ages indicated that the Kluane glaciation was deposited during the late Wisconsinan (MIS 2) and that the Boutellier interval correlated to the mid-Wisconsinan (MIS 3). The Icefield and Shakwak glaciations were assigned to the early Wisconsinan and an earlier glacial period based on correlation to established mid-continental glacial stratigraphy (Denton, 1974). Subsequent examination of the organic-rich sediment in the Boutellier non-glacial interval using pollen and bryophyte analyses indicated that “a tundra meadow, and/or tundra-steppe, with only local willow shrubs” (Schweger and Janssens, 1980, pg. 316) existed in the area between 33 and 30 ^{14}C ka BP.

3.5. Methods

Eleven sites along Silver Creek were investigated during field seasons in 2009 and 2010. Units were defined by sedimentology, organic content, relative weathering and their stratigraphic context to other sites. Organic-rich beds were sampled for macrofossil and pollen analysis and for radiocarbon dating. Units with the appropriate grain size and inferred bleaching history were sampled for IRSL dating. Proximal glacial sediment may have inheritance, resulting in erroneously old ages. Numerous tephras were also sampled, but the associated glass was too heavily weathered to establish the major element geochemistry of the shards, despite repeated attempts. At least 50 clasts with ≥ 3:1 ratios of a- to b-axis lengths were measured for clast fabric analyses. These are shown as equal area, lower hemisphere plots. Preference was given to striated and

keeled clasts. Only one fabric measurement was collected in each diamict reported, limiting the interpretations that can be made using these data.

Plant and arthropod macrofossils in seven samples from Unit 13 were isolated from the sieved residue (0.425 mm mesh opening), similar to Birks (2001). Vascular plant and insect macrofossils were identified and interpreted by Alice Telka of Paleotec Services using comparison of modern reference specimens housed at the Geological Survey of Canada, Ottawa and illustrations, descriptions and checklists in several publications (e.g. Martin and Barkley, 1961; Bousquet, 1991; Danks and Downes, 1997; Cody, 2000). Four macrofossils samples from two units were submitted to the Keck Carbon Cycle AMS Facility at University of California Irvine for radiocarbon dating. Where ever possible, fragile macrofossils were used to limit the potential of reworking. Samples were also collected for paleoecological analysis in other units. However, weathering or a lack of organic-rich material of both macrofossils and pollen in these units prevented detailed analysis.

Pollen analysis was performed on seven samples from Unit 13 and one from Unit 7. A minimum grain count of 300 per sample was attempted, but was only achieved for SC11-PO5. Sub-samples for pollen analysis were processed using standard techniques (sieving, 10% KOH, and 10% HCl washes), followed by heavy liquid separation (s.g. 2.0) and filtering with a fibreglass filter. The filters were then dissolved in hydrofluoric acid and the samples were acetolized (one or two minutes in a boiling water bath with acetic anhydride and sulfuric acid), washed in acetic acid and water and suspended in silicone oil (Faegri and Iversen, 1989; Moore et al., 1991). Pollen identifications were based on comparisons with published atlases (McAndrews et al., 1973; Moriya, 1976; Moore et al., 1991) and with the pollen reference collection housed at the Department of Geology and Geophysics at the University of Alaska Fairbanks.

IRSL samples were collected in three units at different exposures. The IRSL method used here is similar to that in Jensen et al. (2011), where tephra-bounded loess was dated to 106 ± 10 ka. Samples were collected using black opaque PVC tubes to prevent exposure to sunlight. Units were preferentially sampled based on their inferred bleaching history, water content and grain size. It is important to select sediments that

have had a transport history that has allowed sufficient exposure to sunlight to ensure that there is no inheritance. Separate sets of samples were collected for dose rate and moisture content measurements and analyzed at the Université du Québec à Montréal (UQAM). In the laboratory, 125-250 µm feldspars were isolated using standard densimetric techniques. Luminescence signals were detected using a TL/OSL-DA-15 Risø reader, with a ^{90}Sr beta source calibrated at 6.98 Gy/min. Blue-violet luminescence emission was detected through a Schott BG39/Corning 7-59 filter combination. Measurements on the Risø DA15 reader are from a strong 100 second IR illumination, depleting more than 90% of the signal.

The natural luminescence was assessed using 12 to 24 aliquots, from which a sub-set of ca. 6 to 8 aliquots for each sample was dosed in the laboratory to build up a 'standard' luminescence regeneration growth curve. The equivalent dose was evaluated following the methods developed at the Université du Québec à Montréal (see Lamothe, 2004), using a modified version of the single-aliquot regeneration (SAR) technique first (Murray and Wintle, 2000). For feldspar, the same preheat for both the dose and test dose was used (Huot and Lamothe, 2003; Auclair et al., 2003; Lamothe, 2004; Blair et al., 2005). A cut-heat to 280 ^{o}C followed by a further IR stimulation limits the thermal transfer of charges to the test dose IRSL. The weighted mean of the normalized natural luminescence (Ln/Tn) was calculated using the Central Age Model. That average Ln/Tn was interpolated into a "standard growth curve", averaged from a limited number of aliquots, each carrying ~10-100 grains. The low Ln/Tn variability generally observed between aliquots for the same dose allowed measurement of a larger number of natural aliquots and use of elevated regeneration doses. Dose recovery experiments used a solar bleach of two hours from a SOL2 Honle lamp, followed by a dose of 220 Gy. These aliquots were then processed as carrying a natural dose using the same protocol described above. The use of the SAR protocol (Lamothe, 2004) yields satisfactory dose recovery tests (dose recovered/dose given = ca. 1.00) for most samples on which this test has been carried out in the UQAM lab.

Feldspars are prone to anomalous fading, or the loss of luminescence due to the leakage of electrons from traps without stimulation (Wintle, 1973; Aitken, 1998; Auclair et al., 2003). This results in the equivalent dose being lower than the total acquired dose in

the environment since deposition. The latter is assessed from anomalous fading measurements, from which the fading rate (*g* value), is obtained. The radiation dose received by the feldspars since deposition is calculated using the dose rate correction (DRC) equation, as described in Lamothe et al. (2003), providing a fading-corrected age. The DRC equation incorporates the measured fading rate, the laboratory radiation dose rate and the environmental radiation dose rate (Lamothe et al., 2003). The correction method developed by Huntley and Lamothe (2001) is not used here, as the method is known to be only applicable to the linear portion of the growth curve.

3.6. Results

3.6.1. Stratigraphy

The stratigraphy of the Silver Creek exposures is separated into sixteen units and is best exposed at four sites: SC11, SC10, SC8 and SC7 (Figs. 3.3a, 3.4 and 3.5). Figure 3.6 illustrates an interpreted compilation of the stratigraphy at the examined sites. Most of the units are tilted to the north, with older sediment exposed further upstream (to the south). The dip angle increases significantly with age; the upper few units are nearly horizontal, whereas the older units are dipping up to 14^{o}. The modern floodplain has a slope of approximately 2.5^{o}.

Units 1 to 4 are interbedded gravel and diamict. They are only present in the upstream sites and are poorly exposed. Units 1 and 3 are >10 m thick gravel with infrequent sand beds. The gravel in both units is moderately sorted, weakly stratified and supported by a fine- to coarse-grained sand matrix, with well rounded to subangular clasts ranging in size from pebbles to boulders. The matrix and clasts in these units are heavily weathered with disintegrated clasts in some exposures. These two units are interpreted as being deposited in a non-glacial, fluvial environment due to the sorting, stratification and thickness of the units.

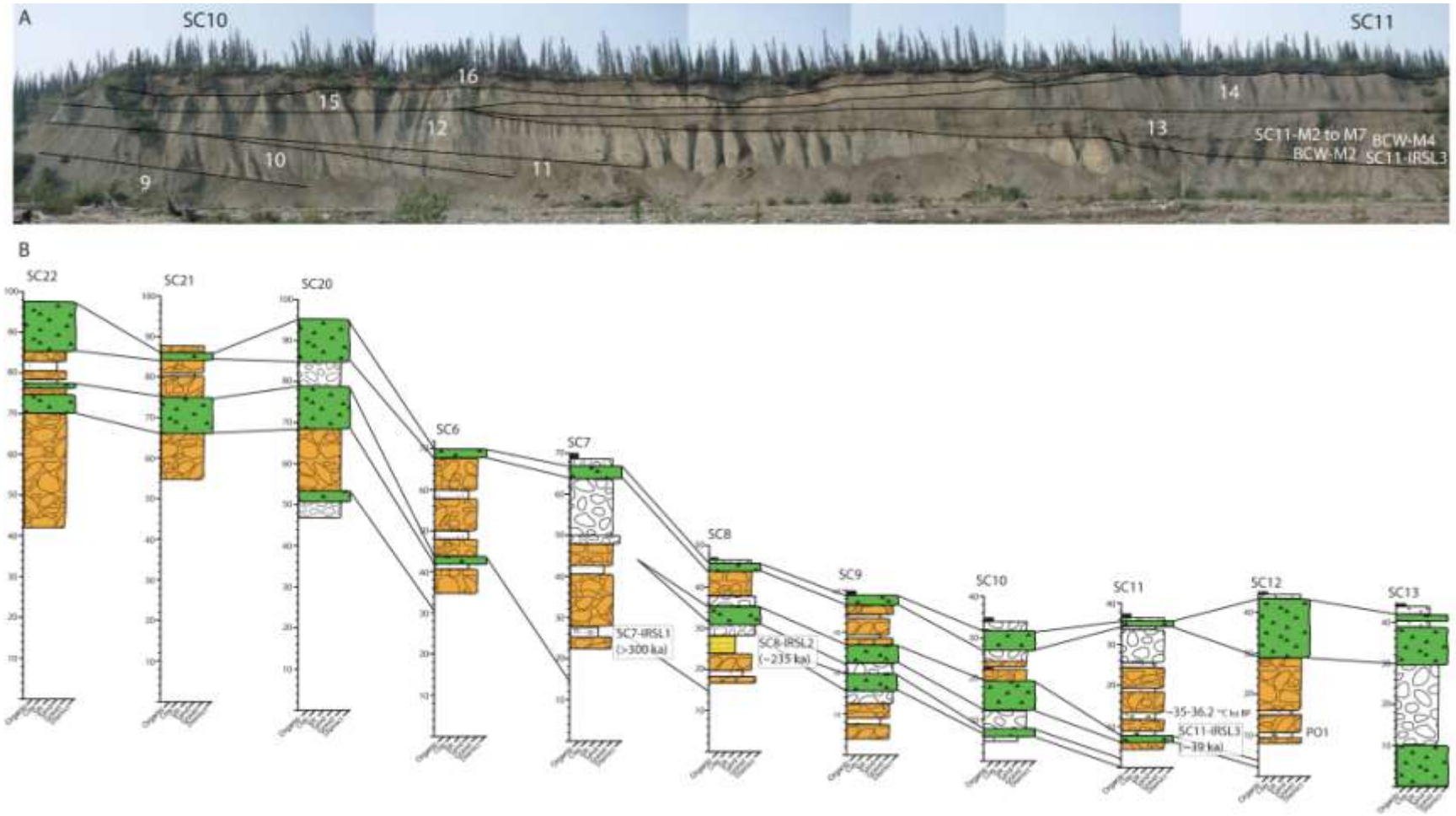

Figure 3.3. **a) Exposures SC10 (left) and SC11 (right), with unit numbers in white. Note the tilting in the upstream (left) exposure; b) Stratigraphic logs for Silver Creek exposures. Heights are in metres, with 0 m representing creek level at each site. Horizontal distances are not to scale. See figure 3.6 for legend.**

Units 2 and 4 are massive, consolidated diamicts. Unit 2 has ~20% well rounded to subangular clasts that range in size from pebble to boulders with a silty-sand matrix. Some of these clasts are bullet-shaped and striated. The lower contact of this unit is sharp, and its upper contact has evidence of subaerial weathering. At SC21, this unit has higher clast content and is fractured, weathered and less consolidated than at SC20 and SC22. Unit 4 is similar to Unit 2, but has 25% heavily weathered clasts and a clayey-silt matrix. Both of these units are interpreted as till rather than colluvium based on their consolidation and the abundance of striated clasts.

Unit 5 consists of interbedded gravel and finer-grained beds. This unit is at least 30 m thick in the upstream exposures and is inclined ~10-15^{o} to the north. The gravel is moderately sorted and supported by a medium- to coarse-grained sand matrix. This unit has well rounded to subangular clasts ranging in size from granules to cobbles. The gravel coarsens and is less weathered at its upper contact at several exposures. Both the gravel matrix and clasts are heavily oxidized and many clasts are disintegrated or frost-shattered. Faulting observed in the gravel is associated with overlying, ~50 cm thick diamict lenses. The finer-grained layers are composed of ~10-20 cm thick, inorganic clay and silt beds, and <2 m thick medium- to coarse-grained sand beds. Several subaerially deposited tephras were also observed. This unit is interpreted as fluvial, deposited over a sufficiently prolonged period to allow deposition of multiple tephras and substantial subaerial weathering.

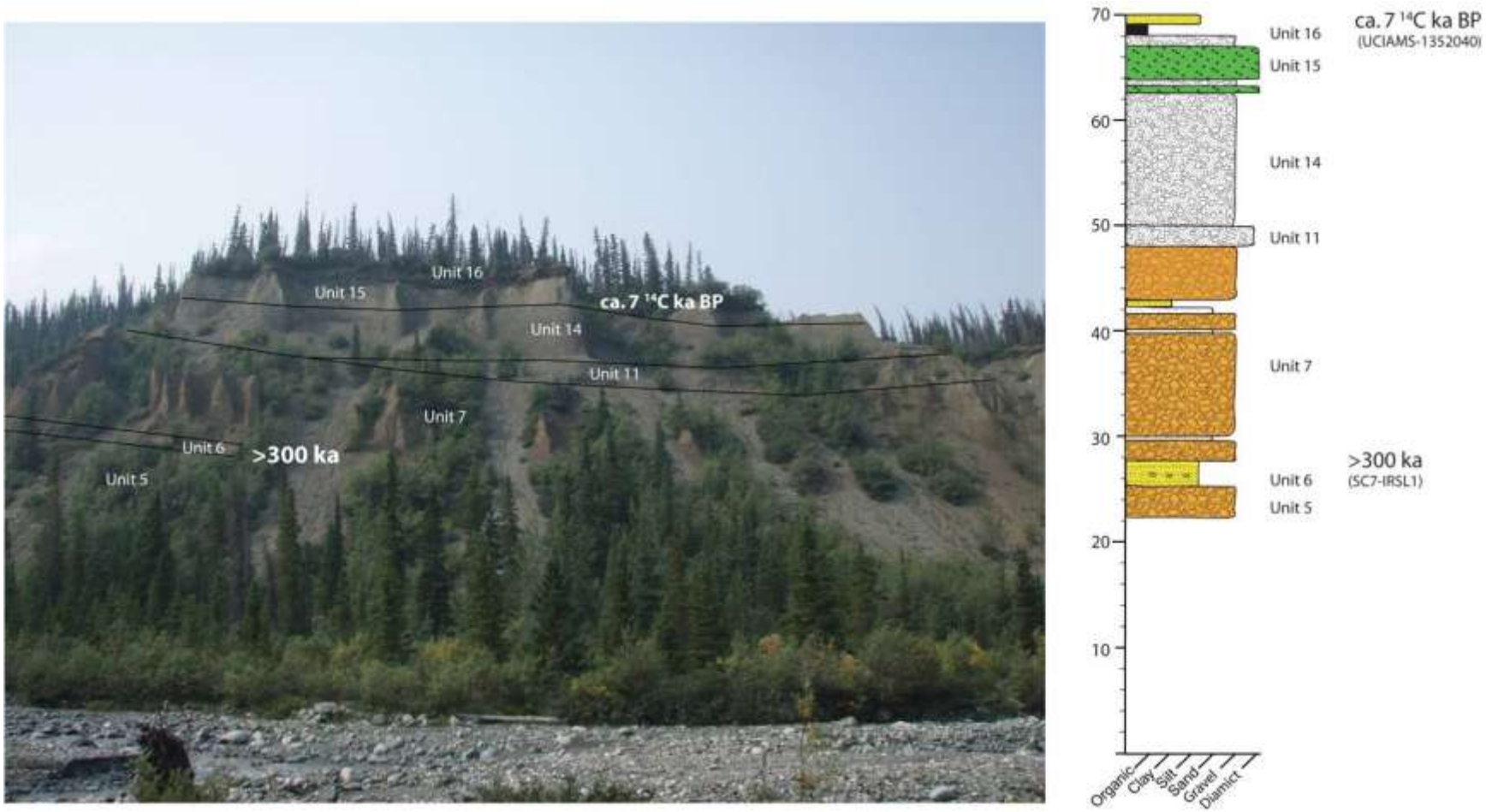

Figure 3.4. Exposure SC7. See figure 3.6 for legend. Exposure is 70 m high.

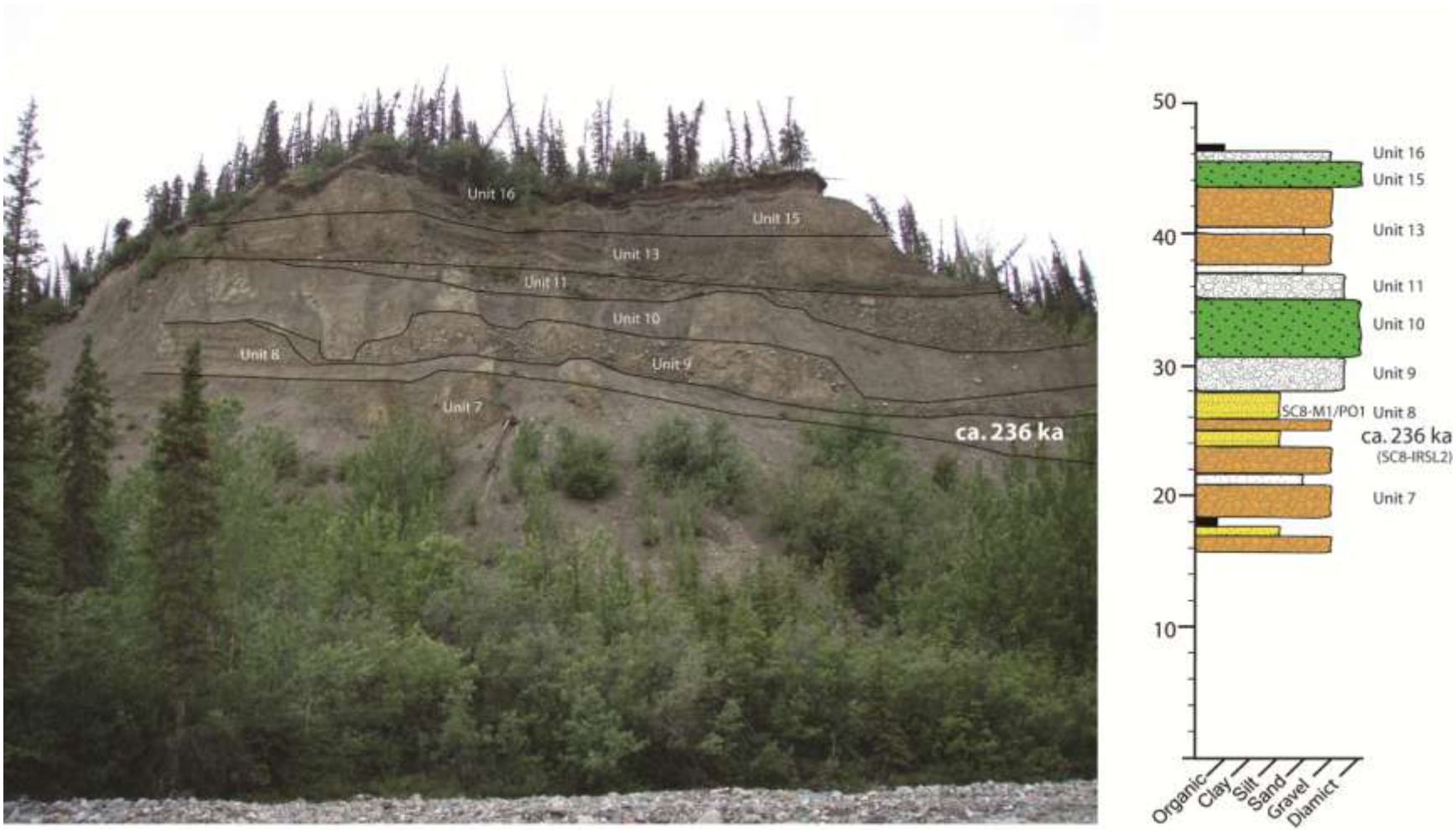

Figure 3.5. Exposure SC8. See figure 3.6 for legend. Exposure is 47 m high.

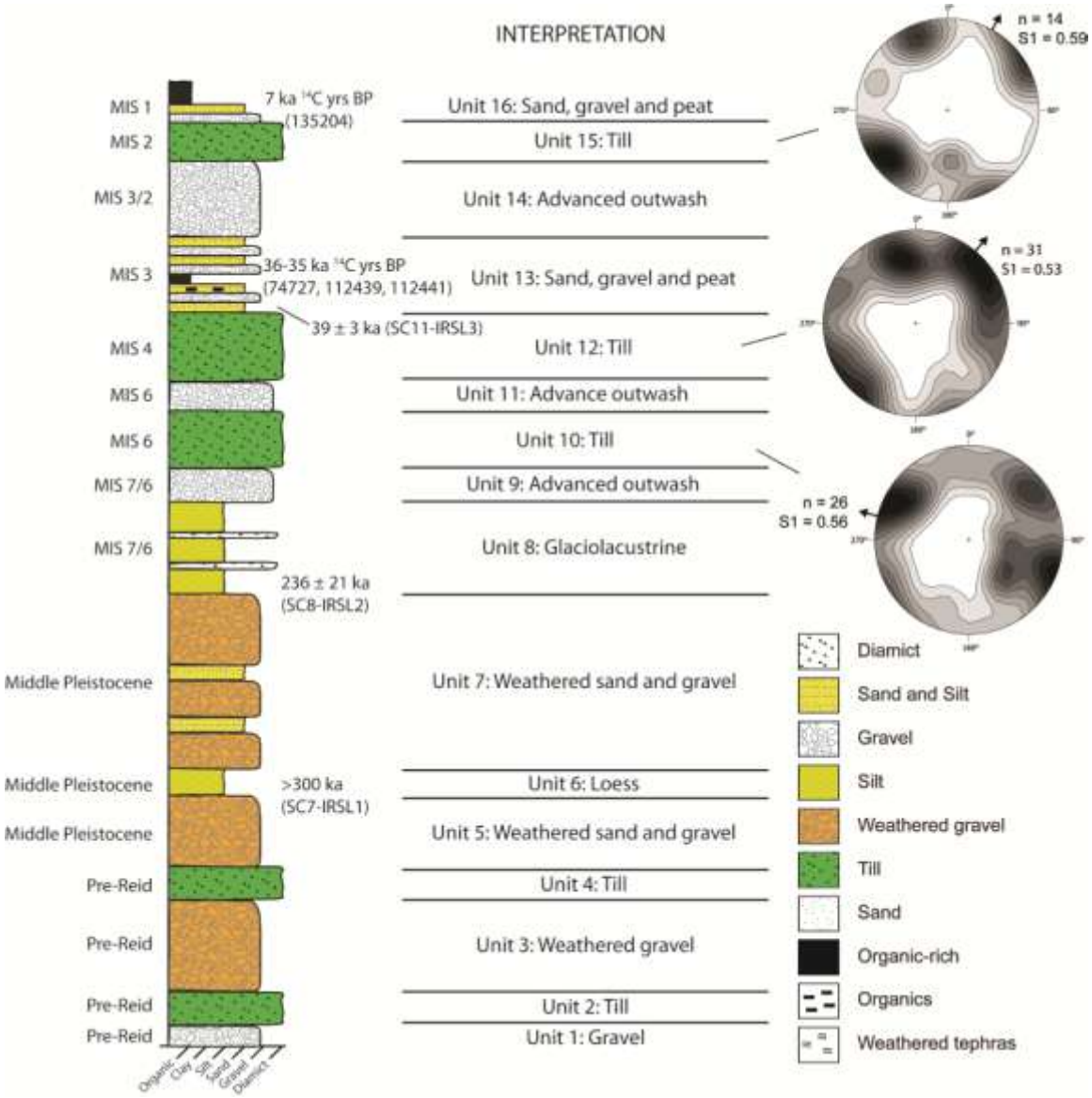

Figure 3.6. Compilation of stratigraphy at Silver Creek from eleven sites. Till a-axis clast fabrics are equal area, lower hemisphere plots with contour intervals of 10. The number of clasts measured (n) and the calculated primary eigenvector (S1) are also noted. Ages on the left are the preferred interpretation of several possibilities. Radiocarbon sample names are prefixed with UCIAMS- in Table 3.1 and in the text.

Unit 6 consists of 2 m of well sorted, massive, silty fine-grained sand. It is dominantly light grey, but weathers light brown to dark grey with zones of oxidation. There are a few pebble- to cobble-sized clasts in the sand. Unit 6 has a conformable lower contact, marked by ~30-50 cm of interbedded medium- to coarse-grained sand,

pebble-rich beds and variably organic-rich silt. This contact undulates by ~35 cm and has potential ice-wedge pseudomorphs, suggesting cryoturbation during deposition. The top 25-50 cm of Unit 6 is weakly stratified with thin beds of silt inclined by 5-15^{o} to the north. Several diffuse tephra beds observed in this unit are potentially the same tephra reworked into multiple horizons. Sample SC7-IRSL1 was collected from silty fine-grained sand at the bottom of Unit 6 for IRSL dating (Fig. 3.4). Unit 6 is interpreted as cryoturbated loess and marks a change in depositional environment from Unit 5 to a period of relatively sparse vegetation and high landscape instability. Unit 7 is similar sedimentologically to Unit 5, also contains tephras and is interpreted as a weathered fluvial deposit.

Unit 8 comprises 1.5-3.5 m of well sorted, bedded and laminated, inorganic, fine- to medium-grained sand, silt and clay with a few pebbles. Its lower contact is interbedded with Unit 7. Ripples, normally graded beds and multiple, 25-50 cm thick diamict beds were observed in this unit. At its upper contact, it is interbedded with trough cross-bedded sand and gravel similar to units 5 and 7. These beds are approximately 30-60 cm thick, and the gravel beds are loaded into the sand beds. The sand beds at the top of the unit are heavily deformed, brecciated, faulted and weakly oxidized.

Unit 8 extends laterally for >40 m at SC8 (Fig. 3.5). The upper and lower contacts and the bedding in this unit are inclined ~11-12^{o} downstream. This unit is interpreted as glaciolacustrine based on the lack of organics, the diamict beds that likely represent frequent mass wasting events into the lake near the ice margin, and the proximity to Unit 10, interpreted below as a till. The inclination of the bedding indicates that this unit, and probably the other inclined beds at Silver Creek, was tilted post-depositionally. Sample SC8-IRSL2 was collected from a sand bed at the bottom of Unit 8 for IRSL dating (Fig. 3.5). Paleomagnetic samples collected in Unit 8 are normally magnetized, but provided no addition information.

Unit 9 is poorly preserved and only exposed at SC8 and SC9. It is composed of massive, coarse-grained gravel. It is interpreted as advanced glaciofluvial outwash because of its coarseness it is and its association with the overlying Unit 10.

Unit 10 is a consolidated, dark grey, 2-4 m thick, silty-sand diamict. It has 30% subrounded to angular clasts ranging in size from pebbles to boulders, with an average size of small pebbles. Many of these clasts are striated. This unit has a sharp lower contact, with a few cobbles and boulders loading into the underlying sand beds. It has a spread bimodal to polymodal fabric near its upper contact (Fig. 3.6; Hicock et al.,1996). The primary eigenvector of this fabric is oriented towards 104^{o}. One sand lens was observed in this unit at its upper contact at SC10. Unit 10 is interpreted as a till based on its consolidation, abundance of striated clasts and its extent.

Unit 11 consists of 2-5 m of poorly sorted gravel with a silty fine- to coarse-grained sand matrix. It is lenticular and has an unconformable lower contact that undulates by ~1 m. This unit is composed of >50% well rounded to angular clasts ranging from pebbles to boulders, with an average grain size of cobble. At SC10, the unit fines upwards with fewer cobbles and boulders. Unit 11 is laterally variable; at both SC10 and 11, the top 1 m comprises unoxidized, interbedded gravel and finer-grained beds composed of deformed <25 cm thick sand and <10 cm silt and clay. It is interpreted as proximal or subglacial glaciofluvial sediment based on its poor sorting, coarseness and association with the tills in units 10 and 12.

Unit 12 is 2-5 m thick, consolidated, light to dark grey, massive, coarse-grained diamict. It contains 20-40% subrounded to subangular, striated, pebble- to boulder-sized clasts of various lithologies. It has a silty fine- to medium-grained sand matrix and a sharp lower contact. At SC10, where it overlies sand and gravel beds, the sand beds are faulted and there are injection features emanating from the diamict that penetrate 50 cm into the gravel beds below. It has a polymodal fabric near its upper contact (Fig. 3.6). There are several heavily deformed lenses of clay, silt and sand throughout this unit. Unit 12 is interpreted as a till based on its consolidation, faulting in underlying units and the presence of striated clasts.

Unit 13 is composed of interbedded sand, gravel and organic-rich beds. Rare 15-50 cm thick laminated clay beds are also present. The sand beds are weakly stratified, light to dark brown and composed of silty fine- to coarse-grained sand. The gravel beds are moderately sorted and either supported by pebble- to cobble-sized, well

rounded to subangular clasts, or by a coarse-grained sand matrix. The clasts are weakly imbricated parallel to the modern creek. The gravel beds include partially weathered clasts and evidence of cryoturbation. Unit 13 has a sharp, unconformable lower contact and thickens downstream at SC11 from ~5-10 m to 15-20 m. It is more weathered and oxidized towards its lower contact. In its upper half, the sand beds thin and have fewer organics, and the gravel beds become well sorted, with a higher matrix content. In the top 2 m however, the clast percentage and grain size increase and the beds are unoxidized. The unit has numerous tephras deposited throughout. Sample SC11-IRSL3 was collected in the lowest sand bed in Unit 13 for IRLS dating to constrain the underlying till. Unit 13 is interpreted as a non-glacial, fluvial floodplain deposit.

Unit 14 is a weakly stratified to massive, pebble to boulder-sized gravel with well rounded to subangular clasts supported in a medium- to coarse-grained sand matrix. It has a sharp lower contact. It is poorly sorted near the lower contact, but the sorting improves with height. It is 8-12 m thick downstream, thins to <1 m upstream and is unoxidized throughout with no evidence of subaerial weathering. At its upper contact, it has <1 m thick beds and lenses of interbedded, well sorted silt and fine- to coarse-grained sand. This unit is interpreted as advance outwash because of its poor sorting, coarseness and association with the till interpreted for Unit 15.

Unit 15 consists of a laterally variable diamict that is exposed near the top of all the sites. At the furthest downstream exposures, it is up to 12 m thick, consolidated, light grey to brown, and has a clast percentage that ranges from 30-35% to >45% at its upper contact. Further upstream, Unit 15 is 2-4 m thick, light brown, only weakly consolidated and has 20-25% clasts, although this percentage also increases at its upper contact. At all locations, it has a medium- to coarse-grained sand matrix, a sharp lower contact and striated, well rounded to angular clasts that range in size from pebbles to >2 m diameter boulders. This unit is interpreted as till because of its erosive lower contact, the abundance of striated clasts, its extent and spread bimodal fabric (Fig. 3.6) at its lower contact that suggests ice flow to the northeast. The higher clast percentage at its upper contact could be a lag from post-depositional weathering in the upper 50 cm or represent a transition to an ablation environment.

Unit 16 is 2-5 m of massive, inorganic, fine-grained sand and well sorted gravel underlying interbedded and laminated peat and organic-rich, fine- to medium-grained sand and silt. The gravel has a silty fine- to coarse-grained sand matrix, subrounded clasts and no observable cobbles or boulders. This gravel is clast supported at some sites. The gravel and sands beds at the lower contact of this unit are interbedded with the underlying diamict at some locations. At SC13, this contact is strongly deformed and faulted, with >1 m sand and gravel beds mixed into the top of the underlying till. The organic-rich beds contain visible woody-debris and a thick, Type II tephra (Preece et al., 2011a) that likely correlates to the late Holocene White River Ash (Lerbekmo et al., 1975; Clague et al., 1995). This unit is interpreted as being deposited on a non-glacial, fluvial floodplain that represents a stable surface prior to incision of the modern creek.

3.6.2. Radiocarbon Chronology

Four samples were analyzed using AMS radiocarbon dating. Three ages from Unit 13 provide mid-MIS 3 ages, between ca. 36.2-35 ^{14}C ka BP (Table 3.1). The error associated with UCIAMS-112441 reflects the small sample mass (0.056 mg C) of the sample following pre-treatment. Unfortunately, the only datable material in this unit was compressed, weathered and likely reworked wood. However, the similarity between the resulting ages, and to the age of the IRSL sample collected from the same unit (see results below) suggest that reworking was limited and does not affect the age interpretation. The fourth radiocarbon date, from Unit 16 (UCIAMS-135204), provides an Early Holocene age of 7095 ± 25 ^{14}C yrs BP.

3.6.3. Infrared Stimulated Luminescence Dating

Three samples were dated from Units 6, 8 and 13 using IRSL (Table 3.2; Figs. 3.7, 3.8). The equivalent doses (De) range from 43 ± 5 Gy to 318 ± 12 Gy (Table 3.2). In the case of samples SC7-IRSL1 and SC8-IRSL2, the natural luminescence is in the slightly supralinear part of the growth curve (Fig. 3.7). Correction for fading thus uses

Table 3.1. Radiocarbon dates from this study, Lowdon et al. (1970) and Denton and Stuiver (1967).

This Study						Lowden et al. (1970)	
Lab #		UCIAMS-112441	UCIAMS-112439	UCIAMS-74727	UCIAMS-135204	GSC-734	GSC-769
Field Sample		09DTSC12-M1	BCW-SC-M2	09DTSC11-M5	13SC7-M1		
Site		SC12	SC11	SC11	SC7	SC11	SC11
Unit		13 (Same as Y-1357)	13 (Same as Y-1357)	13	16	13 (Same as Y-1356)	13 (Same as Y-1385)
Material / Taxon		Weathered wood	Weathered wood	Weathered wood	Weathered wood	Wood-bearing organic lens	Wood-bearing organic lens
$d^{13}C$ (‰)		Sample too small	-28.1	-27.1	-25.3		
±			0.1	0.1	0.1		
Fraction Modern		0.0129	0.0113	0.0110	0.4135		
±		0.0056	0.0008	0.0004	0.0010		
$D^{14}C$ (‰)		-987.1	-988.7	-989.0	-586.5		
±		5.6	0.8	0.4	1.0		
^{14}C age (BP)		35000	36010	36240	7095	>35 000	29600
±		3500	600	310	25		460
Calibrated ages*	from	47018	39857	39582	6010		32691
	to	32629	37482	38253	5928		30838
Calibrated ages**	from	41551	39328	39299	6023		32247
	to	33933	38106	38601	5911		31376

* 95% probability
**68% probability

Denton and Stuiver (1967)

Lab #		Y-1355	Y-1486	Y-1356	Y-1385	Y-1488	Y-1357
Field Sample							
Site		SC8	SC8	SC11	SC7	SC8	SC10
Unit		7	10	13	13	13	16
Material / Taxon		Bulk organics	Bulk organics	Bulk organics	Bulk organics	Bulk organics	Bulk organics
^{14}C age (BP)		>46400	>49000	37700	30100	33400	7340
±				+1500, -1300	600	800	140
Calibrated ages*	from			43325	33469	37767	6462
	to			37549	31110	33937	5930
Calibrated ages**	from			41399	32761	36626	6361
	to			38766	31746	34666	6072

* 95% probability
**68% probability

the dose rate correction (DRC) of Lamothe et al. (2003). Similar correction procedures have been successfully applied to loess from Alaska (e.g. Auclair et al., 2003; Jensen et al., 2011) and Yukon (Turner, unpublished data from the White River sites). Fading values are consistent between samples along the Silver Creek exposures and tend to average ~4.8% per decade. This implies a correction of ca. 40% to the natural luminescence normalized intensities.

The 39 ± 3 ka age from sample SC11-IRSL3 (Unit 13) is within one standard deviation of the calibrated radiocarbon ages above it (ca. 39-38 cal ka BP; Table 3.1). The two stratigraphically lower Silver Creek IRSL samples, SC7-IRSL1 (Unit 6) and SC8-IRSL2 (Unit 8), yielded ages of >300 ka and 236 ± 21 ka, respectively. Sample SC8-IRSL2 was collected from the bottom of a glaciolacustrine bed in Unit 8, below proximal advanced outwash and till in units 9 and 10. This sample site marks a transition from a non-glacial to a glacial environment. It should be noted that this age may be a maximum age as the possibility of partial bleaching cannot be precluded, given the depositional environment.

Table 3.2. Infrared stimulated luminescence data and age assessment for three samples at Silver Creek. For the SC7-IRSL1, the rate is the Do value.

Sample	SC11-IRSL 3a Unit 13	SC8-IRSL2 Unit 8	SC7-IRSL1 Unit 6
^{238}U [ppm]	2.04 ± 0.2	1.42 ± 0.14	1.56 ± 0.16
^{232}Th [ppm]	3.55 ± 0.21	2.97 ± 0.18	3.64 ± 0.22
^{40}K [%]	0.82 ± 0.03	0.98 ± 0.03	0.85 ± 0.03
Water content	13 ± 4	27 ± 3	25 ± 4
Da (Gy/ka)	2.27 ± 0.10	2.06 ± 0.07	2.02 ± 0.07
De (Gy)	43 ± 5	204 ± 10	318 ± 12
Uncorrected Age (ka)	19 ± 2	99 ± 6	157 ± 8
g_{48h} value (%/Decade)	4.9 ± 0.5	5.1 ± 0.5	4.8 ± 0.5
DRC age (ka)	39 ± 3	236 ± 21	320 ± 30[1]

[1] SC7-IRSL1 is interpreted to be a minimum age. An age of >300 ka is used in the text.

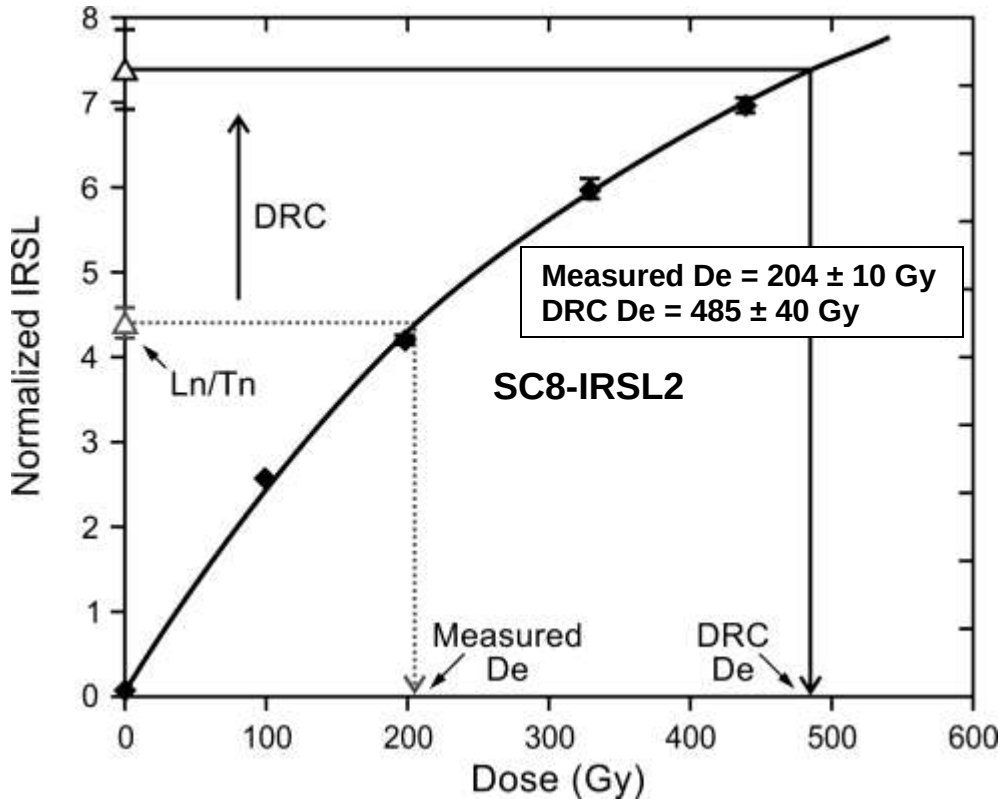

Figure 3.7. Normalized regenerative grown curve to determine the equivalent dose (De) using a modified SAR technique (see text). The De measured and calculated using the dose recovery correction (DRC De) of Lamothe et al. (2003) are shown.

The natural luminescence corrected for anomalous fading for SC7-IRSL1 is not statistically distinguishable from the laboratory saturation luminescence. This sample is thus likely beyond the reasonable limit of the IRSL method and ca. 300 ka is therefore considered a minimum age. This apparent age is calculated using the characteristic dose in the exponential (Do).

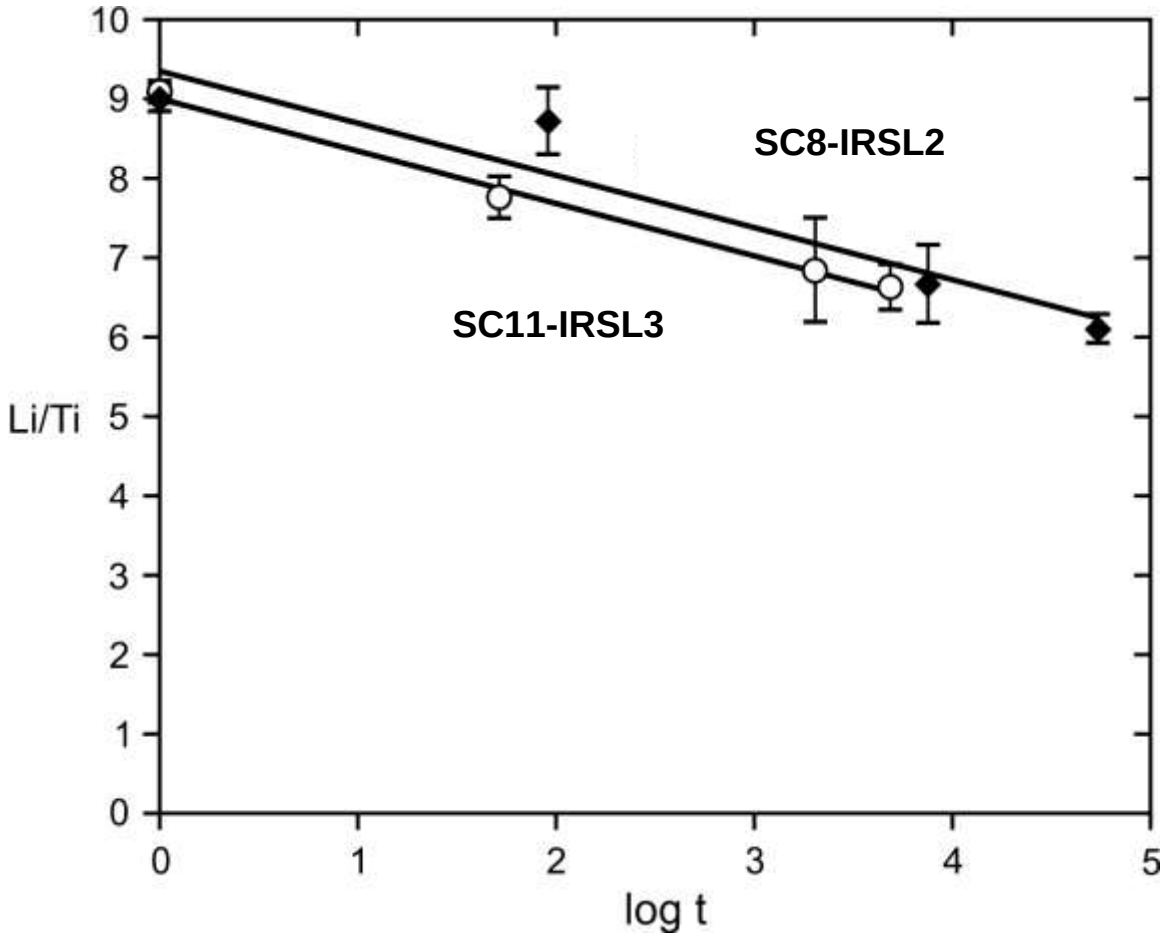

Figure 3.8. Anomalous fading of SC8-IRSL2 and SC11-IRSL3. Each point is an average of about eight aliquots for the delayed measurements and 36 aliquots for the prompt measurement. The time was approximately 0.24 hr and the dose used for regenerating luminescence was 110 Gy.

3.6.4. Paleoecology

Three units were sampled for detailed paleoecological analysis: units 6, 8 and 13. The lack of macrofossils and poor pollen preservation in Unit 6 precludes any interpretation for this unit. There also were no macrofossils present in Unit 8 and the preservation of pollen grains in this sample was too poor to differentiate between *Picea*, *Pinus* or *Abies*. However, the abundance of Pinaceae pollen grains in sample SC8-PO1 (Unit 8; Fig. 3.9) suggests a forest environment existed during deposition of the bottom of this unit.

The plant and insect macrofossil data from Unit 13 indicate a willow-rich riparian environment with alternating high and low energy stream conditions (Tables 3.3 and 3.4). Although distinctive organic-rich beds were sampled, the lack of preservation of macrofossils led to difficulty in identifying plant fossils. Most of the insect fossils consist of small fragments with evidence of pitting and bleaching. Samples SC11-M2 and M3 were deposited in a dry, riparian environment populated by willows (Anderson, 1989, 1997). Comparatively, the plant and insect macrofossils in samples SC11-M5 and BCW-SC-M2 suggest a lower energy, broader floodplain with adjacent pools or thermokarst ponds possibly up to 3 m deep, populated by pondweed (*Potamogeton* sp.), emergent sedges, moss and aquatic insects. This is supported by the presence of <9 cm thick, cryoturbated silt and clay beds in the horizons SC11-M5 and BCW-SC-M2 were sampled from.

The pollen data from Unit 13 generally support the macrofossils and indicate regionally extensive tundra dominated by herbs and forbs, especially grasses and sedges, with almost no trees (Fig. 3.9). Some of these samples have low pollen sums and therefore care should be taken in interpreting the results. However, the low willow percentages in PO3 are interesting considering the abundance of willow macrofossils in M3. Although this may be partly because willow is a poor pollen producer, it also suggests that there is regionally less willow than the relatively local signature of the macrofossils indicates. Sample SC12-PO1 has higher amounts of undifferentiated Pinaceae pollen (19%), suggesting that conifers expanded at least once during deposition of Unit 13.

Table 3.3. Plant macrofossils from SC11. Sample locations shown in Fig. 3a.

Site	SC11	SC11	SC11	SC11	SC11	SC11
Macrofossil sample	BCW-M2	BCW-M4	M2	M3	M5	M7
Fungal remains						
fungal balls			abundant			
fungal sclerotia	8			7		
Non-vascular plants						
Bryophytes	fragments			fragments	fragments	fragments
Sphagnum sp.						
Vascular plants						
Equisetaceae						
Equisetum sp.					1	
Potamogetonaceae						
Potamogeton sp.					4	
Poaceae	15					
Cyperaceae						
Carex lenticular type	~100			2	38	1
Carex trigonous type	7				10	
Eriophorum sp.			3			
Juncaceae						
Juncus/Luzula type	1					
Juncus sp.			19			
Salicaceae						
Salix sp.	2		3	48		
Betulaceae						
Betula sp.			1			
Ranunculaceae						
Ranunculus sp.	9					
Rosaceae						
Potentilla sp.			1			
Potentilla smooth type	8				2	
Wood/twig	~40	Sm. Frag.	Sm. Frag.	Sm. Frag.	Sm. Frag.	Sm. Frag.
Unknown plant macrofossil taxa	~100		6	2	25	1
Reworked pre-Quaternary coal						5

Table 3.4. Insect macrofossils from SC11. Sample locations shown in Fig. 3a.

Site	SC11	SC11	SC11	SC11	SC11
Macrofossil sample	BCW-M2	BCW-M4	M2	M3	M5
ARTHROPODA					
Insecta					
Orthoptera					
Acrididae	1				
Hemiptera					
Cicadellidae		1			
Coleoptera	1		2		Misc. Frag.
Caradibae	4	3			3
Bembidon sp.		3			
Pterostichus sp.					1
Dytiscidae	4				5
Hydroporus sp.	4				2
Hydrophilidae	2				
Helophorus sp.	2				
Curculionidae	1		4	3	1
Connatichela artemisiae Anderson			3?		
Lepidophorus lineaticollis Kirby		8	25	3	
Isochnus? sp.			3		
Trichoptera	4				10
Diptera	1	1			1
Tipulidae					
Tipula sp.	2				1
Hymenoptera					
Ichneumonidae	1				
Arachnida					
Aranea	1				
Erigonida					
Erigone sp.	1				
Unidentified animal taxa				1	

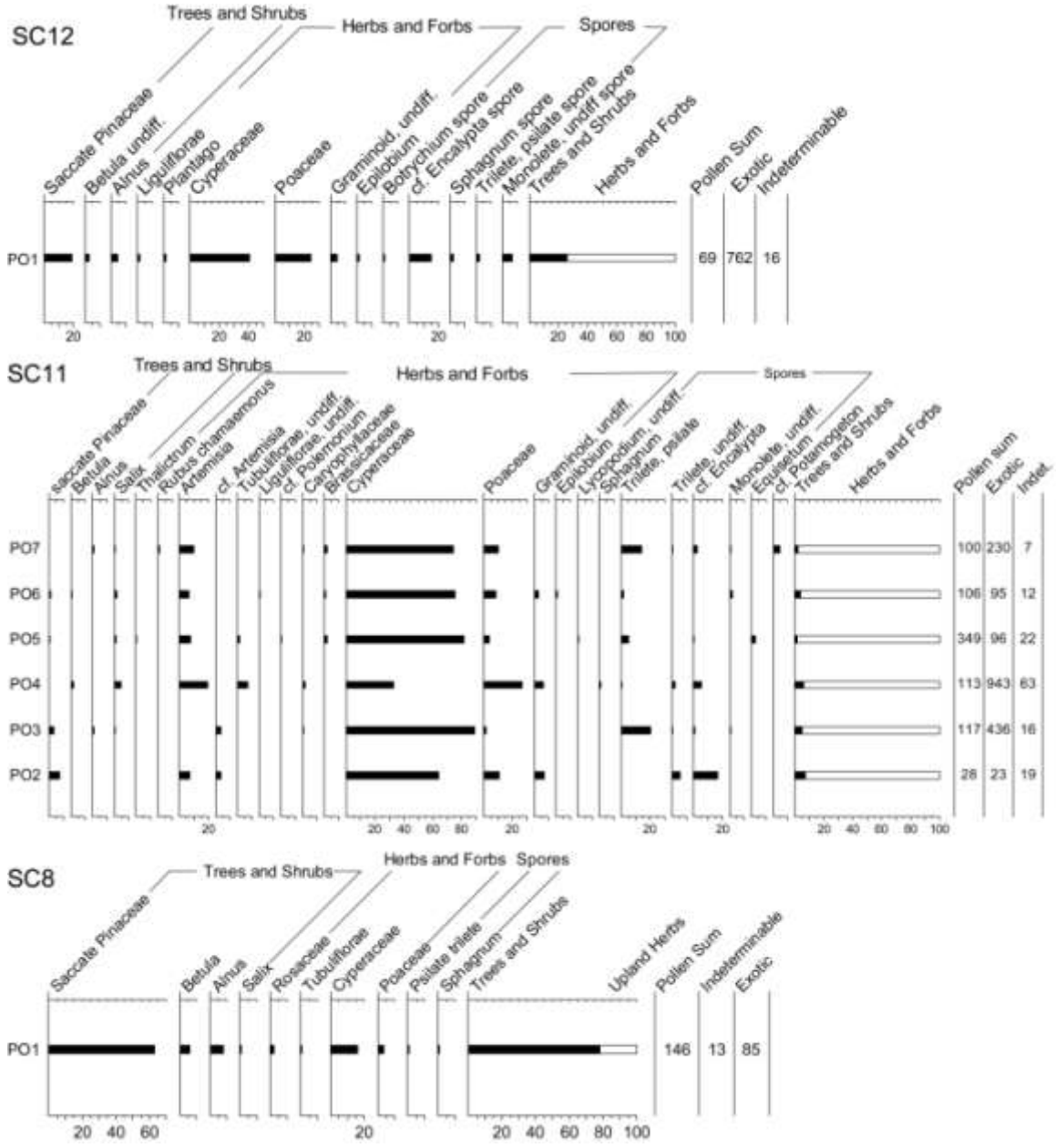

Figure 3.9. Pollen percentages for samples at SC8, 11 and 12. SC12-PO1 and the SC11 samples were collected from Unit 13. SC8-PO1 is from the bottom of Unit 8. Sample locations are shown in figures 3.3-3.5. Pollen (PO) samples at SC11 were collected at the same location as macrofossil samples (M).

3.7. Discussion

Our analysis of the sedimentology and chronology of the Pleistocene record at Silver Creek generally confirms Denton and Stuiver's (1967) interpretation of three glaciations separated by non-glacial weathering intervals and expands the record to include two earlier glaciations (Fig. 3.10). Units 10, 12 and 15 correlate to Denton and Stuiver's (1967) Shakwak, Icefield and Kluane tills, respectively. These three most recent glaciations are constrained by IRSL and radiocarbon dating to being younger than at least MIS 8.

The radiocarbon ages and an IRSL age in Unit 13 indicate that it was deposited ca. 36-35 ^{14}C ka BP, in mid-MIS 3. This unit was named the Boutellier interval by Denton and Stuiver (1967). These ages are tightly spaced, but generally agree with data from Lowdon et al. (1970) and Denton and Stuiver (1967), and indicate that Unit 13 was deposited in just a few thousand years. The environment during this time was a herbaceous tundra, with local willow stands on floodplains. This is similar to Schweger and Janssens' (1980) interpretation of a tundra or meadow-tundra steppe environment with local willow groves. However, the macrofossil data and sedimentology indicate that Silver Creek also experienced periods of lower energy deposition during MIS 3, with up to 3 m deep pools or ponds present on the floodplain. Arboreal pollen in Unit 13 at SC12 suggests a period of forest expansion during MIS 3, although the poor precision on the radiocarbon age from this site makes it unclear if this occurred before or after the samples at SC11. The age of 13SC7-M1 (ca. 7.1 ka ^{14}C BP) is similar to Denton and Stuiver's (1967) age of 7340 ± 140 ^{14}C yrs BP from the same unit, but is younger than some other post-glacial ages in southwest Yukon (e.g. Denton and Stuiver, 1966; Lacourse and Gajewski, 2000; Bunbury and Gajewski, 2009). Early Holocene and MIS 3 ages for units 16 and 13 constrain units 14 and 15 to outwash and till associated with glaciation in MIS 2.

Units 8-12 are constrained by SC8-IRSL2 and overlying radiocarbon dates to between MIS 8-4. Based on the sedimentology of Unit 8 and its association with the overlying outwash and till in units 9 and 10, it was probably deposited in a proglacial lake adjacent to advancing ice. A non-glacial to glacial transition is supported by the arboreal

pollen at the base of Unit 8 that suggests a forest existed in the area prior to formation of the lake. Conifer forest conditions were widespread in eastern Beringia during MIS 5a and 5e (Hamilton and Brigham-Grette, 1991; Reyes et al., 2010a; Schweger et al., 2011; Turner et al., 2013), and have been interpreted for MIS 7 (e.g. Schweger, 2003; Schweger et al., 2011).

If SC8-IRSL2 (236 ± 21 ka) is accurate and units 8-10 were deposited shortly after ca. 236 ka, this non-glacial to glacial transition could represent the MIS 7c/7b boundary. In this scenario, the till in Unit 12 could be from MIS 6 or 4. Alternatively, SC8-IRSL may contain inheritance and overestimate the age of this transition. Given the glaciolacustrine interpretation, it is possible that the sediment sampled were not completely bleached prior to deposition. In this case, units 8-10 could represent the MIS 7/6 boundary (ca. 190 ka) and units 10 and 12 could be from MIS 6 and 4, respectively. The difference in inclination of the beds in units 8-10 (>10^{o}) and units 13-15 (<5^{o}) supports the presence of an unconformity and a >MIS 6 age for Unit 8. However, further work, potentially involving terrestrial cosmogenic nuclide dating, is needed to resolve this part of the record.

Units 1-7 were deposited before 236 ± 21 ka. Units 5-7 are potentially from early MIS 7. However, the >300 ka age for SC7-IRSL1 in Unit 6 suggests that units 5-7 likely span at least one MIS and may contain multiple unconformities. The change from fluvial to eolian deposition in Unit 6, coupled with the lack of identifiable pollen or macrofossils in this unit, indicates a significant transition in environment to an unstable landscape, potentially with less vegetation and a drier climate, than the bounding units 5 and 7. This could indicate stadial conditions, or even a restricted ice advance, sometime before MIS 7. The two lower tills forming units 2 and 4 were deposited during Early to Middle Pleistocene glaciations (e.g. MIS 10, 12, 16, etc.).

The base level of Silver Creek has varied during Pleistocene non-glacial intervals. The height of the former floodplain above the modern creek in MIS 3 and potentially before ca. 7 ^{14}C ka BP (ca. 30-70 m) suggests a higher base level during these two periods. The size of Kluane Lake likely controls this variability. During the Little Ice Age (ca. 1350 – 1850 AD), southern drainage of the lake was blocked by

increased sedimentation from the expansion of the nearby Kaskawulsh Glacier (Clague et al., 2006). This aggradation resulted in a drainage reversal and the rapid rise of the lake level. It is possible that similarly high sediment delivery also blocked the southern drainage during MIS 3 and following MIS 2, leading to increased base levels and decreased erosion in Silver Creek.

3.7.1. Regional Glacial Correlation

The stratigraphy at Silver Creek contains at least five tills and represents the oldest glacial record in southwest Yukon. These glaciations likely correlate to MIS 2, 4, either mid-MIS 7 or 6, and two Early to Middle Pleistocene glaciations (Fig. 3.10). This stratigraphy confirms that Denton and Stuiver's (1967) Kluane glaciation correlates to the MIS 2 McConnell glaciation. The Icefield glaciation likely correlates to the MIS 4 Gladstone glaciation (Ward et al., 2007) in the Aishihik Lake area and the Mirror Creek glaciation (Rampton, 1971) in the Snag-Klutlan area. The Shakwak glaciation either correlates to the MIS 6 Reid glaciation in central Yukon (Ward et al., 2008, Demuro et al., 2012), which was the most extensive Pleistocene ice advance in southwest Yukon (Turner et al., 2013), or to an earlier, mid-MIS 7 advance.

The two older, poorly-exposed tills were deposited by Pre-Reid glaciations. Although Pre-Reid till is found across central Yukon, marking the maximum extent of Cenozoic glaciation in the area (Duk-Rodkin, 1999), it is lacking in southwest Yukon (Hughes et al., 1969; Bond et al., 2008). The identification of two Pre-Reid ice advances at Silver Creek is the first evidence of Early to Middle Pleistocene glaciations in southwest Yukon. Stratigraphic records of Pre-Reid glaciations near Fort Selkirk (Nelson et al., 2009; Jackson et al., 2012), in the Klondike (Froese et al., 2000; Hidy et al., 2013) and in the Tintina Trench (Duk-Rodkin et al., 2010; Barendregt et al., 2010) indicate that the Selwyn lobe of the northern Cordilleran Ice Sheet advanced multiple times throughout the latest Pliocene to Middle Pleistocene. It is unknown if the Pre-Reid tills at Silver Creek represent the same Pre-Reid ice advances, different periods of ice sheet development, or just growth of local ice in the Kluane Ranges. However, it is unlikely that ice advanced from the Kluane Ranges and not from the St. Elias Mountains.

These tills therefore likely represent two periods of Early to Middle Pleistocene formation of the St. Elias lobe that may correlate to advances of the Selwyn lobe in central Yukon.

3.7.2. Estimate of Pleistocene Uplift Rates Along the Denali Fault

The tilting observed at the Silver Creek exposures could be from uplift associated with movement along the Denali Fault, or it could be from tilting due to sediment loading in the Shakwak Trench. However, the proximity of the Denali Fault to the exposures and its continuous activity during the time that these sediments were deposited, suggests that a tectonic signature at least contributed to this tilting.

The Silver Creek exposures are directly north of the extrapolated location of the Denali Fault, a large dextral transverse fault that extends over 2000 km from British Columbia to Alaska (Fig. 3.2; Dodds, 1995). The glaciolacustrine beds and laminations in Unit 8 are 350 m northeast of the mapped extent of the fault and are continuously laterally exposed for at least 40 m at an angle of 11-14^{o}. Assuming SC8-IRSL2 (236 ± 21 ka) is accurate, this suggests uplift of ~65-90 m on the north side of the Denali fault since between 257-215 ka, a rate of 0.25-0.42 mm/yr. However, this could be a significant underestimate, since it relies on the distance between the extrapolated fault and exposure of Unit 8 at SC8. If the same dip angles are assumed to extend to the nearest point on a northwest trend of where the fault is observed crossing Silver Creek, the total uplift and uplift rate increase to between ~315-400 m and ~1.2-1.9 mm/yr, respectively.

3.7.3. Ice Configuration During Glacial Onset

Prior to ice filling the Shakwak Trench in MIS 6, drainage in the trench was blocked and water levels near Silver Creek rose ~100 m above the modern bottom of the trench. The interbedded fluvial and glaciolacustrine beds at the bottom of Unit 8 were deposited in an increasingly inorganic ice marginal lake during glacial onset. Denton (1965) also identified glaciolacustrine sediment at exposures now obscured along nearby Christmas and Boutellier Creeks in the middle of the Shakwak Trench, below till from the last glaciation. This suggests that the development of a trench-wide lake in the

early stages of glacial advance was a repeated event at the onset of at least two glaciations. This was likely caused by early advance of the Kaskawulsh Glacier down the Slims River Valley, before ice flowed out of the Silver Creek headwaters (Kluane Range) or the St. Elias lobe advanced into the Shakwak Trench. The Kaskawulsh Glacier advanced 3 km during the Little Ice Age (Denton and Stuiver, 1966) and would need to advance another 17 km at the beginning of a glaciation to flow east across the trench and block drainage into Kluane Lake. Using the maximum elevation of Unit 8 at SC8, the resulting lake likely flooded the Shakwak Trench and potentially neighbouring valleys. Although this lake may have connected to larger proglacial lake networks to the south and east, it was likely a local proglacial lake.

Figure 3.10. Regional Middle to Late Pleistocene glacial correlations in central and southwest Yukon compared with the marine oxygen isotope record (Lisiecki and Raymo, 2005). Black squares denote approximate ages of tephras: Dt = Dawson tephra (ca. 25,300 ^{14}C yrs BP; Froese et al., 2006); OCt = Old Crow tephra (124 ± 10 ka; Preece et al., 2011a).

3.8. Conclusions

The Pleistocene exposures at Silver Creek contain the longest direct record of Pleistocene glaciation in southwest Yukon. Five glaciations are constrained by radiocarbon and IRSL dating at these exposures. These glaciations correlate to the MIS 2 McConnell, two Middle Pleistocene glaciations between MIS 8-4, and two older, Pre-Reid glaciations. Pollen and macrofossil data collected from non-glacial sediment deposited in MIS 3 indicate that the environment was a fluctuating riparian floodplain with periods of low and high energy, surrounded by a herbaceous tundra with few to no trees. Conifer forest advanced in the area at least once during MIS 3 and potentially during MIS 7, before glaciation in either mid-MIS 7 or 6. The dip of the Early to Middle Pleistocene units suggests average uplift rates along the nearby Denali fault of up to 1.9 mm/yr over the last ca. 236 ka.

Chapter 4. The timing, extent and forcing mechanisms of Plio-Pleistocene glacial limits in Yukon Territory, Canada

Derek G. Turner[1], Duane G. Froese[2], Brent C. Ward[1], Britta J.L. Jensen[2]

[1]Derek G. Turner & Brent C. Ward, Department of Earth Sciences, Simon Fraser University, 8888 University Drive, Burnaby, B.C., V5A 1S6. Ph. 1-778-782-4564; Fax: 1-778-782-4198, dgturner@sfu.ca.

[3]Duane G. Froese & Britta J.L. Jensen, Department of Earth and Atmospheric Sciences, University of Alberta, 1-26 Earth Sciences Building, Edmonton, Alberta, Canada, T6G 2E3.

4.1. Abstract

Yukon and Alaska contain some of the oldest and richest records of glacial response to Quaternary climate change in North America. The timing and extent of these glaciations is constrained by $^{40}Ar/^{39}Ar$ ages, tephrochronology, cosmogenic nuclides, luminescence and radiocarbon dating. Three glacial limits are preserved in central Yukon from the advances of the northern Cordilleran Ice Sheet in the Late Pliocene-Early Pleistocene to early Middle Pleistocene (Pre-Reid), marine oxygen isotope stage (MIS) 6 (Reid) and MIS 2 (McConnell). In southwest Yukon, tightly-spaced glacial limits date from MIS 6, 4 and 2, with no evidence of more extensive Pre-Reid glaciations. New tephra data suggest that this record is consistent with that preserved in the Delta River area of east-central Alaska, implying similar controls on Pleistocene glaciation over ~500 km.

The regional differences in glacial extent suggest differing boundary conditions influenced the separate ice lobes of the northern Cordilleran Ice Sheet through successive glaciations. The large differences in glacial limits in central Yukon suggest a combination of unglaciated topography and a highly-erodible substrate may have contributed to extensive Late Pliocene-Early Pleistocene ice in this area. Middle to Late

Pleistocene glaciations in central Yukon may have been limited by more resistant substrates and changes to atmospheric circulation due to the formation of the Laurentide Ice Sheet, but were unlikely influenced by changing sea levels or tectonics. The record in southwest Yukon and eastern Alaska indicates that continentality in these areas had already been developed in the Late Pliocene and Early Pleistocene and was the primary control on Plio-Pleistocene glacial limits. Variations in other secondary conditions, such as atmospheric circulation, moisture pathways and topographic adjustments influenced the relatively small differences in these glacial limits.

4.2. Introduction

Northwestern North America contains one of the oldest and richest terrestrial records of Arctic Quaternary climate change (Hopkins, 1982; Froese et al., 2009). The repeated expansion of the northern Cordilleran Ice Sheet and local montane glaciers in response to changes in Pleistocene climate left a series of distinct glacial limits across Alaska and Yukon. The application of tephrochronology, Ar-Ar, luminescence, AMS radiocarbon and terrestrial cosmogenic nuclide dating techniques, provides a unique opportunity to date these limits and evaluate potential boundary conditions that influenced them.

Ice advancing from isolated local massifs and the northern Cordilleran Ice Sheet covered large parts of Yukon and Alaska throughout the Pleistocene. This ice sheet is better described as an ice complex due to its formation by semi-independent ice lobes that were precipitation-limited and strongly topographically controlled (Jackson et al., 1991, Ward et al., 2007). The distinct Selwyn, Cassiar, St. Elias and Eastern Coast Mountain ice lobes spread up to 400 km across Yukon from their sources during successive periods of high global ice volume (Fig. 4.1; Duk-Rodkin, 1999). Some of these advances were more extensive than the last glacial maximum in marine oxygen isotope stage (MIS) 2, resulting in the preservation of multiple ice limits from earlier glaciations (Hughes et al., 1969; Duk-Rodkin, 1999). Similar records of more extensive, pre-last glacial maximum limits are preserved from ice advancing out of the Ogilvie Mountains in central Yukon (Vernon and Hughes, 1966) and the Brooks and Alaska Ranges in Alaska (Briner and Kaufman, 2008).

The purpose of this paper is to review the chronology of Cordilleran and montane glacial limits in Yukon and to use these limits to evaluate regional differences in potential forcing mechanisms on glacial extent across Yukon throughout the Pleistocene. Although this paper concentrates on Yukon, we also use new tephra data to correlate the glacial limit record in southwest Yukon to the Delta River area in east-central Alaska, 500 km to the west.

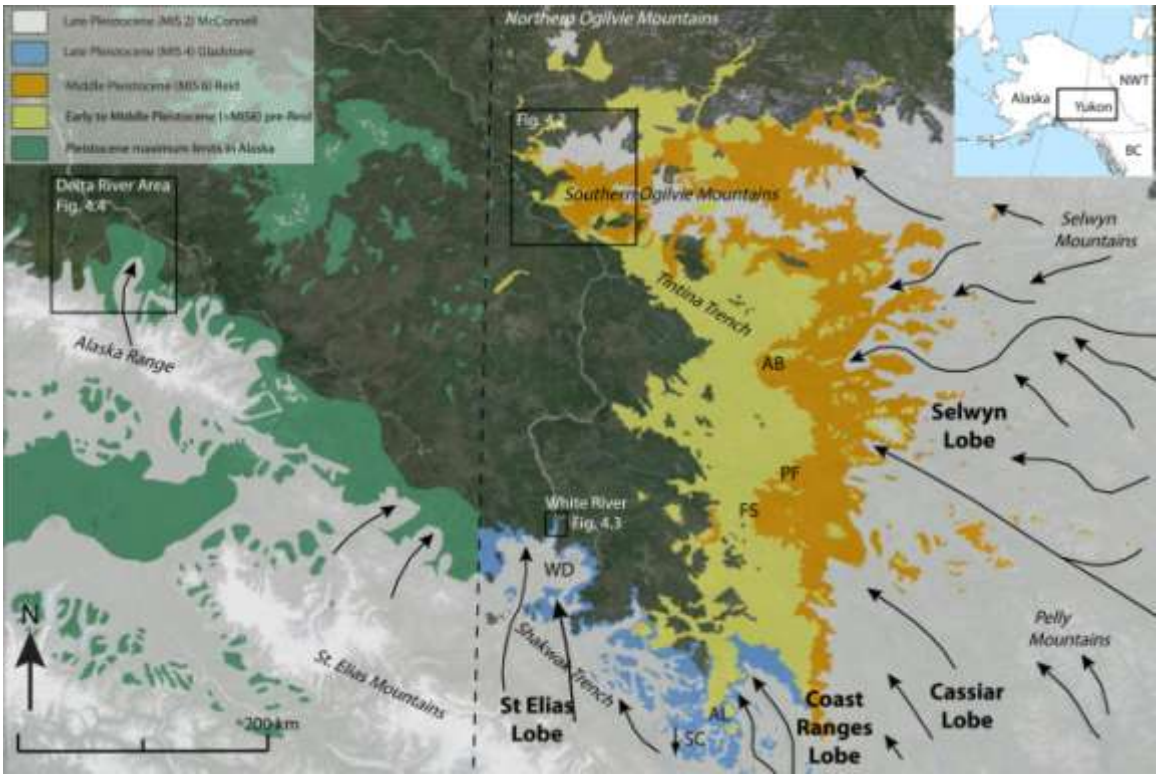

Figure 4.1. Glacial limits of the northern Cordilleran Ice Sheet and local montane ice along the glaciated fringe of Yukon and eastern Alaska. Black boxes show locations of figures 4.2 (Southern Ogilvie Mountains), 4.3 (White River) and 4.4 (Delta River). Locations mentioned in the text: AB = Ash Bend; PF = Pelly Farm; FS = Fort Selkirk; AL = Aishihik Lake; WD = Wellesley Depression. Silver Creek (SC) is located ~50 km south-southwest of Aishihik Lake. Glacial limits in Alaska are from Manley and Kaufman (2002). Yukon glacial limits and black ice flow arrows are from Duk-Rodkin (1999), modified in southwest Yukon based on mapping by Bond et al. (2008).

4.3. Previous Work

Three broadly synchronous glacial surfaces were mapped and correlated across Yukon based on geomorphic expression and soil development (Hughes et al., 1969; Tarnocai et al., 1985; Smith et al., 1986). The youngest McConnell glacial limit is constrained to MIS 2 (Jackson et al., 1991) and comprises sharp-crested moraines and modern soils. The penultimate limit has rounded, moderately-weathered moraines. Recent work has shown that this limit is composed of at least two separate glacial limits deposited in MIS 6 (Reid glaciation) in central Yukon (Ward et al., 2008; Demuro et al., 2012) and MIS 4 (Gladstone glaciation) in southern Yukon (Ward et al., 2007; Turner et al., 2013). In central Yukon and the Southern Ogilvie Mountains, penultimate deposits are covered by the Diversion Creek paleosol that is better developed than the modern soil, suggesting a last interglacial, MIS 5 (*sensu lato*) exposure (Smith et al., 1986). The most extensive limit in central Yukon consists of poorly-preserved glacial surfaces, in some cases only identifiable by meltwater channels and erratics, and the strongly developed Wounded Moose paleosol (Smith et al., 1986; Hidy et al., 2013). This limit is an amalgamation of multiple Early to Middle Pleistocene glaciations and is termed the Pre-Reid limit (Hughes et al., 1969).

4.4. Central Yukon

Central Yukon was glaciated by ice from the Selwyn Mountains to the east and the Cassiar Mountains to the southeast (Fig. 4.1). Early work by Bostock (1966) defined the Reid glaciation in this area as the penultimate limit in the Stewart River Valley, near the Reid Lakes. Hughes et al. (1969) grouped the glacial sediment beyond the Reid limit and used the term Pre-Reid for these glaciations. Based on overlying, non-finite bulk sediment radiometric radiocarbon ages, Hughes et al. (1969) interpreted the Reid to be older than the classical Wisconsinan of the mid-western continental North American stratigraphy.

The earliest and most extensive advance of the Selwyn lobe of the northern Cordilleran Ice Sheet in central Yukon flowed down the Tintina Trench during the latest

Pliocene, merging with montane ice from the Ogilvie Mountains. Paleoflow measurements and clast lithologies indicate a Selwyn Mountain source for this ice (Bond, 1997; Froese et al., 2000). Paleomagnetic, tephrochronolgic and terrestrial cosmogenic nuclide data constrain the glaciofluvial Klondike gravel associated with this advance to the late Gauss Chron, approximately 2.64 $^{+0.02}/_{-0.18}$ Ma (Froese et al., 2000; Hidy et al, 2013). Ice-wedge casts in the underlying, Pliocene-age White Channel gravels indicate that continental conditions suitable for permafrost development first existed at this time (Burn, 1994; Froese et al., 2000).

Although multiple glaciations filled the Tintina Trench northeast of Dawson (see discussion below), the Selwyn lobe only merged with ice from the Ogilvie Mountains during the initial advance. The preservation of outwash gravels of the Klondike gravel-equivalent, late Pliocene Flat Creek beds within the Pre-Reid glacial limit (Bostock, 1942; Froese, 2005) suggests that the Selwyn lobe did not advance over that surface in subsequent glaciations. Mapping in the Mt. Nansen area indicates that the Cassiar lobe was also extensive during the Pre-Reid (Hughes, 1969; Duk-Rodkin, 1999).

There were at least three, less-extensive Pre-Reid advances of the Selwyn lobe in the Fort Selkirk area (Jackson et al., 1996, 2012; Nelson et al., 2009). The earliest of these was the Ne Ch'e Ddhawa glaciation, which is constrained to ca. 2.1 Ma by a volcanic eruption beneath at least 300 m of ice (Jackson et al., 1996, 2012). The second, Fort Selkirk glaciation, occurred between the earlier Ne Che Ddhawa glaciation and deposition of the Fort Selkirk tephra (1.48 ± 0.11 Ma; Westgate et al., 2001). Jackson et al. (2012) interpreted that this event immediately preceded MIS 54. The later Forks glaciation occurred between ca. 1.3 Ma and the end of the Matuyama chron, ca. 0.78 Ma.

Until recently, the age of the Reid glaciation was enigmatic. Initial dating using a $^{40}Ar/^{39}Ar$ age of 311 ± 32 ka on basalt below Reid outwash (Huscroft et al., 2004), and the presence of several tephras, one of which (UT1052) was erroneously correlated to the 190 ± 20 ka Sheep Creek tephra-Fairbanks (SCt-F; Berger et al., 1996), above Reid drift at Ash Bend suggested a MIS 8 age for the Reid glaciation (Westgate et al., 2001). However, further analyses have shown that there are many similar, but distinguishable,

Sheep Creek tephras. The tephras at Ash Bend are considerably younger (<ca. 80 ka; Westgate et al., 2008) than SCt-F. Subsequent identification by Ward et al. (2008) of Old Crow tephra (124 ± 10 ka; Preece et al., 2011a) above Reid outwash at Pelly Farm, and optically stimulated luminescence ages of 158 ± 18 ka and 132 ± 18 ka in glaciofluvial sand bracketing Reid till (Demuro et al., 2012) at Ash Bend, confirm that the penultimate Reid limit in central Yukon was deposited in MIS 6. Cosmogenic ^{10}Be ages on a penultimate surface near the Stewart River (91.4 ± 8.4 ka, 102.0 ± 9.4 ka) also support a MIS 6, rather than MIS 4, age (Stroeven et al., 2010). There is currently no geomorphic or stratigraphic evidence that the MIS 4 Gladstone glaciation was more extensive than the MIS 2 limit in central Yukon (Hughes et al., 1969; Duk-Rodkin, 1999).

The late Wisconsinan (MIS 2), McConnell glaciation in central Yukon covered 25% less area than the maximum Pre-Reid glaciation (Fig. 4.1; Hughes et al., 1969; Jackson, 1994, 2000). The timing of MIS 2 ice advance and retreat of the Selwyn lobe is loosely constrained by radiocarbon and cosmogenic nuclide dating. An AMS radiocarbon age on *Corispermum hyssopifolium* seeds in organic-rich silt and sand overlain by advance glaciofluvial gravel and till in the Mayo area (Matthews et al., 1990b) provided an age of 29 600 ± 300 ^{14}C yrs BP (TO-292). A similar age of 26 350 ± 280 ^{14}C yrs BP (TO-393) obtained from a *Bison* sp. radius in gravel and colluvium below till along the Ketza River (Jackson and Harington, 1991) suggests that the ice sheet developed at the end of MIS 3 at the earliest.

Another radiocarbon date from a separate exposure in the Mayo area of 38 100 ± 1330 ^{14}C yrs BP (GSC-4554) on an *in-situ*, rooted willow stump (Matthews et al., 1990b) is considered unreliable due to the abundance of associated spruce needles and pollen. Two new AMS radiocarbon dates from the same unit returned non-finite ages and indicate a MIS 5 age (Table 4.1). Sample DF08-102, taken from a *Picea* sp. stump 4 m above river level and below McConnell till, returned an age of 54,400 ± 220 ^{14}C yrs BP. This is near radiocarbon background and suggests a non-finite, likely MIS 5 age for the spruce.

Table 4.1. Radiocarbon ages from samples of a tree stump (*Picea* sp.) at 4 m above river level and below McConnell (MIS 2) till at the Mayo Section. These samples were collected from the same unit as GSC-4554 (Matthews et al., 1990b) and suggest a non-finite, likely MIS 5 age.

UCIAMS #	Field Sample	$\delta^{13}C$ (‰)	±	Fraction Modern	±	$\delta^{14}C$ (‰)	±	^{14}C age (BP)	±
51318	QueetsA-batch2	-24.8	0.1	0.0011	0.0001		0.1	54920	430
51325	DF08-102	-16.7	0.4	0.0011	0.0003		0.3	54400	2200

Deglaciation of the Selwyn lobe was achieved by a combination of frontal retreat and stagnation, with deposition of moraines near the limits and evidence of downwasting near ice sources in the Selwyn Mountains (Jackson, 1987, 2000; Jackson et al., 1991). The timing of deglaciation is marked by moraine stabilization in the Pelly Mountains and Tintina Trench ca. 12 ka (Stroeven et al., 2010) and in the Selwyn Mountains between 13 ± 0.6 ka and 9.2 ± 0.2 ka (Turner, 2008), and the disappearance of ice in the Selwyn Mountains by ca. 9 ^{14}C ka BP (MacDonald, 1983). At least one re-advance of the Selwyn lobe into the Pelly Mountains occurred during deglaciation (Plouffe, 1989; Bond and Kennedy, 2005; Bond, 2007).

4.5. Ogilvie Mountains

The southern Ogilvie Mountains were glaciated numerous times during the Plio-Pleistocene (Vernon and Hughes, 1966), with ice extending south to the Tintina Trench (Duk-Rodkin et al., 2010; Barendregt et al., 2010), and north towards the Ogilvie River (Thomas and Rampton, 1982; Duk-Rodkin, 1996). Extensive Pre-Reid sediment extends in both directions, with less extensive penultimate and MIS 2 limits restricted to valley lobes close to their mountain sources (Fig. 4.2). In comparison, ice extents in the lower elevation northern Ogilvie Mountains were more limited, with piedmont ice expanding to the east and valley glacier growth to the west (Duk-Rodkin, 1999). The timing of ice limits in the northern Ogilvie Mountains has not been studied in detail, but is likely similar to the southern Ogilvie Mountains.

The Late Pliocene-Early Pleistocene record of glaciation at the southern extent of the southern Ogilvie Mountains is one of the oldest and most complete in North America

(Duk-Rodkin et al., 2010, Duk-Rodkin and Barendregt, 2011). Ice advanced from its source area into the Tintina Trench, where it initially merged with ice from the Selwyn lobe flowing from the southeast (Duk-Rodkin, 1996). The stratigraphies of the Rock Creek site, near the maximum all-time limit, and of the East and West Fifteenmile River sites, within the penultimate limit (Fig. 4.2) include multiple tills, loess, outwash, colluvium and paleosols. Paleomagnetism and pollen data indicate that this record represents eight glaciations spanning the Late Pliocene to Middle Pleistocene (Duk-Rodkin, 2010; Barendregt et al., 2010).

The penultimate limit on the southwest side of the southern Ogilvie Mountains, ~35 km east of Dawson, is 10-50 km inside the Early Pleistocene limit. Although the penultimate limit could have been deposited in MIS 4, MIS 6 or both, the identification of the Diversion Creek paleosol on its surface suggests that it was present through the last interglacial (MIS 5e), indicating a similar MIS 6 age for the penultimate limit as the Reid in central Yukon (Tarnocai and Smith, 1989). Glaciation during MIS 2 only extended ~25 km from local cirque sources (Duk-Rodkin, 1996).

Two sets of well-developed moraines are present within the Pre-Reid limit on the north side of the southern Ogilvie Mountains (Fig. 4.2). Beierle (2002) interpreted these moraines to be from MIS 2 and a later, Younger Dryas re-advance. This was based on geomorphological relationships and a basal radiocarbon age of 13 200 ± 300 ^{14}C yrs BP on likely re-worked wood from cores from Chapman Lake. This kettle lake developed on the penultimate surface following incision of the moraine by a large meltwater channel that pirated drainage from minor channels flowing across the valley. The elevation of the lake and the smaller channels suggests this incision coincided with subsidence from melting buried morainal ice. The basal date from Chapman Lake therefore suggests that this incision and subsidence occurred after ca. 13 ^{14}C ka BP.

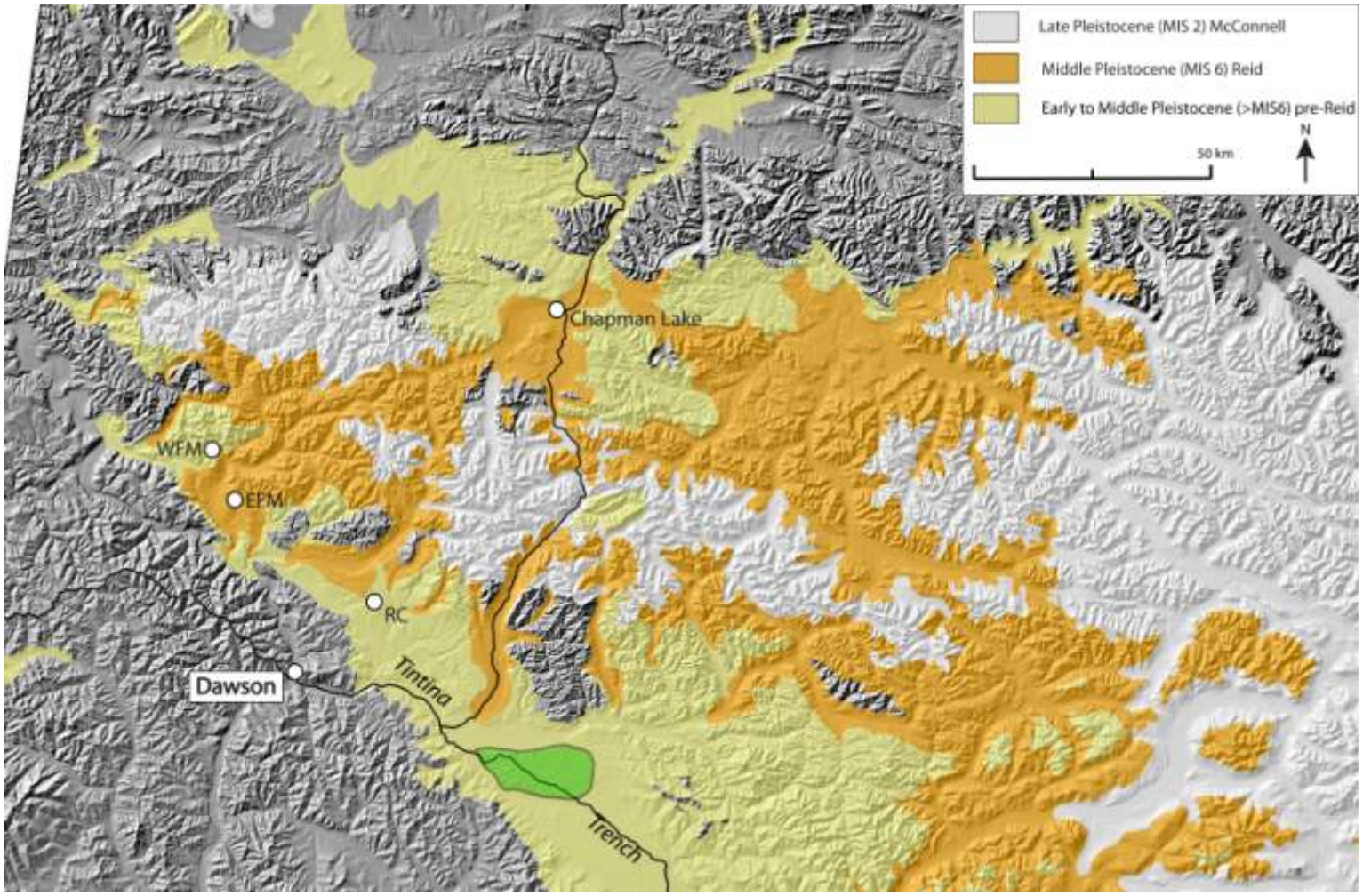

Figure 4.2. Glacial limits in the Southern Ogilvie Mountains (Duk-Rodkin, 1999). The penultimate limit (orange) is assigned a MIS 6 age in this figure, but could be a composite of MIS 4 and MIS 6-aged deposits. The approximate outline of the Flat Creek beds is shown in green (Froese, 2005). Site names mentioned in text: RC = Rock Creek; EFM = East Fifteenmile; WFM: West Fifteenmile.

Beierle (2002) also proposed that the presence of buried ice indicates a MIS 2 age for the penultimate limit, because this ice could not have persisted through a warm interglacial period in MIS 5. Alternatively, the penultimate limit may be from MIS 4. The buried ice would then only have had to stay frozen through MIS 3. However, multiple studies have shown the preservation of deeply buried ice through interglacial periods (Matheus et al., 2003; Froese et al., 2008; Reyes et al., 2010b). Cosmogenic ^{10}Be dates on the less extensive moraine of 9.8 ± 1.1 ka and 9.5 ± 0.9 ka suggest a MIS 2 age for the younger limit (Stroeven et al., 2010), although a Younger Dryas age cannot be precluded. It is therefore likely that the penultimate surface is either from MIS 4 (c.f. Lacelle et al., 2007), MIS 6 (Thomas and Rampton, 1982; Duk-Rodkin, 1996) or a composite of the two. Deglaciation of the more recent MIS 2 advance may have caused incision of the MIS 4/6 limit and melting of the old, buried ice. The kettle lake could have also pre-dated this incision, dried out during arid conditions in MIS 2 and only infilled at ca. 13 ^{14}C ka BP.

4.6. Southwest Yukon

The St. Elias Mountains have a mean elevation range between <1000 m to 3000 m, with peaks exceeding 5900 m (Yukon Ecoregions Working Group, 2004). Uplift of these mountains since the Miocene created a strong precipitation barrier for moisture delivery into southwest Yukon (Foster et al., 2010). Pleistocene ice expanded northeast from these mountains as independent glaciers, filling the northwest-trending Shakwak Trench (Fig. 4.1). As this ice flowed northwest along the trench, it merged with ice flowing down the White and Donjek River valleys before spilling out across the Wellesley Depression to the north (Denton, 1974; Duk-Rodkin, 1999).

Extensive mapping near the terminus of the St. Elias lobe by Rampton (1969, 1971) identified two major ice limits, termed the Macauley and Mirror Creek glaciations. These glaciations were tentatively assigned to the late (MIS 2) and early (MIS 4) Wisconsinan, respectively (Rampton, 1971; Denton, 1974) and have been correlated to the McConnell and Reid glaciations (Hughes et al., 1969; Duk-Rodkin, 1999). Turner et al. (2013) used tephrochronology and radiocarbon dating along the White River at the maximum extent of the St. Elias lobe (Fig. 4.3) to confirm the initial MIS 4 and 2 age

assignments. They also identified a more extensive, MIS 6-aged limit <5 km beyond the MIS 4 extent.

The White River exposures contain up to 30 m of loess, glaciolacustrine, fluvial and colluvial sediment with plant and insect macrofossils, bones and pollen that separate two tills beyond the MIS 2 limit. These non-glacial deposits are constrained to MIS 5 by Old Crow (124 ± 10 ka; Preece et al., 2011a), Woodchopper Creek (ca. 124-106 ka; Jensen et al., 2011), Donjek, Snag and Dominion Creek (82 ± 9 ka; Westgate et al., 2008) tephras. An infrared stimulated luminescence (IRSL) date collected in loess beside Donjek tephra of 88 ± 7 ka supports a MIS 5 age (Turner, unpublished data). This confirms that the MIS 2, 4 and 6 limits of the St. Elias lobe are closely-spaced (<15 km apart). No Pre-Reid glacial sediment has been identified beyond the MIS 6 limit (Bond and Lipovsky, 2010; Turner et al., 2013), in contrast to mapping by Duk-Rodkin (1999).

An early Wisconsinan, MIS 4 age for the penultimate glaciation was also established near Aishihik Lake, southeast of the White River area. Ward et al. (2007) used cosmogenic ^{10}Be ages of 54-51 ka from four boulders in an area affected by the St. Elias and Coast Mountain lobes to define the MIS 4-aged Gladstone glaciation. The Aishihik Lake and White River records indicate that the St. Elias and Coast Mountain lobes responded similarly during the late-Middle and Late Pleistocene, with extensive glaciation in MIS 4 and 6 and more limited Pre-Reid and MIS 2 ice.

Multiple glaciations are recorded further up-ice in the St. Elias lobe at Silver Creek. Denton and Stuiver (1967) interpreted three glaciations from interbedded till, outwash and fluvial sediment. They named them the Shakwak, Icefield and Kluane glaciations in order from oldest to youngest. Conventional radiocarbon ages between 37 700 $^{+1500}/_{-1300}$ ^{14}C yrs BP (Y-1356; Denton and Stuiver, 1967) and 29 600 ± 460 ^{14}C yrs BP (GSC-769; Lowden et al., 1970) from the non-glacial, MIS 3-aged Boutellier interval between the upper Kluane till and middle Icefield till, constrain the former to MIS 2. Subsequent AMS radiocarbon ages of 36 240 ± 310 (UCIAMS-74727), 36 010 ± 600 (UCIAMS-112439) and 35 000 ± 3500 ^{14}C yrs BP (UCIAMS-112441), and an IRSL age of ca. 39 ka from the same interval are in agreement with this age (Chapter 3).

The Icefield and Shakwak tills at Silver Creek likely correlate to MIS 4 and 6. Below the older Shakwak till is 5-40 m of interbedded oxidized sand and gravel, loess and lacustrine sediment. Infrared stimulated luminescence samples from the loess and lacustrine sediment provide ages of >300 ka and 236 ± 21 ka, suggesting that this non-glacial material is Middle Pleistocene in age (Chapter 3). The Icefield and Shakwak tills are therefore between MIS 7-3 in age and may correlate with the Reid and Gladstone glaciations further east. Two older tills were observed below the units the luminescence samples were collected from. Although these confirm that at least two Pre-Reid advances of the St. Elias lobe occurred, their age and extent are not clear.

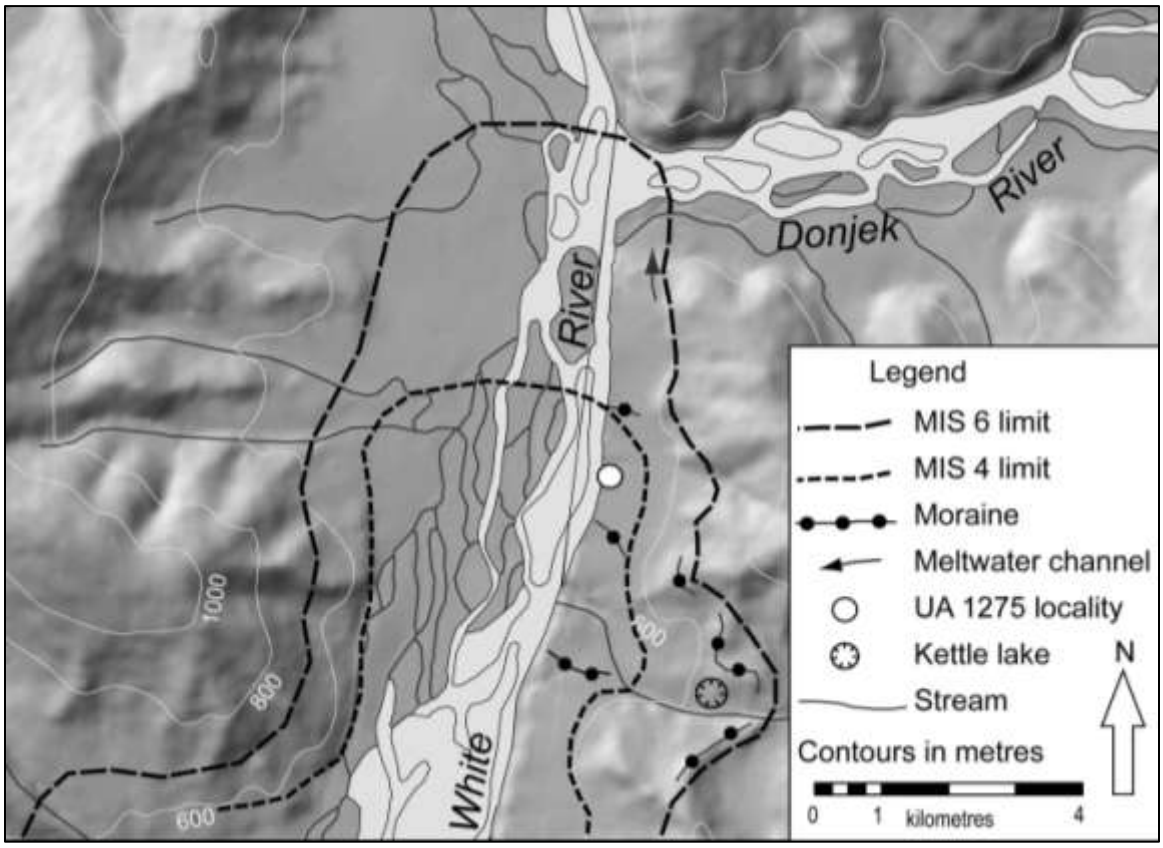

Figure 4.3. Glacial limits in the White River area of southwest Yukon (modified from Turner et al., 2013), based on mapping by Bond and Lipovsky (2010).

Advance of the St. Elias lobe in southwest Yukon during MIS 2 occurred sometime after 29 600 ± 460 ^{14}C yrs BP (GSC-769; Lowden et al., 1970). This age is from organic-rich fluvial sediment in Silver Creek that is separated from the overlying MIS 2-aged till by up to 20 m of outwash. It is therefore likely that ice advanced out of

the St. Elias Mountains and reached its maximum extent 100 km to the north well after this date. Deglaciation of the St. Elias lobe in MIS 2 is constrained near Silver Creek to 12 500 ± 200 ^{14}C yrs BP (Denton and Stuiver, 1967) and north of the Rudy Range to between 14 630 ± 800 and 13 740 ± 500 cal yrs BP (Bond and Lipovsky, 2009). Ages of 10 900 ± 160 ^{14}C yrs BP (Y-2301) and 11 270 ± 200 ^{14}C yrs BP (Y-2306) on frozen peat at the head waters of the White River in the St. Elias Mountains (Denton, 1974) support the interpretation that this ice lobe deglaciated between 11-12.5 ^{14}C ka BP.

4.7. The penultimate Delta glaciation in east-central Alaska

The penultimate glacial limits on the north side of the Alaska Range are largely MIS 4 in age (Briner et al., 2005; Dortch, 2006). Glaciers advancing north from this range deposited sets of moraines in multiple valleys (Pewe, 1953). In each valley studied, the youngest moraines stabilized during MIS 2, and in most, the penultimate moraines stabilized in MIS 4 or early MIS 3 (Briner et al., 2005; Briner and Kaufman, 2008). The one area that may have older penultimate drift is along the Delta River, at the eastern limit of the Alaska Range (Fig 4.4).

Here, two glacial limits are separated by <30 km near the confluence of the Delta and Tanana Rivers (Pewe and Reger, 1983, 1989). The younger of these was deposited by the Donnelly glaciation in MIS 2. The older Delta glacial limit has been dated to MIS 4, based on cosmogenic ^{10}Be ages on weathered boulders, large clasts and gravel from the southeast surface of the Delta moraine (Matmon et al., 2010). Beyond the Delta limit are two discontinuous sets of outwash terraces that extend ~100 km downstream along the Tanana River (Pewe and Reger, 1989; Beget and Keskinen, 2003). The larger, older terrace has been broadly correlated to the Delta moraine and the younger to the Donnelly moraine (Pewe, 1975; Weber et al., 1981; Pewe and Reger, 1989).

Figure 4.4. Glacial limits in the Delta River area in east-central Alaska (Manley and Kaufman, 2002). Two sets of outwash terraces extend downstream from the Delta limit. The larger terraces (in yellow, modified from Beget and Keskinen (2003)) are overlain by MIS 5-aged tephras at Moose Creek (Old Crow tephra) and at Canyon Creek (Sheep Creek tephra – Canyon Creek), suggesting an extensive MIS 6 advance. The black box shows the location of Matmon et al.'s (2010) study area with interpreted MIS 4 cosmogenic nuclide ages.

Two sites exposed in the older of these terraces contain tephra. The Moose Creek site ~80 km downstream from the Delta moraine consists of gravel alluvium, interpreted as outwash, overlain by an organic paleosol with 20-30 cm of Old Crow tephra (Beget and Keskinen, 2003). The recently refined age of Old Crow tephra (124 ± 10 ka; Preece et al., 2011a) provides a minimum age of MIS 6 for this terrace. The Canyon Creek site is located ~40 km beyond the Delta moraine. It consists of outwash gravel associated with the Delta glaciation, overlain by gravel and sand of local and Tanana River origin, fan deposits from the nearby Canyon Creek, and thick loess (Weber et al., 1981; Westgate et al., 2008). A deformed tephra in the fan sediment was correlated to SCt-Fairbanks (Beget and Keskinen, 2003; Westgate et al., 2001). This tephra has since been shown to not be SCt-F, but rather another Sheep Creek tephra bed from the same source. This tephra was named Sheep Creek tephra – Canyon Creek (SCt-CC; Westgate et al., 2008).

A potential correlation of SCt-CC to a tephra at one of the sites along the White River in southwest Yukon may provide a chronology for the Canyon Creek site. At their WR99, Turner et al. (2013) identified a pumiceous Sheep Creek-type tephra that is constrained by other tephras and a subsequent IRSL date (Turner, unpublished data) to MIS 5. Comparison of the mineral assemblages, glass morphology and major element geochemistry of the glass shards in UA 1275 to those of SCt-CC suggests that these are the same tephra (Fig. 4.5). UA 1275 has a frothy morphology and abundant hornblende. It is enriched in SiO_2 and K_2O compared to the SCt-F and Sheep Creek tephra-Klondike (SCt-K), with lower Al_2O_3, FeOt, CaO and Na_2O (c.f. Westgate et al., 2008). It is separated from SCt-Christy at the Ash Bend locality in central Yukon by having less than ~0.1 wt % Cl (Westgate et al.'s (2008) Fig. 16). Given the available data, UA 1275 likely correlates to SC-CC, making it the only other known occurrence of SCt-CC in eastern Beringia. Strengthening this correlation is the presence of rare western camel (*Camelops hesternus*) fossils at both sites (Zazula et al., 2011).

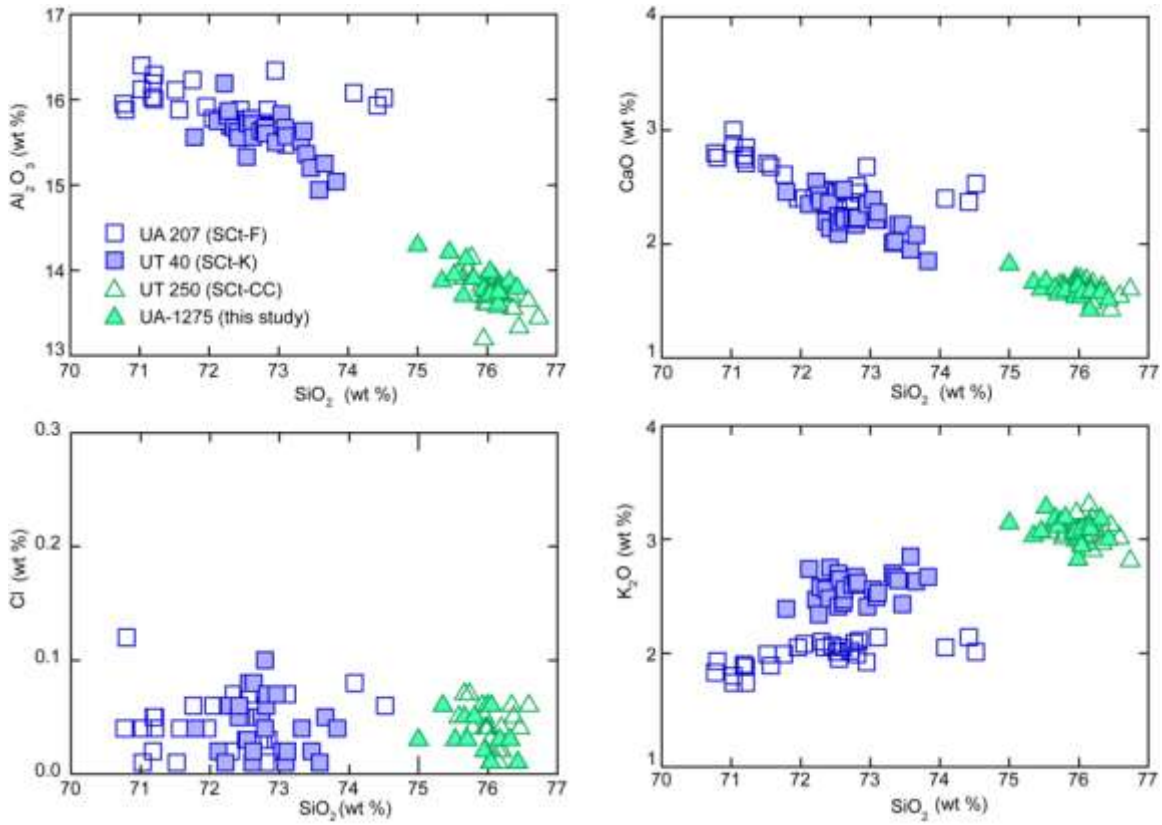

Figure 4.5. Comparison of major element glass chemistry weight %s of Sheep Creek tephra Fairbanks (UA 207), Klondike (UT 40), Canyon Creek (UT 250) and sample UA 1275. UA 1275 and UT 250 (SCt-CC) were analyzed together using a JEOL 8900 electron microprobe operating at 15 eV accelerating voltage with a 10 µm diameter beam and 6 ηA beam current. Standardization used rhyolitic obsidian (ID3506) and Old Crow tephra. A Cl wt % of <0.1 distinguishes SCt-CC from SCt-Christie (Westgate et al., 2008).

A MIS 5-age for SCt-CC suggests that the underlying outwash terrace dates to MIS 6 and is roughly synchronous with the Moose Creek terrace to the north. This indicates that an extensive glaciation occurred in this area during MIS 6 that correlates to the Reid glaciation in Yukon. However, a MIS 6-age for the Delta glaciation is not consistent with Matmon et al.'s (2010) cosmogenic ^{10}Be ages. The lack of ages >70 ka was interpreted as suggesting that this portion of the moraine stabilized in MIS 4 or early MIS 3 (Matmon et al., 2010). One alternative explanation for this is that denudation of the MIS 6 surface during a more limited glaciation in MIS 4 resulted in younger cosmogenic exposure ages than the true age of the Delta limit. Another possibility is that the Delta moraine is from MIS 4, but that MIS 6-aged ice was of similar extent, such

that it was extensive enough to deposit the large outwash terraces downstream of the Delta limit. In either case, ice in the Delta River valley was likely more extensive in MIS 6 than during MIS 2, forming closely-spaced limits similar to those in the White River area in southwest Yukon.

4.8. Discussion

4.8.1. Summary of Glacial Limits in Yukon and the Delta River area in Alaska

The youngest and least extensive glacial advance of the northern Cordilleran Ice Sheet is loosely constrained to MIS 2. The St. Elias, Eastern Coast Mountain, Cassiar and Selwyn lobes advanced after ca. 29-26 ^{14}C ka BP (Matthews et al., 1990b; Jackson and Harington, 1991). The youngest age below MIS 2-aged till in Yukon is 23.9 ^{14}C ka BP, from southeastern Yukon in an area affected by the southeast-flowing Liard lobe (Klassen, 1987). Although it is possible that advance of the Liard lobe was delayed by a lack of precipitation, these independent ice lobes were probably broadly synchronous. However, the reliability of this bulk organic silt radiocarbon date is uncertain.

Termination of glaciation in MIS 2 initiated before 12-13 ^{14}C ka BP (Denton and Stuiver, 1967; Bond and Lipovsky, 2009; Stroeven et al., 2010), with melting of all but local alpine glaciers being complete by ca. 9 ka ^{14}C yrs BP (Jackson et al., 1991). Yukon was sufficiently ice-free by ca. 11.3 ^{14}C ka BP to allow the southern dispersion of Beringian bison into northern British Columbia (Shapiro et al., 2004; Ives et al., 2013). Deglaciation of the northern Cordilleran Ice Sheet may have preceded the retreat of ice in the Southern Ogilvie Mountains, constrained by ^{10}Be nuclide ages of ca. 9.8-9.5 ka (Stroeven et al., 2010).

The penultimate glacial limit in Yukon is now known to vary across the territory. In central Yukon, bracketing OSL dates of 158 ± 18 ka and 132 ± 18 ka (Demuro et al., 2012), and Old Crow tephra overlying outwash (Ward et al., 2008), constrain the intermediate limit of the Selwyn lobe to the MIS 6-aged Reid glaciation. However, in southwest Yukon the penultimate limit of the St. Elias and Coast Mountain lobes is

constrained by ^{10}Be nuclide dating, numerous MIS 5-aged tephras and IRSL data to the MIS 4-aged Gladstone glaciation (Ward et al., 2007; Turner et al., 2013). Retreat of the St. Elias and Coast Mountain lobes during the Gladstone glaciation began before ca. 54-51 ka (Ward et al., 2007), likely coinciding with the end of MIS 4. Ice retreated to at least the margin of the St. Elias Mountains by ca. 36 ^{14}C ka BP (Denton and Stuiver, 1967; Chapter 3), although this probably occurred well before this time. The penultimate limit on the north side of the Southern Ogilvie Mountains is likely either MIS 4 or 6 in age. Further work, potentially using cosmogenic nuclide dating, is necessary to confirm these ages.

The Late Pliocene to Middle Pleistocene Pre-Reid limit comprises at least three separate glaciations (Duk-Rodkin et al., 2010; Jackson et al., 2012). In central Yukon, this limit extends up to 100 km beyond the penultimate, MIS 6-aged Reid glaciation (Duk-Rodkin, 1999), although recent field work suggests this limit is less extensive (Bond and Lipovsky, 2010). Further south, at the maximum extent of the Eastern Coast Mountain lobe, the Pre-Reid limit is <25 km past the penultimate, MIS 4 Gladstone glacial limit (Hughes et al., 1969; Ward et al., 2007). No Pre-Reid equivalent drift exists beyond the MIS 4 and 6 limits at the maximum extent of the St. Elias lobe (Bond et al., 2008; Turner et al., 2013), or in east-central Alaska (Briner and Kaufman, 2008).

New tephrostratigraphic data and existing ^{10}Be-nuclide records may indicate that the MIS 4 and 6 limits in the Delta River area in Alaska are closely-spaced. The potential correlation of SCt-CC at Canyon Creek to UA 1275 at White River supports Beget and Keskinen's (2003) assertion that the large outwash terraces along the Tanana River pre-date MIS 5, suggesting an extensive MIS 6 glaciation. However, ^{10}Be-nuclide dates from the southeast portion of the penultimate moraine (Matmon et al., 2010) indicate that at least part of this surface may date to MIS 4. The most probable scenario is that ice advanced close to the maximum limit in both MIS 4 and 6. The similarity in limits at Delta River, White River and near Aishihik Lake suggest similar boundary conditions controlled glaciation from the eastern Alaska Range to the St. Elias and eastern Coast Mountains, a distance of more than 500 km.

4.8.2. Forcing Mechanisms for Plio-Pleistocene Glacial Extents in Yukon

The most remarkable aspect of the Yukon glacial record is the extensive Late Pliocene – Early Pleistocene glaciations in central Yukon relative to the more restricted and closely-spaced Middle to Late Pleistocene glaciations in southwest Yukon. This does not correspond to the varying intensities of global ice volume or summer insolation records (Fig. 4.6; Hays et al., 1976; Berger, 1978; Raymo and Huybers, 2008). The timing of the extensive Pre-Reid glaciations are broadly correlative with the onset of global cooling and obliquity-driven, 40 kyr cycles (Huybers, 2006; Lisiecki and Raymo, 2007), but this on its own does not adequately explain the pattern of limits in either central or southwest Yukon. Other possible controls include tectonics, sea level, bed conditions, atmospheric circulation and topographic adjustment to a glacial landscape. In this section, we use the differing glacial limits records to discuss the influence each of these had on ice sheet growth in Yukon during the Plio-Pleistocene.

Tectonic uplift of the St. Elias and Wrangell Mountains and the Alaska Range greatly affected glaciation in eastern Beringia. Uplift of the St. Elias orogen likely occurred from the Eocene through to the Pliocene (O'Sullivan and Currie, 1996; Enklemann et al., 2008, 2009). Ongoing uplift throughout the Pleistocene has been suggested as the primary control on Yukon glacial limits (Duk-Rodkin et al., 2004; Barendregt et al., 2010). This 'snow fence' hypothesis states that continually rising mountain ranges progressively limited precipitation into Yukon, creating successively smaller glacial limits. However, the lack of MIS 4-aged limits in central Yukon, and Pre-Reid limits in southwest Yukon and eastern Alaska, indicate that Yukon glacial limits do not follow a progressively more limited pattern. In addition, Late Pliocene and Early Pleistocene periglacial features in Yukon (Froese et al., 2000) and Alaska (Pewe et al., 2009), as well as paleobotanical records (White et al., 1997) across eastern Beringia, suggest that a continental climate was already established in Yukon by the latest Pliocene (Burn, 1994). Tectonics therefore was likely not a primary mechanism controlling variations in glacial limits in Yukon throughout the Pleistocene.

Changes in sea level may also have influenced glaciation in eastern Beringia (Hopkins, 1982). During periods of high global ice volume, lower sea levels expose

large areas of the shallow continental shelf currently underlying the Bering and Chukchi seas. Sea level dropped approximately 120 m in MIS 2 (Fig. 4.6; Hopkins, 1973; Clark and Mix, 2002; Hu et al., 2010). The resulting reduced moisture delivery to interior Alaska has been used to explain MIS 4-aged maximum glacial limits in Alaska (Brigham-Grette, 2001). However, restricted ice in central Yukon during MIS 4 and in southwest Yukon during Pre-Reid glaciations, both periods when sea level was higher than in MIS 2, suggests that this is not a significant control on glaciation in Yukon. It is likely that the established continentality and distance to the Bering and Chukchi seas limited the effectiveness of precipitation differences associated with high sea levels.

Variable bed conditions could have shaped central Yukon ice limits through the Pleistocene. Clark and Pollard (1998) hypothesized that lower ice volumes, but equally extensive ice limits for the Laurentide Ice Sheet in the Early Pleistocene compared to the Late Pleistocene were caused by a change in the substrate from a soft-bedded, clay-rich regolith to a mixed hard-soft bed. This may have resulted in a change in ice sheet morphology from a thin and extensive ice sheet to a thicker and less extensive one (Roy et al., 2004; Clark et al., 2006). Similar conditions possibly influenced ice limits in central Yukon. The Wounded Moose paleosol is a Luvisol that developed on Pre-Reid glacial surfaces. It has well developed argillic horizons, clay loam to sandy clay loam textures, strong oxidation and cryoturbated and heavily weathered clasts (Smith et al., 1986). Tertiary Luvisols and Podzols indicative of warm and moist conditions (cf. Tarnocai and Schweger, 1991) suggest that deep, well-developed, clay-rich soils were likely present to preferentially lubricate the base of Late Pliocene-Early Pleistocene glaciations in central Yukon.

Pleistocene soil conditions in southwest Yukon are unknown. Established rain shadow effects and burial from relatively continuous aggradation of sediment from the St. Elias Mountains may have resulted in shallower, more rigid beds in valleys in southwest Yukon compared to in central Yukon, limiting Pre-Reid glaciations in this area.

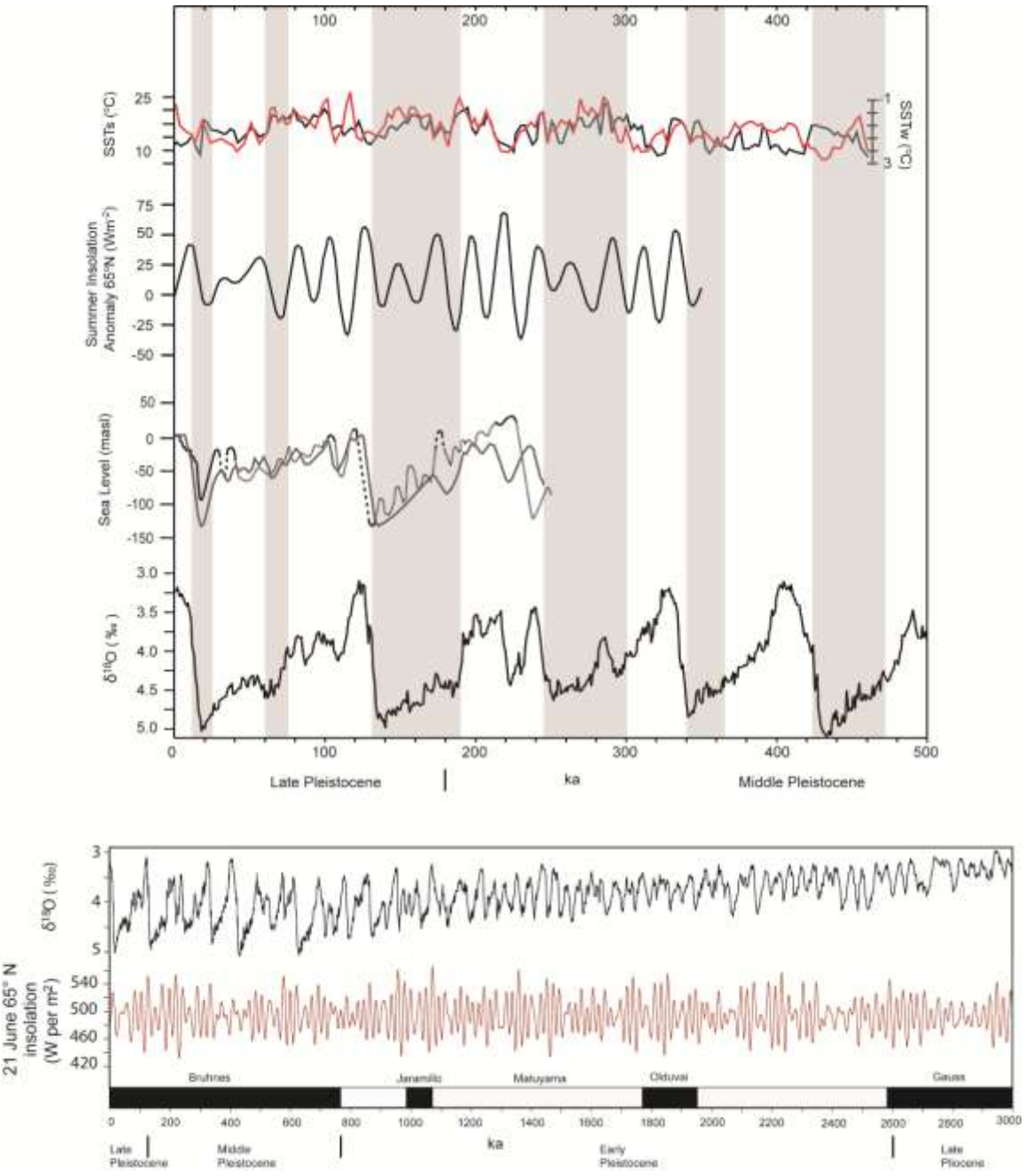
100
200
300
400
SSTs (°C)
25
10
SSTw (°C)
Summer Insolation Anomaly 65°N (Wm⁻²)
75
50
25
0
-25
-50
Sea Level (masl)
50
0
-50
-100
-150
δ18O (‰)
3.0
3.5
4.0
4.5
5.0
0
100
200
300
400
500
Late Pleistocene
ka
Middle Pleistocene
δ18O (‰)
3
4
5
21 June 65° N insolation (W per m²)
540
500
460
420
Bruhnes
Jaramillo
Matuyama
Olduvai
Gauss
0
200
400
600
800
1000
1200
1400
1600
1800
2000
2200
2400
2600
2800
3000
ka
Late Pleistocene
Middle Pleistocene
Early Pleistocene
Late Pliocene

Figure 4.6. **A) Middle to Late Pleistocene summer insolation, sea level and marine oxygen isotope curve. Summer insolation anomaly values from Bartlein et al. (1991), calculated using the routines of Berger (1978). Sea levels curves include a global record (grey line) from the Huon Peninsula, recalculated using a correlation to core V19-30 (Chappell and Shackleton, 1986), Hopkins' (1973) firm (solid black), inferred (dashed black) and hypothetical (dotted black) Beringian sea level curves and Hu et al.'s (2010) relative sea level for the Bering Strait region (red). The orange line is the modern Bering Sea depth (Hu et al., 2010). Oxygen isotope curve is from the LR04 benthic $\delta^{18}O$ stack (Lisiecki and Raymo, 2005). Vertical shaded bars approximately bracket marine oxygen isotope stages of significant global ice volume. B) LR04 benthic $\delta^{18}O$ curve (after Lisiecki and Raymo, 2005) and insolation (from Raymo and Huybers, 2008) for the Late Pliocene and Pleistocene, shown with the paleomagnetic time scale. Labeled Early Pleistocene Yukon glaciations are from Jackson et al., (2012). White boxes denote interpreted Late Pliocene to Middle Pleistocene glaciations from the Ogilvie Mountains (Barendregt et al., 2010).**

Ice growth in Yukon was also influenced by changes in atmospheric circulation caused by the development of the Laurentide and Cordilleran ice sheets during MIS 2. These effects have been repeatedly modeled, with two main results: 1) the splitting of the jet stream (Bromwich et al., 2004; Toracinta et al., 2004); and, 2) the formation of a large anticyclone over North America (e.g. Broccoli and Manube, 1987; Bartlein et al., 1998; Bromwich et al., 2004). In Yukon, the anticyclone brought southeasterly air masses from across the western portion of the ice sheets, delivering cold, dry air and potentially limiting glaciation. However, this effect may only have been significant when the ice sheets exceeded their ca. 14 ka size (Bartlein et al., 1991). Considering that the Laurentide Ice Sheet itself was more restricted during glaciations prior to MIS 2 (Barendregt and Irving, 1998; Jackson et al., 2011), this effect was probably only substantial during the Late Pleistocene. Recent revision of the glacial extents in the western Arctic (England et al., 2009; Lakeman and England, 2012, 2013) suggests that the maximum limit was deposited in the Late Pleistocene. This indicates higher moisture delivery to this area during MIS 2, which may be a result of a stronger split jet and anticyclone during the Late Pleistocene than during previous Plio-Pleistocene glaciations.

Topography also may have controlled ice extents in Yukon throughout the Pleistocene. The coupling of climate and topography in glaciated environments (e.g. Anders et al., 2010) may be linked to glacial erosion and ice extents. Glacial erosion causes a greater concentration of surface area below snowline (Whipple et al., 1999; Brocklehurst and Whipple, 2004). The combination of smaller accumulation areas and increased ice capacity of broad, U-shaped glacial valleys, results in less extensive ice compared to unglaciated landscapes (MacGregor et al., 2000; Kaplan et al., 2009; Pedersen and Egholm, 2013). This may have contributed to more extensive ice growth across unglaciated central Yukon during Late Pliocene – Early Pleistocene glaciations. In addition, glacial erosion of the St. Elias and Wrangell Mountains throughout the Pleistocene may have created lower-elevation moisture pathways in the late-Middle to Late Pleistocene compared to the Late Pliocene – Middle Pleistocene, contributing to more extensive St. Elias lobe extents.

Simulations also show that with the change from 41 kyr to 100 kyr climate cycles, ice growth in well-developed glacial landscapes responds non-linearly as the equilibrium line drops below the pre-established hypsometric maximum (Pedersen and Egholm, 2013). This results in significantly more-extensive ice growth following the 41-100 kyr transition, followed by steadily more limited ice as the negative feedback between glacial erosion and extent is re-established. This effect may have influenced the Forks Glaciation (Jackson et al., 2012) and three extensive ice advances from the Ogilvie Mountains (Duk-Rodkin et al., 2010; Barendregt et al., 2010) between ca. 1 – 0.7 Ma, but more data are needed to make this connection.

This discussion of potential forcing mechanisms on glaciation in eastern Beringia reveals that multiple conditions may have contributed to promote maximum ice extents during the Late Pliocene – Early Pleistocene in central Yukon. Deep regolith substrates and unglaciated topography in the Cassiar and Selwyn Mountains may have been more significant factors than tectonics or sea level in allowing the Selwyn lobe to reach its maximum extent in the latest Pliocene. These would also act to restrict further glaciation throughout the Pleistocene, as saprolite substrates eroded and the topography adjusted to a glacial landscape. Yet the lack of Pre-Reid limits in southwest Yukon suggests that

these mechanisms were insufficient to cause the St. Elias and Eastern Coast Mountain lobes to advance past their Late Pleistocene extents.

Ice growth in southwest Yukon and eastern Alaska was more extensive in the late Middle Pleistocene – Late Pleistocene than at any previous time in the Plio-Pleistocene. The glacial limits in these areas are also more closely-spaced than in central Yukon. It may be that the Pre-Reid limits at the Delta and White Rivers areas are close to the MIS 4/6 limits, and that the glacial rain shadow of the St. Elias and Wrangell Mountains and the Alaska Range limited glaciation to the point that other variables caused only minor variations. In this scenario, the only glaciation that differed substantially was MIS 2, when the impact of the Laurentide Ice Sheet on atmospheric circulation further restricted ice growth. However, Pre-Reid cirques in southwest Yukon suggest sufficient precipitation for alpine ice growth. Alternatively, the topographic transition of the St. Elias Mountains and Alaska Range from unglaciated to glacial-modified may have carved out lower-level moisture pathways for precipitation-starved southwest Yukon and eastern Alaska and created a topographic adjustment that favored non-linear ice growth (MacGregor et al., 2000; Pedersen and Egholm, 2013). These effects could have contributed to more extensive Middle to Late Pleistocene ice than in previous glaciations.

4.8.3. Summary

This paper reviews the Late Pliocene to Late Pleistocene glacial limits produced by the Cordilleran Ice Sheet and montane ice in Yukon Territory and speculates on possible forcing mechanisms that controlled them. In central Yukon, the most extensive ice advances were in the Late Pliocene - Early Pleistocene, followed by in MIS 6, MIS 2 and finally in MIS 4. Comparatively, in southwest Yukon and the Delta River area of east-central Alaska, ice was extensive in MIS 6 and 4, and less extensive in MIS 2 and in the Late Pliocene - Early Pleistocene.

The forcing mechanisms that influenced glacial extents in Yukon varied spatially and temporally over the past ca. 2.6 Ma. A combination of varying bed conditions, topographic adjustments to a glacial landscape and circulation effects of the Laurentide

and Cordilleran ice sheets potentially influenced ice growth in central Yukon. In southwest Yukon, established continentality and the rain shadow effect of the Alaska Range and the St. Elias and Wrangell Mountains restricted glaciation throughout the Plio-Pleistocene. Other factors, such as changes in atmospheric circulation during MIS 2 and erosion of lower-elevation moisture pathways, were possible secondary contributors to the resulting glacial limits in Yukon.

Chapter 5. Summary and Conclusions

5.1. Synthesis

The glacial limits and paleoenvironments of southwest Yukon were previously under-studied and poorly constrained. The primary objective of this study was to examine the Quaternary stratigraphy and sedimentology along the White River and Silver Creek to determine the timing of advances of the St. Elias lobe. Secondary objectives were to: 1) investigate Pleistocene paleoenvironments of southwest Yukon; and 2) to correlate the limits to other areas in eastern Beringia. Most of the sites used to reconstruct Pleistocene environments are located in the unglaciated region of Yukon and Alaska. Few sites within the glaciated fringe have been studied to directly constrain the glacial limits of Yukon.

The White River sites are located beyond the MIS 2 extent, but within the limit of two, more extensive, glaciations. These sites contain well-preserved glacial and non-glacial sediment spanning the Middle to Late Pleistocene. Analysis of the major element geochemistry of tephras sampled at these sites identified eleven different tephras, including well-documented tephras such as Old Crow, Dominion Creek and Dawson tephras, as well as previously unnamed tephras such as Donjek and Snag tephras. These tephras allow correlation between different sites at White River and to other locations across Alaska and Yukon. The tephrochronology and both finite and non-finite radiocarbon ages constrain the two pre-MIS 2 glacial limits to MIS 6 and 4. This record contrasts with the record from central Yukon, where the maximum limit is from the latest Pliocene (Froese et al., 2000; Hidy et al., 2013).

The Silver Creek sites contain a longer, but more poorly-constrained glacial record. The chronology of the stratigraphy at Silver Creek was determined using radiocarbon and IRSL dating, generally confirming Denton and Stuiver's (1967)

interpretations. These exposures contain till from at least five glaciations in MIS 7 or 6, MIS 4, MIS 2 and two older, Pre-Reid glaciations. The two older tills are the first evidence of Pre-Reid advance of the St. Elias ice lobe in southwest Yukon. The tilting of the older units at Silver Creek suggest between 65-90 m of uplift since MIS 7 (~0.25 - 0.42 mm/yr) along the north side of the Denali Fault. The White River and Silver Creek sites provide a greater understanding of the timing of ice advances in southwest Yukon throughout the Pleistocene.

Another objective was to reconstruct the environments that existed in southwest Yukon during Middle to Late Pleistocene non-glacial intervals. The exceptional preservation of paleoecological material at White River provided an ideal means for this. Pollen and plant and insect macrofossils were collected from sediment dating to various sub-stages of MIS 5 and from the transition from MIS 3 to MIS 2. Two expansions of boreal forest are documented in MIS 5, during MIS 5e and 5a. The last interglacial period in MIS 5e is commonly described as being as warm as, or warmer than, present in eastern Beringia. However, MIS 5a is rarely cited as having a similar climate. It is possible that some MIS 5e sites in eastern Beringia actually date to MIS 5a. The paleoecological record at Silver Creek complements the White River record with data from MIS 7 and MIS 3. Pollen data indicate that a boreal forest expanded across southwest Yukon at some point during MIS 7. In MIS 3, Silver Creek comprised a riparian floodplain within a herbaceous tundra with few trees. At White River, the transition from MIS 3 to MIS 2 is marked by a classic Mammoth Steppe associated with Dawson tephra.

A third objective was to correlate the glacial record in southwest Yukon to other areas in Yukon and eastern Alaska. This increases our understanding of the conditions that existed during the large variations in climate that occurred throughout the Late Pliocene and Pleistocene. The MIS 6, 4 and 2 advances of the St. Elias lobe, previously termed the Shakwak, Icefield and Kluane by Denton and Stuiver (1967), correlate to the Reid, Gladstone and McConnell glaciations defined in central and southern Yukon. These limits are closely-spaced in the White River area with no earlier, Pre-Reid glacial sediment beyond them. This contrasts with central Yukon and the Southern Ogilvie Mountains, where MIS 2, MIS 6 and multiple Pre-Reid limits are separated by up to 100

km and there is no evidence of a MIS 4-aged glaciation. The MIS 4 and 2 glaciations represented at Silver Creek also correlate to the Gladstone and McConnell glaciations. The next oldest glacial limit likely correlates to the MIS 6-aged Reid glaciation, but may be from a previously-unrecognized, Pre-Reid, MIS 7 ice advance.

The difference in glacial limits in central Yukon and southwest Yukon was likely determined by regional differences in forcing mechanisms throughout the Pleistocene. The large separation of the glacial limits in central Yukon was likely due to ideal conditions for extensive ice in the Late Pliocene and Early Pleistocene, including a deeply weathered substrate and a lack of established glacial topography. In southwest Yukon, Pleistocene glaciations were limited by the rain shadow produced by Tertiary uplift of the St. Elias and Wrangell Mountains to the southwest. Relatively small differences in ice extents were potentially influenced by other factors such as the creation of lower-level moisture pathways into southwest Yukon and the varying affect on atmospheric circulation by the Laurentide and Cordilleran ice sheets. Previously-cited forcing mechanisms such as pervasive tectonics and changing sea level did not significantly affect the Plio-Pleistocene glacial limits of Yukon.

5.2. Future Work

Future work on the Pleistocene glacial stratigraphy and chronology in Yukon should focus on the following aspects:

1) Examine sites that reconnaissance studies indicate may have datable Pleistocene glacial sediment, organics and tephras. These sites may contain sediment that correlate to White River or Silver Creek, providing more chronological and paleoecological constraint on Pleistocene environments in southwest Yukon. Such sites have previously been identified at Wolverine Creek, Telluride Creek and in the headwaters of the White River in eastern Alaska (Denton, 1974);
2) Improve the constraints on MIS 2 deglaciation of the St. Elias and Selwyn lobes using radiocarbon and cosmogenic nuclide dating;
3) Utilize further developments in IRSL and cosmogenic nuclide dating to establish a more precise chronology of the glacial sediment at Silver Creek, including accurate ages for the two Pre-Reid tills;
4) Document the detailed paleoenvironmental, sedimentological and stratigraphic context and the minor element and Fe-Ti oxide

geochemistry for the tephras at White River. This is significant for future correlation of these tephras to other sites across Yukon and Alaska;

5) Establish a chronology for the glacial limits in the Southern Ogilvie Mountains, possibly using tephrochronology or cosmogenic nuclide dating;

6) Further examine the glacial limits record in the Delta River area of eastern Alaska, potentially using a depth profile of cosmogenic nuclide samples and pedogenic comparisons to soils in central Yukon;

7) Use models of Pleistocene climatological conditions and landscape adjustment to glacial erosion to investigate possible forcing mechanisms that resulted in the differing glacial limits records in Yukon;

8) Complete a comprehensive clast fabric, structural and sedimentological analysis on the tills at Silver Creek to determine ice flow configurations at the onset of successive glaciations and during deglaciation.

References

Aitken, 1998. An Introduction to Optical Dating. Oxford University Press, London.

Anders, A.M., Mitchell, S.G., Tomkin, J.H., 2010. Cirques, peaks, and precipitation patterns in the Swiss Alps: Connections among climate, glacial erosion, and topography. Geology, 38, 239-242.

Anderson, P.M., Lozhkin, A.V., 2001. The Stage 3 interstadial complex (Karginskii/middle Wisconsinan interval) of Beringia: variations in paleoenvironments and implications for paleoclimatic interpretations. Quaternary Science Reviews, 20, 93-125.

Anderson, R.S., 1989. Revision of the subfamily Rhynchaeninae in North America (Coleoptera: Curculionidae). Transactions of the American Entomological Society, 115, 207-312.

Anderson, R.S., 1997. Weevils (Coleoptera: Curculionoidea, excluding Scolytinae and Platypodinae) of the Yukon. In H.V. Danks, J.A. Downs (Ed.), *Insects of the Yukon*, (pp. 523-556).

Auclair, M., Lamothe, M., Huot, S., 2003. Measurement of anomalous fading for feldspar IRSL using SAR. Radiation and Measurements, 37, 487-492.

Auclair, M., Lamothe, M., Lagroix, F., Banerjee, S.K., 2007. Luminescence investigation of loess and tephra from Halfway House section, Central Alaska. Quaternary Geochronology, 2, 34-38.

Arkle, J.C., Armstrong, P.A., Haeussler, P.J., Prior, M.G., Hartman, S., Sendziak, K.L., Brush, J.A., 2013. Focused exhumation in the syntaxis of the western Chugach Mountains and Prince William Sound, Alaska. GSA Bulletin, 125, 776-793.

Barendregt, R.W., Irving, E., 1998. Changes in the extent of North American ice sheets during the late Cenozoic. Canadian Journal of Earth Science, 35, 504-509.

Barendregt, R.W., Enkin, R.J., Duk-Rodkin, A., Baker, J., 2010. Paleomagnetic evidence for multiple late Cenozoic glaciations in the Tintina Trench, west-central Yukon, Canada. Canadian Journal of Earth Science, 47, 987-1002.

Bartlein, P.J., Anderson, P.M., Edwards, M.E., McDowell, P.F., 1991. A framework for interpreting paleoclimatic variations in eastern Beringia. Quaternary International, 10-12, 73-83.

Bartlein, P.J., Anderson, K.H., Anderson, P.M., Edwards, M.E., Mock, C.J., Thompson, R.S., Webb, R.S., Webb III, T., Whitlock, C., 1998. Paleoclimate simulations for North America over the past 21,000 years: features of the simulated climate and comparisons with paleoenvironmental data. Quaternary Science Reviews, 17, 549-585.

Beget, J.E., Keskinen, M.J., 2003. Trace-element geochemistry of individual glass chards of the Old Crow tephra and the age of the Delta glaciation, central Alaska. Quaternary Research, 60, 63-69.

Beget, J.E., Edwards, M.E., Hopkins, D., Keskinen, M., Kukla, G., 1991. Old Crow tephra found at Palisades of the Yukon, Alaska. Quaternary Research, 35, 291-297.

Beierle, B.D., 2002. Late Quaternary glaciation in the Northern Ogilvie Mountains: revised correlations and implications for the stratigraphic record. Canadian Journal of Earth Science, 39, 1709-1717.

Berger, A.L., 1978. Long-term variations of caloric insolation resulting from the Earth's orbital elements. Quaternary Research, 9, 139-167.

Berger, G.W., Pewe, T.L., Westgate, J.A., Preece, S.J., 1996. Age of Sheep Creek Tephra (Pleistocene) in Central Alaska from thermoluminescence dating of bracketing loess. Quaternary Research, 45, 263-270.

Birks, H.H., 2001. Plant macrofossils. In: Smol, J.P., Birks, H.J.B., Last, W.M. (Eds.), Tracking environmental change using lake sediments. Vol. 3: Terrestrial, Algal, and Siliceous Indicators (pp. 49-74). Kluwer Academic Publishers, Dordrecht, The Netherlands.

Blair, M.W., Yukihara, E.G., McKeever, S.W.S., 2005. Experiences with single-aliquot OSL procedures using coarse-grain feldspars. Radiation Measurements, 39, 361-374.

Bond, J.D., 1997. Late Cenozoic history of McQuesten (115P), Yukon Territory. Unpublished M.Sc. thesis, University of Alberta, Edmonton, Alberta, 161 p.

Bond, J.D., 2007. Late Wisconsinan McConnell glaciation of the Big Salmon Range, Yukon. In D.S. Emond, L.L. Lewis, L.H. Weston (Eds.), Yukon Exploration and Geology 2006 (pp. 105-122). Yukon Geological Survey.

Bond, J.D., Kennedy, K.E., 2005. Late Wisconsinan McConnell ice-flow and sediment distribution patterns in the Pelly Mountains, Yukon. In D.S. Emond, L.L. Lewis, G.D. Bradshaw (Eds.), Yukon Exploration and Geology 2004 (pp.67-82). Yukon Geological Survey.

Bond, J.D., Lipovsky, P.S., 2009. Surficial Geology of Talbot Creek (NTS 115G/09) Yukon (1:50 000 scale). Yukon Geological Survey, Energy, Mines and Resources, Yukon Government, Open File 2009-48.

Bond, J.D., Lipovsky, P.S., 2010. Pre-Reid surficial geology investigations in southwest McQuesten map area (115P). In K.E. MacFarlane, L.H. Weston, L.R. Blackburn (Eds.), Yukon Exploration and Geology 2009 (pp. 103-117). Yukon Geological Survey.

Bond, J.D., Lipovsky, P.S., von Gaza, P., 2008. Surficial geology investigations in Wellesley basin and Nisling Range, southwest Yukon. In D.S. Emond, L.R. Blackburn, R.P. Hill, L.H. Weston (Eds.), Yukon Exploration and Geology 2007 (pp. 125-138). Yukon Geological Survey.

Bousquet, Y. (Ed.), 1991. Checklist of beetles of Canada and Alaska. Research Branch, Agriculture Canada, Publication 1861/E, 430 pp.

Bostock, H.B., 1942. Ogilvie map-area. Geological Survey of Canada, Map 711A

Bostock, H.B., 1966. Notes on glaciation in central Yukon Territory. Geological Survey of Canada. Paper 65-56, 18 p.

Brigham-Grette, J., 2001. New perspectives on Beringian Quaternary paleogeography, stratigraphy, and glacial history. Quaternary Science Reviews, 20, 15-24.

Brigham-Grette, J., Hopkins, D.M., 1995. Emergent marine record and paleoclimate of the last interglaciation along the northwest Alaskan coast. Quaternary Research, 43, 159-173.

Briner, J.P., Kaufman, D.S., 2008. Late Pleistocene mountain glaciation in Alaska: key chronologies. Journal of Quaternary Science, 23, 659-670.

Briner, J.P., Kaufman, D.S., Manley, W.F., Finkel, R.C., Caffee, M.W., 2005. Cosmogenic exposure dating of late Pleistocene moraine stabilization in Alaska. Geological Society of America Bulletin, 117, 1108-1120.

Broccoli, A.J., Manabe, S., 1987. The effects of the Laurentide Ice Sheet on North American climate during the Last Glacial Maximum. Geographie Physique et Quaternaire, 41, 291-299.

Brock, F., Froese, D.G., Roberts, R.G., 2010. Low temperature (LT) combustion of sediments does not necessarily provide accurate radiocarbon ages for site chronology. Quaternary Geochronology, 5, 625-630.

Brocklehurst, S.H., Whipple, K.X., 2004. Hypsometry of glaciated landscapes. Earth Surface Processes and Landforms, 29, 907-926.

Bromwich, D.H., Toracinta, E.R., Wei, H., Oglesby, R.J., Fastook, J.L., Hughes, T.J., 2004. Polar MM5 simulations of the winter climate of the Laurentide Ice Sheet at the LGM. Journal of Climate, 17, 3415-3433.

Bunbury, J., Gajewski, K., 2009. Postglacial climates inferred from a lake at treeline, southwest Yukon Territory, Canada. Quaternary Science Reviews, 28, 354-369.

Burn, C.R., 1994. Permafrost, tectonics, and past and future regional climate change, Yukon and adjacent Northwest Territories. Canadian Journal of Earth Science, 31, 182-191.

Chappell, J., Shackleton, N.J., 1986. Oxygen isotopes and sea level. Nature, 324, 137-140.

Clague, J.J., Evans, S.G., Rampton, V.N., Woodsworth, G.J., 1995. Improved age estimates for the White River and Bridge River tephras, western Canada. Canadian Journal of Earth Science, 32, 1172-1179.

Clague, J.J., Luckman, B.H., Van Dorp, R.D., Gilbert, R., Froese, D., Jensen, B.J.L., Reyes, A.V., 2006. Rapid changes in the lake level of Kluane Lake in Yukon Territory over the last millennium. Quaternary Research, 66, 342-355.

Clark, P.U., Pollard, D., 1998. Origin of the middle Pleistocene transition by ice sheet erosion of regolith. Paleoceanography, 13 (1), 1-9.

Clark, P.U., Mix, A.C., 2002. Ice sheets and sea level of the Last Glacial Maximum. Quaternary Science Reviews, 21, 1-7.

Clark, P.U., Archer, D., Pollard, D., Blum, J.D., Rial, J.A., Mix, A.C., Pisias, N.G., Roy, M., 2006. The middle Pleistocene transition: characteristics, mechanisms, and implications for long-term changes in atmospheric pCO2. Quaternary Science Reviews, 25, 3150-3184.

Cody, J.W., 2000. Flora of the Yukon Territory, Second edition. NRC Research Press, Ottawa, Ontario, Canada, 669 pp.

Danks, H.V., Downes, J.A. (Eds.), 1997. Insects of the Yukon. Biological Survey of Canada Monograph series No. 2, Biological Survey of Canada (Terrestrial Arthropods), Ottawa, 1034 pp.

Demuro, M., Roberts, R.G., Froese, D.G., Arnold, L.J., Brock, F., Bronk Ramsey, C., 2008. Optically stimulated luminescence dating of single and multiple grains of quartz from perennially frozen loess in western Yukon Territory, Canada: Comparison with radiocarbon chronologies for the late Pleistocene Dawson tephra. Quaternary Geochronology, 3, 346-364.

Demuro, M., Froese, D.G., Arnold, L.J., Roberts, R.G., 2012. Single-grain OSL dating of glaciofluvial quartz constrains Reid glaciation in NW Canada to MIS 6. Quaternary Research, 77, 305-316.

Denton, G.H., 1965. Late Pleistocene glacial chronology, northeastern St. Elias Mountains. Unpublished Ph.D. dissertation, Yale University, 88 p.

Denton, G.H., 1974. Quaternary glaciations of the White River Valley, Alaska, with a regional synthesis for the northern St. Elias Mountains, Alaska and Yukon Territory. Geological Society of America Bulletin, 85, 871-892.

Denton, G.H., Stuiver, M., 1966. Neoglacial chronology, northeastern St. Elias Mountains, Canada. American Journal of Science, 264, 577-599.

Denton, G.H., Stuiver, M., 1967. Late Pleistocene glacial stratigraphy and chronology, northeastern St. Elias Mountains, Canada. American Journal of Science, 264, 577-599.

Dodds, C.J., 1995. Denali fault system. In H. Gabrielse, C.J. Yorath (Eds.), Structural styles, Chapter 17, Geology of the Cordilleran Orogen in Canada (pp. 656-657). Geological Survey of Canada, Geology of Canada, no. 4.

Dortch, J., 2006. Defining the timing of glaciation in the central Alaska Range using terrestrial cosmogenic nuclide and optically stimulated luminescence dating of moraines and terraces. Master's thesis, University of Cincinnati.

Duk-Rodkin, A., 1996. Surficial geology, Dawson, Yukon Territory. Geological Survey of Canada, Open File 3288, scale 1:125,000.

Duk-Rodkin, A., 1999. Glacial limits map of Yukon Territory; Geological Survey of Canada, Open File 3694, Indian and Northern Affairs Canada Geoscience Map 1999-2, scale 1:1 000 000.

Duk-Rodkin, A., Barendregt, R.W., 2011. The glacial history of northwestern Canada. In J. Ehlers, P.L. Gibbard, P.D. Hughes (Eds.), Quaternary Glaciations – Extent and Chronology, Part IV: A Closer Look, Elsevier, pp. 661-698.

Duk-Rodkin, A., Barendregt, R.W., Froese, D.G., Weber, F., Enkin, R.J., Smith, I.R., 2004. Timing and extent of Plio-Pleistocene glaciations in North-West Canada and East-Central Alaska. In J. Ehlers, P.L. Gibbard (Eds.), Quaternary Glaciations – Extent and Chronology, Part II: North America. Quaternary Science Reviews, Elsevier, pp. 313-345.

Duk-Rodkin, A., Barendregt, R.W., White, J.M., 2010. An extensive late Cenozoic terrestrial record of multiple glaciations preserved in the Tintina Trench, west-central Yukon: stratigraphy, paleomagnetism, paleosols, and pollen. Canadian Journal of Earth Science, 47, 1003-1028.

Ehlers, J., Gibbard, P.L., 2003. Quaternary Glaciations – Extent and Chronology, Part II: North America. Quaternary Science Reviews, 22, 1561-1568.

Elias, S.A., 2000. Late Pleistocene climates of Beringia, based on analysis of fossil beetles. Quaternary Research, 53, 229-235.

England, J.H., Furze, M.F.A., Doupe, J.P., 2009. Revision of the NW Laurentide Ice sheet: implications for paleoclimate, the northeast extremity of Beringia, and Arctic Ocean sedimentation. Quaternary Science Reviews, 28, 1573-1596.

Enkelmann, E., Garver, J.I., Pavlis, T.L., 2008. Rapid exhumation of ice-covered rocks of the Chugach-St. Elias orogen, Southeast Alaska. Geology, 36, 915-918.

Enkelmann, E., Zeitler, P.K., Pavlis, T.L., Garver, J.I., Ridgway, K.D., 2009. Intense localized rock uplift and erosion in the St. Elias orogen of Alaska. Nature Geoscience, 2, 360-363.

Faegri, K., and Iversen, J., 1989. "Textbook of Pollen Analysis." John Wiley & Sons, Chichester.

Foster, G.L., Lunt, D.J., Parrish, R.R., 2010. Mountain uplift and the glaciation of North America – a sensitivity study. Climate of the Past, 6, 707-717.

Froese, D.G., 2005. Surficial Geology, Flat Creek, Yukon Territory. Geological Survey of Canada, Open File 4592, scale 1:50 000.

Froese, D.G., Barendregt, R.W., Enkin, R.J., Baker, J., 2000. Paleomagnetic evidence for multiple Late Pliocene – Early Pleistocene glaciations in the Klondike area, Yukon Territory. Canadian Journal of Earth Science, 37, 863-877.

Froese, D.G., Smith, D.G., Westgate, J.A., Ager, T.A., Preece, S.J., Sandhu, A., Enkin, R.J., Weber, F., 2003. Recurring middle Pleistocene outburst floods in east-central Alaska. Quaternary Research, 60, 50-62.

Froese, D.G., Zazula, G.D., Reyes, A.V., 2006. Seasonality of the late Pleistocene Dawson tephra and exceptional preservation of a buried riparian surface in central Yukon Territory, Canada. Quaternary Science Reviews, 25, 1542-1551.

Froese, D.G., Westgate, J.A., Reyes, A.V., Enkin, R.J., Preece, S.J., 2008. Ancient permafrost and a future, warmer Arctic. Science, 321, 1648 p.

Froese, D.G., Zazula, G.D., Westgate, J.A., Preece, S.J., Sanborn, P.T., Reyes, A.V., Pearce, N.J.G., 2009. The Klondike goldfields and Pleistocene environments of Beringia. GSA Today, 19 (8), 4-10.

Goetcheus, V.G., Birks, H.H., 2001. Full-glacial upland tundra vegetation preserved under tephra in the Beringia National Park, Seward Peninsula, Alaska. Quaternary Science Review, 20, 135-147.

Guthrie, R.D., 2001. Origin and causes of the mammoth steppe: a story of cloud cover, woolly mammal tooth pits, buckles, and inside-out Beringia. Quaternary Science Reviews, 20, 549-574.

Hamilton, T.D., Brigham-Grette, J., 1991. The last interglaciation in Alaska: stratigraphy and paleoecology of potential sites. Quaternary International, 10-12, 49-71.

Hays, J.D., Imbrie, J., Shackleton, N.J., 1976. Variations in the Earth's orbit: pacemaker of the ice ages. Science, 194, 1121-1132.

Hidy, A.J., Gosse, J.C., Froese, D.G., Bond, J.D., Rood, D.H., 2013. A latest Pliocene age for the earliest and most extensive Cordilleran Ice Sheet in northwest Canada. Quaternary Science Reviews, 61, 77-84.

Hicock, S.R., Goff, J.R., Lian, O.B., Little, E.C., 1996. On the interpretation of subglacial till fabric. Journal of Sedimentary Research, 66, 928-934.

Hopkins, D.M. (ed.), 1967. The Bering Land Bridge. Stanford University Press, Stanford.

Hopkins, D.M., 1973. Sea level history in Beringia during the past 250,000 years. Quaternary Research, 3, 520-540.

Hopkins, D.M., 1982. Aspects of the paleogeography of Beringia during the late Pleistocene. In D.M. Hopkins, J.V. Matthews, Jr., C.E. Schweger, S.B. Young (Eds.), Paleoecology of Beringia (pp. 3-28). Academic Press, New York.

Hu, A., Meehl, G.A., Otto-Bliesner, B.L., Waelbroeck, C., Han, W., Loutre, M-F., Lambeck, K., Mitrovica, J.X., Rosenbloom, N., 2010. Influence of Bering Strait flow and North Atlantic circulation on glacial sea-level changes. Nature Geoscience, 3, 118-121.

Hughes, O.L., 1990. Surficial geology and geomorphology, Aishihik Lake, Yukon Territory. Geological Survey of Canada Paper 87-29, 23 p.

Hughes, O.L., Campbell, R.B., Muller, J., Wheeler, J.D., 1969. Glacial limits and flow patterns, Yukon Territory south of 65^{o} N latitude. Geological Survey of Canada Paper 68-34, 9 p.

Hunt, J.B., Hill, P.G., 1993. Tephra geochemistry: a discussion of some persistent analytical problems. The Holocene, 3, 271-278.

Huntley, D.J., Lamothe, M., 2001. Ubiquity of anomalous fading in K-feldspars and the measurement and correction for it in optical dating. Canadian Journal of Earth Sciences, 38, 1093-1106.

Huot, S., Lamothe, M., 2003. Variability of infrared stimulated luminescence properties from fractured feldspar grains. Radiation Measurements, 37, 499-503.

Huscroft, C.A., Ward, B.C., Barendregt, R.W., Jackson, Jr., L.E., Opdyke, N.D., 2004. Pleistocene volcanic damming of Yukon River and the maximum age of the Reid Glaciation, west-central Yukon. Canadian Journal of Earth Science, 41, 151-164.

Huybers, P.J., 2006. Early Pleistocene glacial cycles and the integrated summer insolation forcing. Science, 313, 508-511.

Ives, J.W., Froese, D., Supernant, K., Yanicki, G., 2013. Vectors, vestiges, and valhallas – rethinking the corridor. In Graf, K.E., Ketron, C.V., Waters, M.R. (eds.), Paleoamerican Odyssey (pp. 149-160). Center for the Study of First Americans, Department of Anthropology, Texas A&M University, College Station, Texas, USA.

Jackson, L.E., Jr., 1987. Terrain inventory and Quaternary history of Nahanni map area, Yukon Territory and Northwest Territories. Geological Survey of Canada, Paper, 86-18, p. 23.

Jackson, L.E., Jr., 1994. Terrain inventory and Quaternary history of the Pelly River area, Yukon Territory. Geological Survey of Canada, Memoir, 437, p. 41.

Jackson, L.E., Jr., 2000. Quaternary geology of the Carmacks map area, Yukon Territory, Geological Survey of Canada Bulletin 539, p. 74.

Jackson, L.E., Jr., Harington, C.R., 1991. Middle Wisconsinan mammals, stratigraphy, and sedimentology at the Ketza River site, Yukon Territory. Geographie physique et Quaternaire, 45, 69-77.

Jackson, L.E., Jr., Ward, B.C., Duk-Rodkin, A., Hughes, O.L., 1991. The latest Cordilleran ice sheet in Yukon Territory. Geographie Physique et Quaternaire, 45-3, 341-354.

Jackson, L.E., Jr., Barendregt, R.W., Baker, J., Irving, E., 1996. Early Pleistocene volcanism and glaciation in central Yukon: a new chronology from field studies and paleomagnetism. Canadian Journal of Earth Science, 33, 904-916.

Jackson, L.E., Jr., Andriashek, L.D., Phillips, F.M., 2011. Limits of successive middle and late Pleistocene continental ice sheets, Interior Plains of southern and central Alberta and adjacent areas. Developments in Quaternary Science, 15, 575-589.

Jackson, Jr., L.E., Nelson, F.E., Huscroft, C.A., Villeneuve, M., Barendregt, R.W., Storer, J.E., Ward, B.C., 2012. Pliocene and Pleistocene volcanic interaction with Cordilleran ice sheets, damming Yukon River and vertebrate palaeontology, Fort Selkirk Volcanic Group, west-central Yukon, Canada. Quaternary International, 260, 3-20.

Jensen, B.J.L., Froese, D.G., Preece, S.J., Westgate, J.A., Stachel, T., 2008. An extensive middle to late Pleistocene tephrochronologic record from east-central Alaska. Quaternary Science Reviews, 27, 411-427.

Jensen, B.J.L., Preece, S.J., Lamothe, M., Pearce, N.J.G., Froese, D.G., Westgate, J.A., Schaefer, J., Beger, J., 2011. The variegrated (VT) tephra: A new regional marker for middle to late marine isotope stage 5 across Yukon and Alaska. Quaternary International, 246, 312-323.

Kaplan, M.R., Hein, A.S., Hubbard, A., Lax, S.M., 2009. Can glacial erosion limit the extent of glaciation? Geomorphology, 103, 172-179.

Kennedy, K.E., Froese, D.G., Zazula, G.D., Lauriol, B., 2010. Last glacial maximum age for the northwest Laurentide maximum from the Eagle River spillway and delta complex, northern Yukon. Quaternary Science Reviews, 29, 1288-1300.

Klassen, R., 1987. The Tertiary-Pleistocene stratigraphy of the Liard Plain, southeastern Yukon Territory. Geological Survey of Canada, Paper 86-17, 16 p.

Kuhn, S., Froese, D.G., Shane, P.A.R., INTAV Intercomparison Participants, 2011. Quaternary International, 246, 19-47.

Lacelle, D., Lauriol, B., Clark, I.D., Cardyn, R., Zdanowicz, C., 2007. Nature and origin of a Pleistocene-age massive ground-ice body exposed in the Chapman Lake moraine complex, central Yukon Territory, Canada. Quaternary Research, 68, 249-260.

Lacourse, T., Gajewski, K., 2000. Late Quaternary vegetation history of Sulphur Lake, Southwest Yukon Territory, Canada. Arctic, 53, 27-35.

Lakeman, T.R., England, J.H., 2012. Paleoglaciological insights from the age and morphology of the Jesse moraine belt, western Canadian Arctic. Quaternary Science Reviews, 47, 82-100.

Lakeman, T.R., England, J.H., 2013. Late Wisconsinan glaciation and postglacial relative sea-level change on western Banks Island, Canadian Arctic Archipelago. Quaternary Research, 80, 99-112.

Lamothe, M., 2004. Optical dating of pottery, burnt stones, and sediments from selected Quebec archaeological sites. Canadian Journal of Earth Sciences, 41, 659-667.

Lamothe, M., Auclair, M., Hamzaoui, C., Huot, S., 2003. Towards a prediction of long-term anomalous fading of feldspar IRSL. Radiation Measurements, 37, 493-498.

Lerbekmo, J.F., Westgate, J.A., Smith, D.G.W., Denton, G.H., 1975. New data on the character and history of the White River volcanic eruption, Alaska. In R.P. Suggate, M.M. Cresswell (Eds.), Quaternary studies (pp. 203-209). Royal Society of New Zealand, Wellington, N.Z.

Lisiecki, L.E., Raymo, M.E., 2005. A Pliocene-Pleistocene stack of 57 globally distributed benthic δO18 records. Paleoceanography, 20, 10.1029/2004PA001071.

Lisiecki, L.E., Raymo, M.E., 2007. Plio-Pleistocene climate evolution: trends and transitions in glacial cycle dynamics. Quaternary Science Reviews, 26, 56-69.

Lowdon, J.A., Wilmeth, R., Blake, W., Jr., 1970. Geological Survey of Canada radiocarbon dates X. Radiocarbon, 12, 472-485.

MacDonald, G.M., 1983. Holocene vegetational history of the upper Natia River area, Northwest Territories, Canada. Arctic and Alpine Research, 15, 169-180.

MacGregor, K.R., Anderson, R.S., Anderson, S.P., Waddington, E.D., 2000. Numerical simulations of glacial-valley longitudinal profile evolution. Geology, 28, 1031-1034.

Manley, W.F., Kaufman, D.S., 2002. Alaska PaleoGlacier Atlas, Vol. 1. Institute of Arctic and Alpine Research (INSTAAR), University of Colorado.

Martin, A.C., Barkley, W.E., 1961. Seed identification manual. California University Press, Berkeley, 221 pp.

Martinson, D.G., Pisias, N.G., Hays, J.D., Imbrie, J., Moore, T.C., Jr., Shackleton, N.J., 1987. Age dating and the orbital theory of the Ice Ages: development of a high-resolution 0 to 300,000-year chronostratigraphy. Quaternary Research, 27, 1-29.

Matheus, P., Beget, J., Mason, O., Gelvin-Reymiller, C., 2003. Late Pliocene to late Pleistocene environments preserved at the Palisades Site, central Yukon River, Alaska. Quaternary Research, 60, 33-43.

Matmon, A., Briner, J.P., Carver, G., Bierman, P., Finkel, R.C., 2010. Moraine chronosequence of the Donnely Dome region, Alaska. Quaternary Research, 74, 63-72.

Matthews, J.V., Schweger, C.E., Janssens, J.A., 1990a. The last (Koy-Yukon) interglaciation in the northern Yukon: evidence from Unit 4 at Ch'ijee's Bluff, Bluefish Basin. Geographie Physique et Quaternaire, 44, 341-362.

Matthews, J.V., Schweger, C.E., Hughes, O.L., 1990b. Plant and insect fossils from the Mayo Indian Village Section (Central Yukon): new data on Middle Wisconsinan environments and glaciation. Geographie physique et Quaternaire, 44, 15-26.

McAndrews, J. H., Berti, A. A., and Norris, G., 1973. Key to the Quaternary Pollen and spores of the Great Lakes Region. Royal Ontario Museum, Toronto.

Moore, P. D., Webb, J. A., and Collinson, M. E., 1991. Pollen Analysis. Blackwell Scientific Publications, Oxford.

Moriya, K., 1976. Flora and Palynomorphs of Alaska. Kodansha Pub. Co, Tokyo.

Morley, J.J., Pisias, N.G., Leinen, M., 1987. Late Pleisticene time series of atmospheric and ocean variables recorded in sediments from the subarctic Pacific. Paleoceanography, 2, 49-62.

Muhs, D.R., Ager, T.A., Beget, J.E., 2001. Vegetation and paleoclimate of the last interglacial period, central Alaska. Quaternary Science Reviews, 20, 41-61.

Murray, A.S., Wintle, A.G., 2000. Luminescence dating of quartz using an improved single-aliquot regenerative-dose protocol. Radiation Measurements, 32, 57-73.

Nelson, F.E., Barendregt, R.W., Villeneuve, M., 2009. Stratigraphy of the Fort Selkirk volcanogenic complex in central Yukon and its paleoclimatic significance: Ar/Ar and paleomagnetic data. Canadian Journal of Earth Science, 46, 381-401.

O'Sullivan, P.B., Currie, L.D., 1996. Thermotectonic history of Mt. Logan, Yukon Territory, Canada: implications of multiple episodes of middle to late Cenozoic denudation. Earth and Planetary Letters, 144, 251-261.

Pedersen, V., Egholm, D.L., 2013. Glaciations in response to climate variations preconditioned by evolving topography. Nature, 493, 206-210.

Pewe, T.L., 1953. Big Delta area, Alaska. In Pewe, T.L. (Ed.), Multiple Glaciations in Alaska (pp. 8-10). U.S. Geological Survey Circular 289.

Pewe, T.L., 1975. The Quaternary geology of Alaska. U.S. Geological Survey Professional Paper 385.

Pewe, T.L., Reger, R.D., 1983. Richardson and Glenn Highways, Alaska: guidebook to permafrost and Quaternary Geology. Alaska Division of Geological and Geophysical Surveys Guidebook 1.

Pewe, T.L., Reger, R.D., 1989. Quaternary geology and permafrost along the Richardson and Glenn Highways between Fairbanks and Anchorage, Alaska. Field Trip Guidebook T102. 28th International Geological Congress.

Pewe, T.L., Berger, G.W., Westgate, J.A., Brown, P.M., 1997. Eva Interglaciation Forest Bed, Unglaciated East-Central Alaska: Global Warming 125,000 Years Ago, Geological Society of America Special Paper 319, 54 p.

Plouffe, A., 1989. Drift prospecting and till geochemistry in Tintina Trench, Southeastern Yukon. Unpublished M.Sc. thesis, Carleton University, Ottawa, Ontario, 81 p.

Preece, S.J., Westgate, J.A., Gorton, M.P., 1992. Compositional variation and provenance of late Cenozoic distal tephra beds, Fairbanks area, Alaska. Quaternary International, 13/14, 97-101.

Preece, S.J., Westgate, J.A., Stemper, B.A., Pewe, T.L., 1999. Tephrochronology of late Cenozoic loess at Fairbanks, central Alaska. Geological Society of America Bulletin, 111, 71-90.

Preece, S.J., Pearce, N.J.G., Westgate, J.A., Froese, D.G., Jensen, B.J.L., Perkins, W.T., 2011a. Old Crow tephra across eastern Beringia: a single cataclysmic eruption at the close of Marine Isotope Stage 6. Quaternary Science Reviews, 30, 2069-2090.

Preece, S.J., Westgate, J.A., Froese, D.G., Pearce, N.J.G., Perkins, W.T., 2011b. A catalogue of late Cenozoic tephra beds in the Klondike goldfields and adjacent areas, Yukon Territory. Canadian Journal of Earth Sciences, 48, 1386-1418.

Rampton, V.N., 1969. Pleistocene geology of the Snag-Klutlan area, southwestern Yukon Territory, Canada. Ph.D. dissertation, University of Minnesota, 237 pp.

Rampton, V.N., 1971. Late Pleistocene glaciations of the Snag-Klutlan area, Yukon Territory, Arctic, 24, 277-300.

Raymo, M.E., Huybers, P., 2008. Unlocking the mysteries of the ice ages. Nature, 451, 284-285.

Reimer, P.J., Baillie, M.G.L., Bard, E., Bayliss, A., Beck, J.W., Blackwell, P.G., Bronk Ramsey, C., Buck, C.E., Burr, G.S., Edwards, R.L., Friederich, M., Grootes, P.M., Guilderson, T.P., Hajdas, I., Heaton, T.J., Hogg, A.G., Hughen, K.A., Kaiser, K.F., Kromer, B., McCormac, F.G., Manning, S., Reimer, R.W., Richards, D.A., Southon, J.R., Talamo, S., Turney, C.S.M., van der Plicht. J., Weyhenmeyer, C.E., 2009. IntCal09 and Marine09 radiocarbon age calibration curves, 0-50,000 years cal BP. Radiocarbon, 51, 1111-1150.

Reyes, A.V., Jensen, B.J.L., Zazula, G.D., Ager, T.A., Kuzmina, S., La Farge, C., Froese, D.G., 2010a. A late-Middle Pleistocene (Marine Isotope Stage 6) vegetated surface buried by Old Crow tephra at the Palisades, interior Alaska. Quaternary Sciences Reviews, 29, 801-811.

Reyes, A.V., Froese, D.G., Jensen, B.J.L., 2010b. Permafrost response to last interglacial warming: field evidence from non-glaciated Yukon and Alaska. Quaternary Science Reviews, 29, 3256-3274.

Roy, M., Clark, P.U., Raisbeck, G.M., Yiou, F., 2004. Geochemical constraints on the regolith hypothesis for the middle Pleistocene transition. Earth Planetary Science Letters, 227, 281-296.

Sanborn, P.T., Pawluk, S., 1989. Microstructure diversity in Ah horizons of Black Chermozemic soils, Alberta and British Columbia (Canada). Geoderma, 45, 221-240.

Shackleton, N.J., 1987. Oxygen isotopes, ice volume and sea level. Quaternary Science Reviews, 6, 183-190.

Shapiro, B., Drummond, A.J., Rambaut, A., Wilson, M.C., Matheus, P.E., Sher, A.V., Pybus, O.G., Gilbert, M. Thomas P., Barnes, I., Binladen, J., Willerslev, E., Hansen, A.J., Baryshnikov, G.F., Burns, J.A., Davydov, S., Driver, J.C., Froese, D.G., Harington, C.R., Keddie, G., Kosintsev, P., Kunz, M.L., Martin, L.D., Stephenson, R.O., Storer, J., Tedford, R., Zimov, S., Cooper, A., 2004. Rise and fall of the Beringian Steppe Bison. Science, 306, 1561-1565.

Schweger, C.E., 2003. Paleoecology of two Marine Oxygen Isotope stage 7 sites correlated by the Sheep Creek tephra, northwestern North America. Quaternary Research, 60, 44-49.

Schweger, C.E., Janssens, J.A.P., 1980. Paleoecology of the Boutellier Nonglacial Interval, St. Elias Mountains, Yukon Territory. Arctic and Alpine Research, 12 (3), 309-317.

Schweger, C., Froese, D., White, J.M., Westgate, J.A., 2011. Pre-glacial and interglacial pollen records over the last 3 Ma from northwest Canada: Why do Holocene forests differ from those of previous interglaciations? Quaternary Science Reivews, 30, 2124-2133.

Schweger, C.E., Matthews, Jr., J.V., 1991. The last (Koy-Yukon) interglaciation in the Yukon: Comparisons with Holocene and interstadial pollen records. Quaternary International 10-12, 85-94.

Smith, C.A.S., Tarnocai, C., Hughes, O.L., 1986. Pedological investigations of Pleistocene glacial drift surfaces in the central Yukon. Geographie Physique et Quaternaire, 40 (1), 29-37.

Stroeven, A.P., Fabel, D., Codilean, A.T., Kleman, J., Clague, J.J., Miguens-Rodriguez, M., Xu, S., 2010. Investigating the glacial history of the northern sector of the Cordilleran Ice Sheet with cosmogenic ^{10}Be concentrations in quartz. Quaternary Science Reviews, 29, 3630-3643.

Tarnocai, C., Schweger, C.E., 1991. Late Tertiary and Early Pleistocene paleosols in Northwest Canada. Arctic, 44, 1-11.

Tarnocai, C., Smith, C.A.S., 1989. Micromorphology and development of some Central Yukon paleosols, Canada. Geoderma, 45, 1450162.

Thomas, R.D., Rampton, V.R., 1982. Surficial geology and geomorphology, Upper Blackstone River, Yukon Territory. Geological Survey of Canada, Map 7-1982, scale 1:100,000.

Toracinta, E.R., Bromwich, D.H., Oglesby, R., Fastook, J., Hughes, T., 2004. LGM summer climate of the Laurentide Ice Sheet simulated by Polar MM5. Journal of Climate, 17, 3415-3419.

Turner, D.G., 2008. Quaternary Geology of Howard's Pass and Applications to Drift Prospecting. Unpublished M.Sc. Thesis, Simon Fraser University, 212 p.

Turner, D.G., Ward, B.C., Bond, J.D., Jensen, B.J.L., Froese, D.G., Telka, A.M., Zazula, G.D., Bigelow, N.H., 2013. Middle to Late Pleistocene ice extents, tephrochronology and paleoenvironments of the White River area, southwest Yukon. Quaternary Science Reviews, 75, 59-77.

Vernon, P., Hughes, O.L., 1966. Surficial Geology, Larsen Creek, and Nash Creek map areas, Yukon Territory. Geological Survey of Canada, Bulletin 136, 25 pp.

Ward, B.C., Bond, J.D., Gosse, J.C., 2007. Evidence for a 55-50 ka (early Wisconsin) glaciation of the Cordilleran ice sheet, Yukon Territory, Canada. Quaternary Research, 68, 141-150.

Ward, B.C., Bond, J.D., Froese, D., Jensen, B., 2008. Old Crow tephra (140 ± 10 ka) constrains penultimate Reid glaciations in central Yukon Territory. Quaternary Science Reviews, 27, 1909-1915.

Weber, F.R., Hamilton, T.D., Hopkins, D.M., Repenning, C.A., Haas, H., 1981. Canyon Creek: a Late Pleistocene vertebrate locality in interior Alaska. Quaternary Research, 16, 167-180.

Westgate, J.A., Walter, R.C., Pearce, G.W., Gorton, M.P., 1985. Distribution, stratigraphy, petrochemistry, and palaeomagnetism of the late Pleistocene Old Crow tephra in Alaska and the Yukon. Canadian Journal of Earth Science, 22, 893-906.

Westgate, J.A., Stemper, B.A., Pewe, T.L., 1990. A 3 m.y. record of Pliocene-Pleistocene loess in interior Alaska. Geology, 18, 858-861.

Westgate, J.A., Preece, S.J., Froese, D.G., Walter, R.C., Sandhu, A.S., 2001. Dating Early and Middle (Reid) Pleistocene glaciations in central Yukon by tephrochronology. Quaternary Research, 56, 335-348.

Westgate, J.A., Preece, S.J., Froese, D.G., Pearce, N.J.G., Roberts, R.G., Demuro, M., Hart, W.K., Perkins, W., 2008. Changing ideas on the identity and stratigraphic significance of the Sheep Creek tephra beds in Alaska and the Yukon Territory. Quaternary International, 178, 183-209.

Whipple, K.X., Kirby, E., Brocklehurst, S.H., 1999. Geomorphic limits to climate-induced increases in topographic relief. Nature, 401, 39-43.

White, J.M., Ager, T.A., Adam, D.P., Leopold, E.B., Liu, G., Jette, H., Schweger, C.E., An 18 million year record of vegetation and climate change in northwestern Canada and Alaska: tectonic and global climate correlates. Paleogeography, Paleoclimatology, Paleoecology, 130, 293-306.

Wintle, A.G., 1973. Anomalous fading of thermoluminescence in mineral samples. Nature, 245, 143-144.

Wood, R.D., Imahori, K., 1965. Monograph of the Characeae, Vol. 1. Cramer, Wertheim, pp. 904.

Yukon Ecoregions Working Group, 2004. St. Elias Mountains. In C.A.S. Smith, J.C. Meikle, C.F. Roots (Eds.), Ecoregions of the Yukon Territory: Biophysical properties of Yukon landscapes (pp/ 169-178). Agriculture and Agri-Food Canada, PARC Technical Bulletin No. 04-01, Summerland, British Columbia.

Zazula, G.D., Schweger, C.E., Beaudoin, A.B., McCourt, G.H., 2006a. Macrofossil and pollen evidence for full-glacial steppe within an ecological mosaic along the Bluefish River, eastern Beringia. Quaternary International, 142-143, 2-19.

Zazula, G.D., Froese, D.G., Elias, S.A., Kuzmina, S., La Farge, C., Reyes, A.V., Sanborn, P.T., Schweger, C.E., Scott Smith, C.A., Mathewes, R.W., 2006b. Vegetation buried under Dawson tephra (25,300 ^{14}C years BP) and locally diverse late Pleistocene paleoenvironments of Goldbottom Creek, Yukon, Canada.

Zazula, G.D., Telka, A.M., Harington, C.R., Schweger, C.E., Mathewes, R.W., 2006c. New spruce (*Picea* spp.) macrofossils from Yukon Territory: implications for Late Pleistocene refugia in Eastern Beringia. Arctic, 59, 391-400.

Zazula, G.D., Froese, D.G., Elias, S.A., Kuzmina, S., Mathewes, R.W., 2007. Arctic ground squirrels of the mammoth-steppe: paleoecology of Late Pleistocene middens (~24 000 – 29 450 ^{14}C yr BP), Yukon Territory, Canada. Quaternary Science Reviews, 979-1003.

Zazula, G.D., Turner, D.G., Ward, B.C., Bond, J.D., 2011. Last Interglacial western camel (*Camelops hesternus*) from Eastern Beringia. Quaternary Science Reviews, 30, 2355-2360.

Appendix A.

Site Sedimentological and Stratigraphic Descriptions

Appendix A site descriptions are included on the attached DVD. Sites are displayed from south to north. These diagrams were created and exported as PDFs using Adobe Illustrator and may be opened with any PDF program.

File Name: Appendix A Site Descriptions.pdf

Appendix B.

Tephra Data

Appendix B tephra data are included as a multi-tab spreadsheet on the attached DVD. This spreadsheet was created using Microsoft Excel 2007 and may be opened with most spreadsheet programs.

File Name: Appendix B Tephra Data.xlsx

Appendix C.

Plant and Insect Macrofossil Reports

Appendix C reports are included as PDFs on the attached DVD and may be opened with most spreadsheet programs. The following catalogue shows the field sample names, sites and collection year for the samples analyzed.

File Name: Appendix C Macrofossil Reports.pdf

White River

Sample names	Site	Year collected
07JB63-M1	WR94	2007
07JB63-M2	WR94	2007
10WR94-M1	WR94	2010
07JB53-M1	WR98	2007
07JB53-M3	WR98	2007
07JB52B-M1	WR99	2007
07JB52B-M2	WR99	2007
07JB52B-M3	WR99	2007
07JB52B-M5	WR99	2007
07JB52B-M7	WR99	2007
07JB52B-M8	WR99	2007
07JB52B-M10	WR99	2007
07JB52B-M11	WR99	2007

Silver Creek

Sample names	Site	Year collected
09DTSC7-M2	SC7	2009
BCW-SC-M1	SC8	2009
09DTSC11-M2	SC11	2009
09DTSC11-M3	SC11	2009
09DTSC11-M5	SC11	2009
09DTSC11-M7	SC11	2009
BCW-SC-M2	SC11	2010
BCW-SC-M4	SC11	2010

Appendix D.

Pollen Data

Appendix D data are included as spreadsheets on the attached DVD and may be opened with most spreadsheet programs. Both pollen count and pollen percentage data are included for the White River and Silver Creek sites. The following catalogue shows the field sample names, sites and collection year for the samples analyzed.

File Names: Appendix D Pollen Data White River.xlsx, Appendix D Pollen Data Silver Creek.xlsx

White River

Sample names	Site	Year collected
10WR54-M1	WR54	2010
10WR54-M2	WR54	2010
10WR93-M1	WR92	2010
10WR95-M1	WR95	2010
10WR95-M2	WR95	2010
07JB52B-M1	WR99	2007
07JB52B-M2	WR99	2007
07JB52B-M3	WR99	2007
07JB52B-M5	WR99	2007
07JB52B-M7	WR99	2007
07JB52B-M8	WR99	2007
07JB52B-M10	WR99	2007
07JB53-M1	WR98	2007
07JB53-M3	WR98	2007
07JB63-M1	WR94	2007
07JB63-M2	WR94	2007

Silver Creek

Sample names	Site	Year collected
09DTSC08-PO1	SC8	2009
09DTSC11-PO2	SC11	2009
09DTSC11-PO3	SC11	2009
09DTSC11-PO4	SC11	2009
09DTSC11-PO5	SC11	2009
09DTSC11-PO6	SC11	2009
09DTSC11-PO7	SC11	2009
09DTSC12-PO1	SC12	2009

Appendix E.

Mammal Fossils

Appendix E data show the sites, elements, taxon identification and Yukon Government Species number for all mammal fossils recovered from the White River sites.

Taxon	Site	Unit	Common Name	Element	Yukon Government Species #
Urocitellus parryii		16	Arctic ground squirrel	Humerus	308.18
Microtus pennsylvanicus	WR98	14	Meadow vole	Mandibles and cranium	
Mammuthus primigenius	WR98	14	Mammoth	Tibia fragment	308.9
Mammuthus primigenius	WR98	14	Mammoth	Post-cranial	308.10
Equus sp.	WR98	14	Horse	Metatarsal	308.19
Equus sp.	WR98	14	Horse	Thoracic vertebra	354.12
Equus sp.	WR98	14	Horse	Thoracic vertebra	354.13
Bison cf. *priscus*	WR98	14	Steppe bison	Cranium	400.1
Bison cf. *priscus*	WR98	14	Steppe bison	Partial cranium	308.11
Bison cf. *priscus*	WR98	14	Steppe bison	Mandibular molar	354.1
Rangifer tarandus	WR98	14	Caribou	Metatarsal fragment	354.7
cf. Ovis dalli	WR98	14	Sheep	Naviculo-cuboid	354.15
Camelops hesternus	WR99	9	Western camel	Partial proximal phalanx	400.6
Bison cf. *priscus*	WR98	Unknown	Steppe bison	Radius fragment	308.4
Equus sp.	WR98	Unknown	Horse	Scapula fragment	308.7

Appendix F.

Pedological Thin Sections

Appendix F thin section pictures are included on the attached DVD. These images from the White River sites may be opened with any PDF program. The file name includes the site number and a brief description in parentheses.

File Name: Appendix F Pedological Thin Sections.pdf